NASA CONTRACTOR
REPORT

NASA CR-61364

SPACE RADIATION HAZARDS TO PROJECT SKYLAB PHOTOGRAPHIC FILM

Phase II

By C. W. Hill and C. F. Neville

Lockheed-Georgia Company
Marietta, Ga. 30060

October 1971

Final Report

Prepared for

NASA-GEORGE C. MARSHALL SPACE FLIGHT CENTER
Marshall Space Flight Center, Alabama 35812

TECHNICAL REPORT STANDARD TITLE PAGE

1. REPORT NO.	2. GOVERNMENT ACCESSION NO.	3. RECIPIENT'S CATALOG NO.
NASA CR-61364		

4. TITLE AND SUBTITLE	5. REPORT DATE
SPACE RADIATION HAZARDS TO PROJECT SKYLAB PHOTOGRAPHIC FILM: Phase II, Final Report	October 1971
	6. PERFORMING ORGANIZATION CODE

7. AUTHOR(S)	8. PERFORMING ORGANIZATION REPORT #
C. W. Hill and C. F. Neville	ER 11192

9. PERFORMING ORGANIZATION NAME AND ADDRESS	10. WORK UNIT NO.
Lockheed-Georgia Company Marietta, Ga. 30060	
	11. CONTRACT OR GRANT NO. NAS 8-26441
	13. TYPE OF REPORT & PERIOD COVERED High Series Contractor Final
12. SPONSORING AGENCY NAME AND ADDRESS National Aeronautics and Space Administration Washington, D. C. 20546	14. SPONSORING AGENCY CODE

15. SUPPLEMENTARY NOTES

16. ABSTRACT

The results of a study of space radiation hazards to Project Skylab photographic film are presented. Radiation components include trapped protons, trapped electrons, bremsstrahlung, and galactic cosmic radiation. The shielding afforded by the Skylab cluster is taken into account with a 5000 volume element mathematical model. A preliminary survey of expected proton spectrometer data is reported.

17. KEY WORDS	18. DISTRIBUTION STATEMENT
Radiation Skylab Film Hazards	X Martin O. Bussell Unclassified-unlimited

19. SECURITY CLASSIF. (of this report)	20. SECURITY CLASSIF. (of this page)	21. NO. OF PAGES	22. PRICE
U	U	125	$3.00

MSFC - Form 3292 (May 1969)

FOREWORD

This technical report is submitted to the George C. Marshall Space Flight Center, National Aeronautics and Space Administration, Alabama, according to the requirements of Contract NAS8-26441. The Contract Officer's Representatives are M. O. Burrell, S&E-SSL-N, and C. A. Best, S&E-ASTN-SDI. The ATM portion of the study is directed by W. Nelson, ATM Experiment Office.

TABLE OF CONTENTS

1.0 INTRODUCTION

Extensive quantities of photographic film will be used for data recording during the Project Skylab program. Film with diverse radiation sensitivities will be placed in low earth orbit for periods ranging from 29 to 236 days. Storage and experimental locations offer varying amounts of protection from space radiation-induced fogging to the Skylab films.

Earlier studies[8,9] of the Skylab film radiation hazard have been made. The present study concentrates on updating the geometric model and improving the computational techniques for estimating film fogging. Detailed spectral analyses are included for proton, electron, and bremsstrahlung components. Approximate damage estimates are included for the galactic cosmic radiation component.

A summary of the study and recommendations are given in Section 2. The radiation environment is discussed in Section 3. Film response to radiation is outlined in Section 4. The ATM film radiation analysis is detailed in Section 5. Radiation damage data to films stored in the OWS vault and at the T027 and S190 experiment locations is presented in Section 6. A preliminary analysis of the MSFC proton spectrometer experiment is given in Section 7.

2.0 SUMMARY AND RECOMMENDATIONS

The trapped proton environment is taken from the current Vette AP7 model.[21] The trapped electron environment is taken from the 1968 (projected) model.[21] A revised electron environment model is in preparation at the National Space Sciences Data Center, Goddard Space Flight Center, NASA, but is not yet available. The galactic cosmic radiation (GCR) dose rate estimates in the Skylab orbit are provided by Burrell and Wright.[3] These estimates are in good agreement with available flight measurements.

The geometry model of the Skylab cluster is revised and updated. The model of the film vaults, MDA, OWS, ATM, T027 experiment, and S190 experiment received particular attention.

The LSVDC4 space radiation transport program[10] is revised to include radiation damage response functions for trapped protons, trapped electrons, and bremsstrahlung. Damage response functions are not available for galactic cosmic radiation at this time. Fog estimates are given on the assumption that equal doses of GCR and trapped protons produce equal fogging.

Film damage estimates are developed for each of the 24 ATM cameras. Daily dose and fogging rates are given in each location, together with their totals. The eight NRL cameras are well below tolerance by factors ranging from 1.8 to 6. The load 1 cameras for the other four telescopes are below tolerance by factors ranging from 4 to 6. Of the remaining 12 cameras, six are slightly under tolerance by margins of 1 to 20 percent; five are over tolerance by margins of 4 to 25 percent; and one is over tolerance by 90 percent.

Dose rates and film damage estimates are developed at 11 magazine locations within the OWS vault. Dose rates, excluding the GCR component, range from 6.42 to 56.6 millirad per day (1 rad = .01 Joule/Kg).

Dose rates and film damage estimates are developed at the T027 boom-mounted camera and at a temporary location within the Scientific Airlock. No timeline is available to permit the estimation of total radiation fogging. A minimum value of 0.421 fog density is achieved by placing the magazines in the heavily shielded part of the OWS vault for 29 days. This value could rise to a value of two or higher depending upon the actual timeline.

Dose rate and film damage rate estimates are developed for three of the six S190 cameras in the operating location and at five storage locations in the OWS vault. Daily dose rates vary from 55 to 61 millirad per day in the MDA and from 6.42 to 9.40 millirad per day in the vault, exclusive of the 10 millirad per day GCR contribution.

A small effort is devoted to examining the behavior of the MSFC proton spectrometer. It is concluded that an eight month sample period will permit good corrections to the radiation environment model for the Skylab orbit. A two month sample period will permit corrections to be derived with a somewhat greater effort. A one week sample requires still greater effort plus favorable vehicle orientation during anomaly passes.

Recommendations for future work include:

- o Develop radiation damage estimates for other film-using experiments.

- o Refine the GCR primary and secondary estimates. Film damage functions should be developed for each component.

- o Develop a proton and electron monitoring technique using present on-board instrumentation. Data obtained in this manner would be used to update film damage estimates so that timely mission planning could be made.

- Provide additional shielding for the H-Alpha 1 cameras in the MDA vault. The removal of the load 4 NRL cameras which provided significant shielding has increased the radiation damage to these films to above-tolerance values.

- Add an electron shield to four sides of the boom-mounted T027 camera. A 1/32 inch lead, 0.15 inch aluminum shield may reduce the damage rate on the boom by a factor of three. The factor of ten uncertainty in the electron environment makes this action particularly important.

- Reassess the electron and bremsstrahlung hazard when the new electron environment models are issued by the National Space Sciences Data Center.

- Periodically test radiation sensitivity of Skylab film up to the procurement date.

3.0 RADIATION ENVIRONMENT

The Skylab cluster is assumed to be in a 440 km (235 n.m.), 50 degree circular orbit. The flight profile is assumed to include the last eight months of 1973, a period near solar minimum. Potentially damaging radiations for this mission include trapped protons, trapped electrons, and galactic cosmic radiation (GCR). Solar flux events, while unpredictable, should have minimal effect on the mission because of low probability of occurrence and partial shielding by the magnetosphere. No known appreciable sources of nuclear radiation are on-board. The three significant radiation components are discussed below.

3.1 Trapped Protons

The proton environment is calculated by M. O. Burrell and J. J. Wright[3] for the Skylab orbit from the Vette model environment AP7[21]. The average daily proton flux, differential in energy, is given in Table 3.1. The uncertainty in the proton environment is a factor of two. Recent measurements indicate that peak fluxes are within 20 percent of predicted values at the Skylab orbit.

The actual flux above 50 MeV varies somewhat from day to day, depending upon the particular orbit. During a typical six day interval, four daily fluxes are 90 percent of the average and two are 120 percent of the average as indicated in Table 3.2. Table 3.2 also shows that each daily flux arrives in 8 or 9 pulses as the orbit penetrates the South Atlantic magnetic anomaly. The small pulses last about 5 minutes and contain few high-energy protons. The largest pulses last 16 minutes with 90 percent of these protons incident during an 8 minute peak interval.

A graphical illustration of the Table 3.2 data is given in Figure 3.1. Here, pulses containing less than four percent of the average daily flux are omitted. It is apparent that 12 hours each day are free of trapped protons.

TABLE 3.1: AVERAGE PROTON SPECTRUM - $\frac{p}{cm^2 - MeV - Day}$

(235 n.m., 50 degrees)

E (MeV)	Flux
20	37000.
50	23000.
100	9700.
150	4800.
200	2200.
300	630.
400	170.
500	56.
600	15.
800	1.5

TABLE 3.2: PROTON PULSE DISTRIBUTION - PERCENT OF DAILY AVERAGE

Pulse/Day	1	2	3	4	5	6
1	13.8	22.4	28.2	18.2	25.6	13.1
2	.7	3.1	9.1	1.6	5.3	.6
3	.6	3.7	1.0	6.9	2.0	.6
4	10.9	24.3	15.7	27.4	20.6	11.3
5	28.2	20.8	27.9	15.0	24.8	28.4
6	10.7	2.0	5.8	1.4	3.0	10.0
7	1.3	2.3	1.4	3.2	1.8	1.3
8	4.3	11.4	6.1	15.7	8.5	4.4
9	20.0		24.9		28.1	20.6
Total	90.5	90.0	120.1	89.4	119.7	90.3

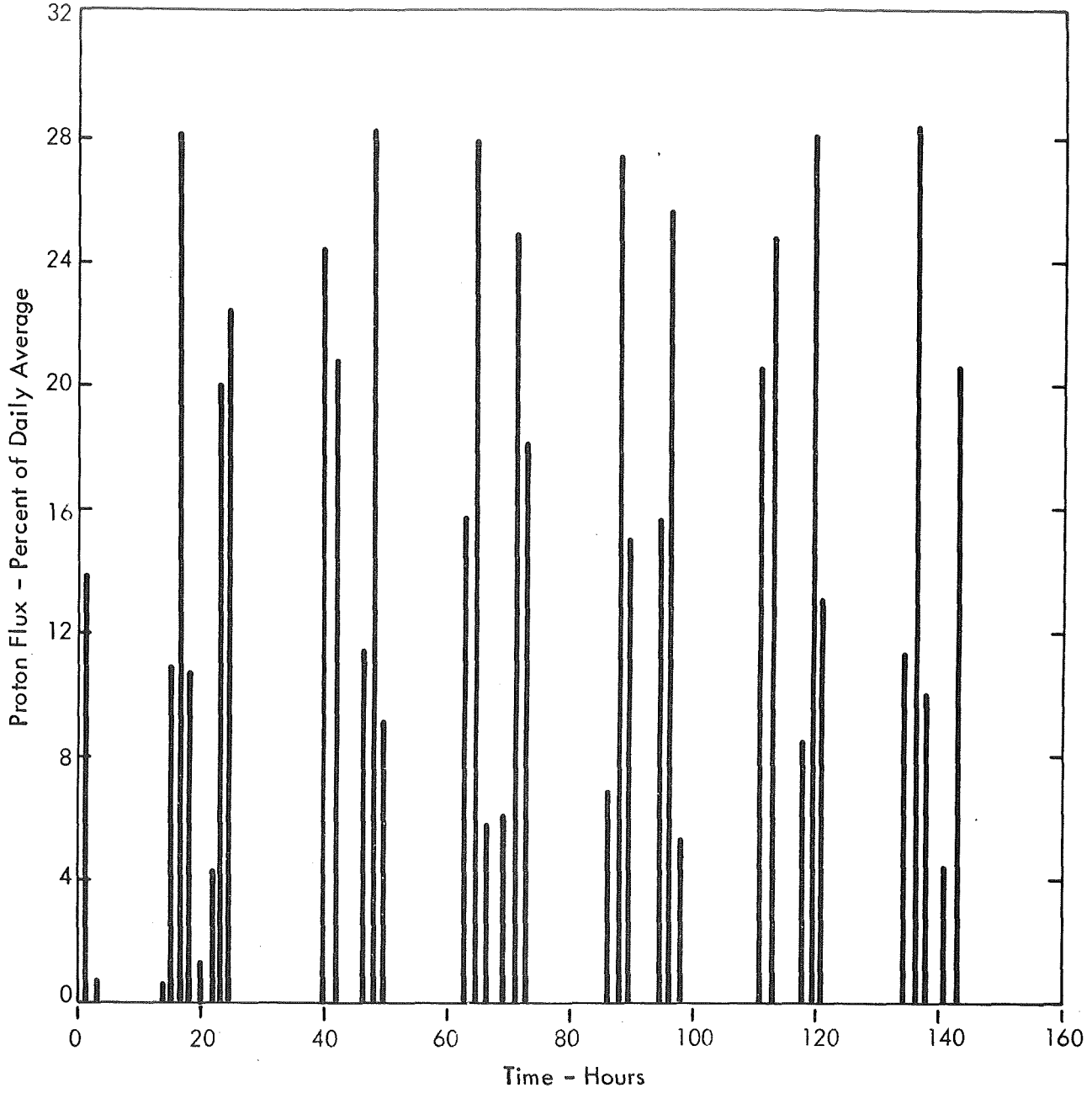

FIGURE 3.1: PROTON PULSE HISTORY

The temporal behavior of trapped protons is important for the proton spectrometer and for film-using experiments temporarily mounted in exposed locations. It has little significance for stored film.

3.2 Trapped Electrons

The electron environment is calculated by M. O. Burrell and J. J. Wright[3] for the Skylab orbit from the Vette model environment AE2 projected to 1968.[21] The average daily electron flux, differential in energy, is given in Table 3.3. Additional data and interpretation were provided by Drs. Mike Teague and Wayne Singley, Goddard Space Flight Center, NASA.

Approximately one-third of the trapped electron flux above 0.5 MeV is due to inner belt electrons. The other two-thirds arises from Skylab penetration of the "horns" of the outer belt. One-fourth of the flux is received in the northern hemisphere.

Electron flux is received during approximately 18 pulses per day, each pulse lasting a few minutes to half an hour. In the case of the longer pulses, almost all the electrons arrive during a ten minute peak interval. A plot of the 16 largest pulses and their percent of the total flux above 0.5 MeV is shown in Figure 3.2. A semilogarithmic plot is used in order to show the smaller pulses clearly. The very steep dose-depth relationship for these electrons may limit EVA activity during moderately small to large pulses.

The electron pulses of Figure 3.2 correlate with the proton pulses during the first 24 hours of Figure 3.1 because both computer runs started at zero latitude and longitude, and proceeded northeast initially.

TABLE 3.3: AVERAGE ELECTRON SPECTRUM - $\frac{e}{cm^2 - MeV - Day}$

(235 n.m., 50 degrees)

E(MeV)	Flux
.0001	2.9 + 11
.25	4.5 + 10
.5	1.0 + 10
1.0	1.2 + 9
1.5	3.5 + 8
2.0	1.1 + 8
4.0	2.5 + 6
6.5	2.9 + 5
10.0	7.0 + 4

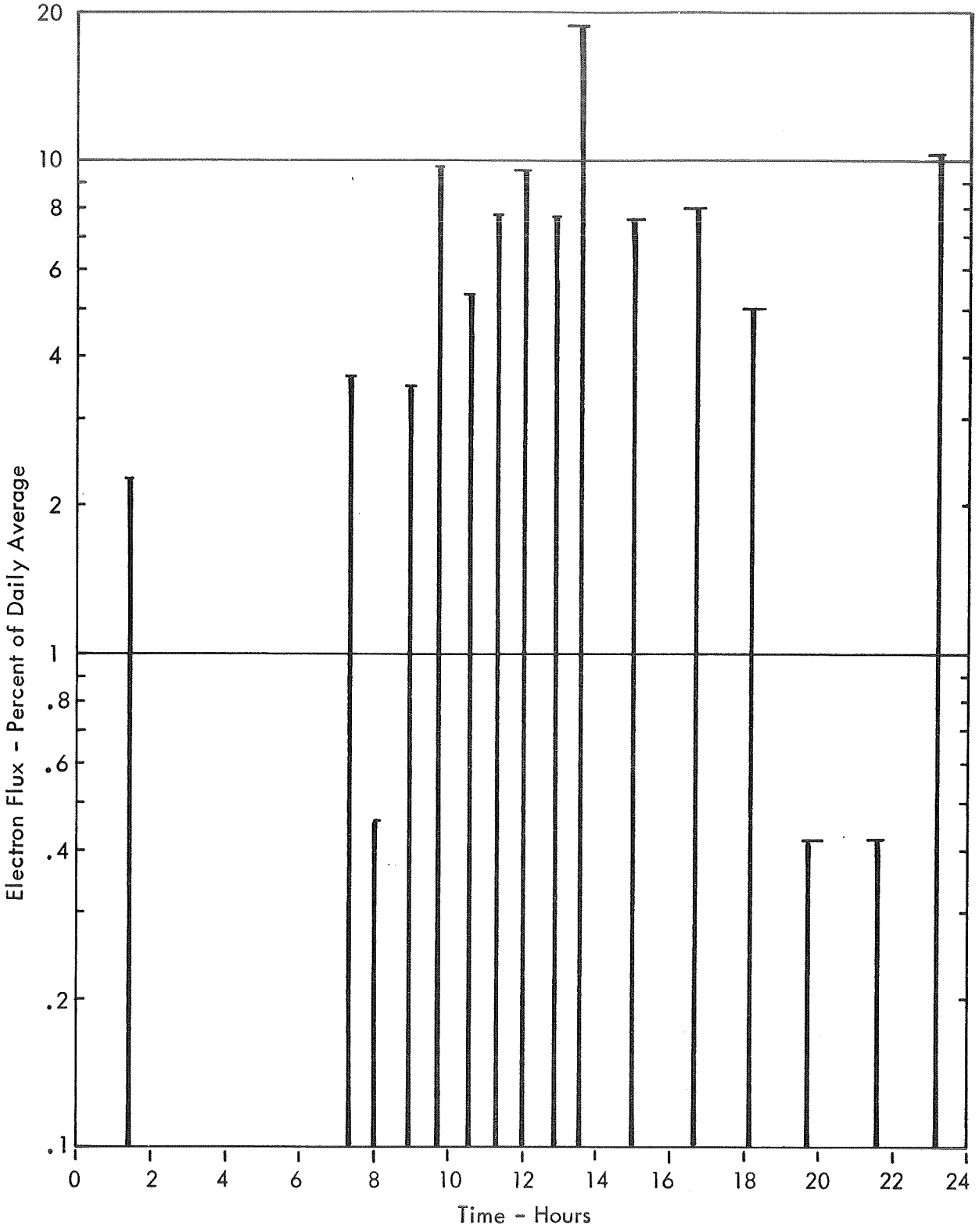

FIGURE 3.2: ELECTRON PULSE HISTORY

Caution should be used in interpreting electron and bremsstrahlung results based upon the 1968 electron model environment. A factor of ten uncertainty may be appropriate for the Skylab orbit. The original AE2 model is for 1964 near solar activity minimum. These data were projected to 1968, near solar activity maximum under the assumption that outer belt peak fluxes move inward during the maximum. Later studies have shown that solar maximum causes a filling of the slot between the belts rather than a movement of the peak. Further, only two sets of data near the region important to Skylab were available for the construction of the outer belt model. Neither set measured electrons below 0.5 MeV which are important for bremsstrahlung production because of the large flux below 0.5 MeV. The Skylab-orbit, outer-belt estimates are primarily extrapolations from higher altitudes.

A new electron model is being developed at the Goddard Space Flight Center, NASA. Revised model data are not available for the present study.

3.3 Galactic Cosmic Radiation (GCR)

GCR includes energetic charged particles such as protons, alphas, and other stripped nuclei with atomic numbers up to approximately $Z = 28$. The energy of these particles in interplanetary space near earth ranges from 10 MeV up to at least 10^{15} MeV. The low energy portion of the GCR is modulated by the solar activity cycle. The free space dose rate is reduced by a factor of about two at solar maximum compared to solar minimum due to the increased screening afforded by the extended solar magnetic field during disturbed solar conditions. The magnetosphere and shadowing effect of the earth also reduce GCR intensity in low, earth orbit.

M. O. Burrell and J. J. Wright have computer GCR dose rates at solar minimum within shielded enclosures.[3] Their computed values are usually within 20 percent of measured values for physical dose rates behind thin shields. The uncertainty is somewhat greater for thick shields. Table 3.4 shows their results in free space near the orbit of the earth about the sun. They treat 14 groups of atomic numbers. Certain approximations are invoked in treating nuclear collisions and secondary transport, but the results may be valid to a thickness as large as 20 gm/cm^2 aluminum or

TABLE 3.4: TOTAL GCR DOSE RATE - FREE SPACE - RAD TISSUE/YEAR

(Normalized to 4 $\frac{\text{Particles above 30 MeV}}{\text{cm}^2 - \text{sec}}$)

Shield Thickness - gm/cm^2	1	5	10	20	35	50	Relative Abundance
Z-Group							
1	4.78	4.73	4.68	4.57	4.40	4.24	.847
2	3.30	3.24	3.14	2.96	2.76	2.61	.1355
4	0.30	0.29	0.28	0.25	0.23	0.21	.00311
6	1.11	1.03	0.95	0.85	0.76	0.69	.00508
7	0.67	0.61	0.56	0.50	0.44	0.40	.00226
8	1.09	0.98	0.90	0.80	0.69	0.62	.00282
9	0.14	0.13	0.11	0.10	0.09	0.08	.00028
10	0.51	0.45	0.41	0.36	0.31	0.27	.00085
11	0.39	0.35	0.31	0.27	0.23	0.20	.00054
12	0.77	0.67	0.60	0.52	0.44	0.38	.00090
13	0.18	0.15	0.14	0.12	0.10	0.09	.00017
14	0.39	0.34	0.30	0.26	0.21	0.18	.00034
18	0.69	0.58	0.51	0.43	0.35	0.28	.00037
25	2.81	2.31	1.99	1.61	1.23	0.98	.00079
Total	17.13	15.86	14.88	13.60	12.24	11.23	1.00001

greater. For the sake of completeness, equivalent biological dose rates using recommended quality factors are shown in Table 3.5. However, the proper quality factors to use are highly controversial and other assumptions may lead to rem dose rates that are a factor of two lower.

Of more interest to the Skylab mission, Table 3.6 shows GCR dose rates for a 250 n.m., 50 degree orbit. The daily dose rate ranges from 11.6 mrad/day behind 1 gm/cm^2 to 9.6 mrad/day behind 50 gm/cm^2 aluminum. A value of about 8 to 10 mrad/day is probably correct to use in the present study because the mission will take place slightly before solar minimum. The rad-tissue unit is about 10 percent higher than the rad-air unit.

Biological dose rates for the above orbit are approximately 50 to 60 mrem/day (an effective quality factor of 6 is assumed), though more detailed calculations should be made.

TABLE 3.5: TOTAL GCR BIOLOGICAL DOSE RATE - FREE SPACE - REM/YEAR

(Normalized to 4 $\frac{\text{Particles above 30 MeV}}{\text{cm}^2 - \text{sec}}$)

Shield Thickness - gm/cm^2	1	5	10	20	35	50
Z-Group						
1	4.06	4.01	3.96	3.86	3.71	3.58
2	3.68	3.60	3.43	3.17	2.91	2.72
4	0.65	0.59	0.54	0.47	0.42	0.38
6	4.02	3.50	3.08	2.61	2.23	1.97
7	3.02	2.57	2.25	1.88	1.59	1.41
8	5.97	4.99	4.33	3.60	3.02	2.66
9	0.89	0.75	0.65	0.54	0.45	0.40
10	3.77	3.16	2.73	2.25	1.87	1.63
11	3.28	2.74	2.37	1.98	1.64	1.42
12	7.16	5.91	5.10	4.22	3.49	3.00
13	1.83	1.51	1.31	1.08	0.89	0.77
14	4.43	3.64	3.14	2.59	2.12	1.78
18	9.86	8.03	6.89	5.64	4.52	3.66
25	51.95	42.13	36.07	29.02	22.02	17.45
Total	104.57	87.13	75.85	62.91	50.88	42.83

TABLE 3.6: TOTAL GCR DOSE RATE - 250 N M, 50 DEGREES - RAD TISSUE/YEAR

(Normalized to 4 $\frac{\text{Particles above 30 MeV}}{\text{cm}^2 - \text{sec}}$)

Shield Thickness - gm/cm^2	1	5	10	20	35	50
Z-Group						
1	0.44	0.44	0.44	0.45	0.45	0.45
2	0.97	0.98	0.97	0.97	0.96	0.94
4	0.09	0.09	0.09	0.09	0.09	0.08
6	0.33	0.33	0.32	0.32	0.30	0.29
7	0.20	0.20	0.20	0.19	0.18	0.17
8	0.32	0.32	0.32	0.31	0.29	0.28
9	0.04	0.04	0.04	0.04	0.04	0.04
10	0.15	0.15	0.15	0.14	0.13	0.13
11	0.12	0.12	0.11	0.11	0.10	0.10
12	0.23	0.23	0.22	0.21	0.20	0.18
13	0.05	0.05	0.05	0.05	0.05	0.04
14	0.12	0.12	0.11	0.11	0.10	0.09
18	0.21	0.21	0.20	0.19	0.17	0.15
25	0.88	0.85	0.81	0.74	0.63	0.55
Total	4.15	4.13	4.03	3.92	3.69	3.49

4.0 RESPONSE OF PHOTOGRAPHIC FILM TO SPACE RADIATION

Radiations encountered in the Skylab orbit deposit energy locally in photographic emulsions, activating a fraction of the silver halide grains. Partial explanations of the mechanisms involved may be obtained from the literature.[5] The effect is termed radiation fogging or radiation darkening.

In the case of black and white film, the result of radiation damage is a darkening measured in terms of change in optical density of the developed film. Optical density is defined as the logarithm of the reciprocal of transmittance.

In the case of color films proposed for Skylab, a color reversal process is used so that increasing exposure results in decreasing density. For this reason the net density change is quoted in this report without reference to sign. Net density changes for color films are quoted for the visible spectral region (white light), plus red, green, and blue regions. Differing responses to space radiation in the various dye layers may cause loss of color fidelity.

Radiation-induced fogging of photographic film is dependent upon several factors including type of emulsion, type of radiation, quality of radiation, and quantity of radiation. In order to account for these factors, the LSVDC4 dose code[10] was modified to compute and tabulate the flux spectra arriving at the detector for proton, alpha, electron, and bremsstrahlung radiations. These spectra are weighted by energy-dependent response functions for 13 black and white films plus 5 color films in 4 spectral regions, then integrated over energy to yield net fogging density.

The films investigated in the present study are listed in Table 4.1. Multiple entries under the "Film Type" heading usually imply that similar emulsions are coated on different backing materials or thicknesses; or that the gel overcoat is changed. The "Inverse Sensitivity" values give a measure of the 1.25 MeV gamma ray dose

TABLE 4.1: KODAK FILMS INCLUDED IN STUDY

Film Type	Inverse Sensitivity* - Rad(Air)/0.2 Net Density				Reference
	Visible	Red	Green	Blue	
So-166, 2485	.12				12
No-Screen	.13				12
103-0 u.v.	.60				12
SC-5	.74				12
Plus-X, 3401	.90				12
Pan-X, 3400, SO-114, SO-212, 026-02	4.5				12
SWR, 104-06	12.0**				12, 17
SO-375	17.5				12
SO-392, SO-101	5.6				17
2403, 3403	.20				17
103 a-f	.80				17
SO-246	.80				17
IN-Spectroscopic	6.0				17
SO-168 (Color)	.30	.25	.42	.50	17
5242 (Color)	.73	1.15	1.1	.60	17
SO-368 (Color)	.80	1.2	1.4	1.8	17
SO-180 (Color)	.85	.70	2.2	1.8	17
SO-121 (Color)	1.2	1.7	2.4	3.5	17

* Cobalt - 60 rads (air) required for 0.2 net density change

** Recent tests indicate a value of 36 rads(air)/0.2 net density change

required to achieve a net fogging density of 0.2. The dose versus density relationship is generally linear for densities less than 0.6. It should be noted that curve smoothing or different experimental values may alter inverse sensitivity by 20-30 percent. Such anomalies have been observed for SO-166, No-Screen, and Pan-X. Evidently the composition of SWR emulsion has changed between 1967 and 1970 because the inverse sensitivity is now larger by a factor of three.

Kodak film 101-01 (101-06) is not included in Table 4.1 because early studies gave anomalous results, probably due to an easily damaged emulsion surface. The Adams data show that 101-01 fogging is about 20 percent greater than Pan-X fogging.

Experimental film fogging data from several sources is available.[1,12,13,16,17,18,22] Several evaluations of the data have been made.[11,15] The techniques used to derive response functions from experimental data are outlined below.

4.1 Proton Response Functions

The density versus dose curve for one film is shown in Figure 4.1. Damage response functions are derived from such data. The damage response functions for protons on eight film types are shown in Figure 4.2. These data are taken from a Kodak-MSFC-Langley study.[12] The values at 10, 17.6, 50, 90, and 130 MeV are derived from proton accelerator experiments. The values at 450 MeV are taken from cobalt-60 tests. This equivalence is suggested by the work of Cormack and Johns[4] who showed that the mean LET (linear energy transfer) of the Compton electrons produced in water by cobalt-60 gamma rays is 1.4 times the LET of a minimum ionizing singly charged particle. Thus it is expected that the sensitivity of film to cobalt-60 gamma rays is similar to the sensitivity to 450 MeV protons whose LET is also 1.4 times the LET for minimum ionizing protons. A further extension to 2500 MeV is made on the basis of relative LET to minimum LET which occurs at 2500 MeV for protons in air. Trapped protons possess energies less than 2500 MeV.

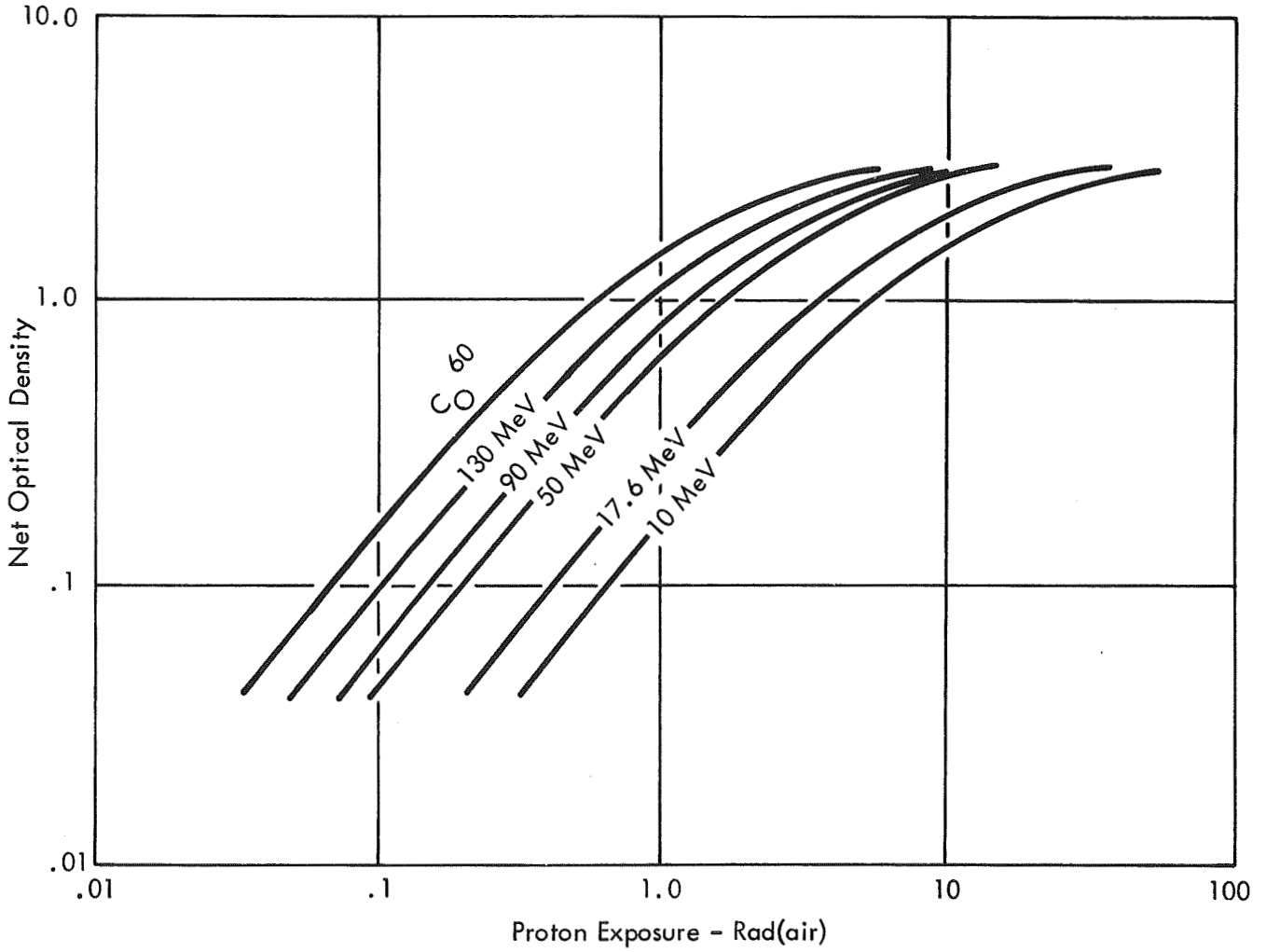

FIGURE 4.1: RADIATION RESPONSE OF FILM TYPE SO-166

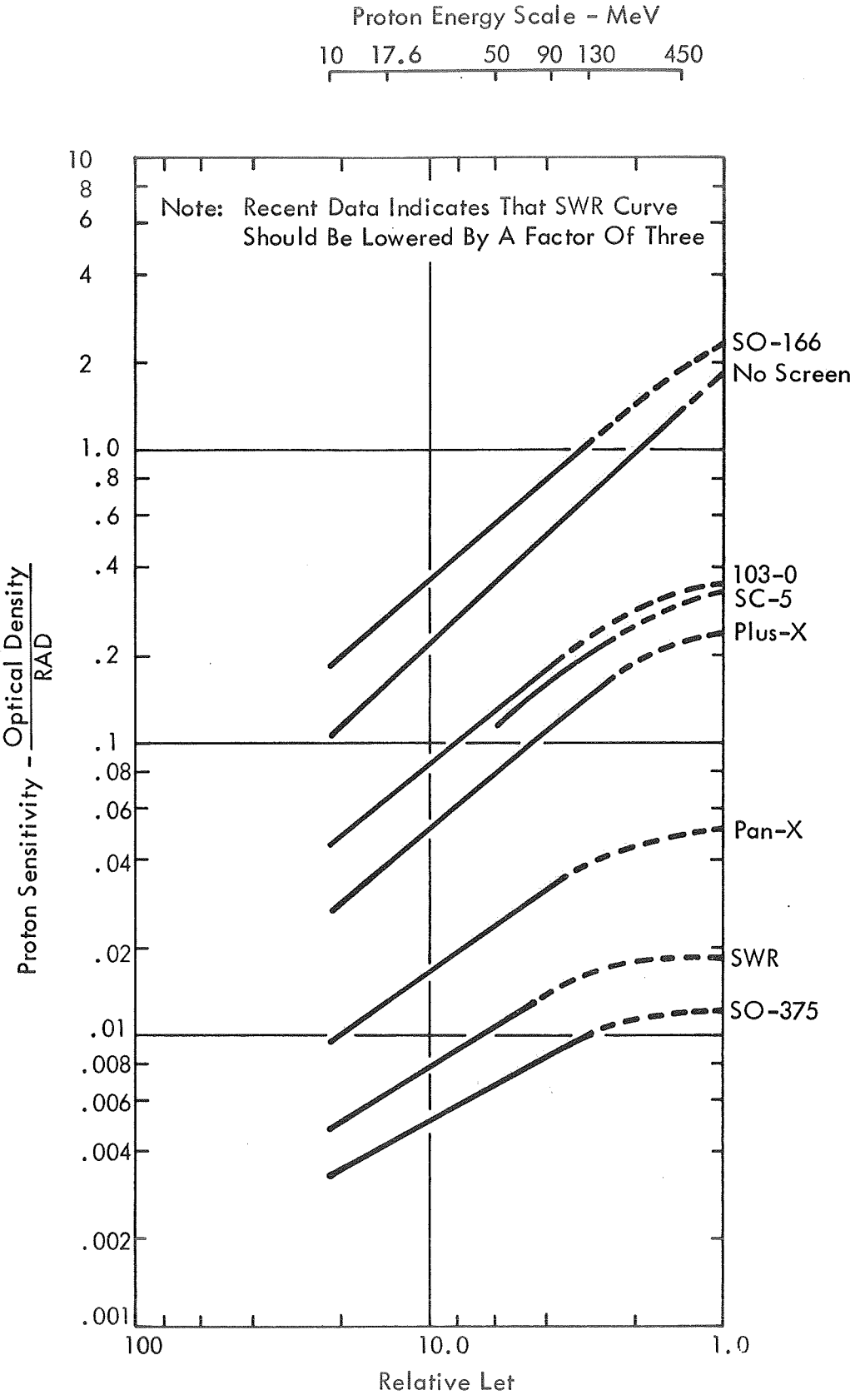

FIGURE 4.2: PROTON SENSITIVITY OF EIGHT FILMS

The damage response function for Kodak film SO-166 versus proton energy is shown in Figure 4.3. Damage response functions for films not included in Figure 4.2 are interpolated according to sensitivity to cobalt-60 radiation.

4.2 Alpha Response Functions

Radiation fogging induced by alpha (helium nuclei) are not computed explicitly in this study. Alpha radiation is an insignificant component of the trapped radiation belts and is ignored. Cosmic radiation damage (including alphas) is discussed in Section 4.5 below. However, the capability of treating alphas is included in the dose code. Damage response functions for alphas are derived from those for protons on a relative LET basis. Figure 4.3 includes an alpha energy scale so that values of the alpha response function may be read directly from the figure for SO-166.

4.3 Electron Response Functions

Experimental data showing the electron-induced fogging density as a function of energy are not available for the films of interest to Skylab. In general, sensitivity has been found to increase with increasing electron energy up to approximately 1 MeV which is the energy of a minimum ionizing electron in air.[5] Above 1 MeV the sensitivity remains approximately constant.[19,20]

The interaction of electrons with emulsion is by direct ionization and secondary ionization caused by electron-produced delta rays (secondary electrons). Below minimum ionization, the effect is similar to the ionizing effect of protons. Electron damage response functions are derived from proton damage response functions on a relative LET basis. Figure 4.3 includes an electron energy scale so that values of the electron response function may be read directly from the figure for SO-166.

It is claimed that the fogging density per unit dose for 1 MeV gamma rays is equal to the fogging density per unit dose for 1 MeV electrons.[19] Therefore, the value

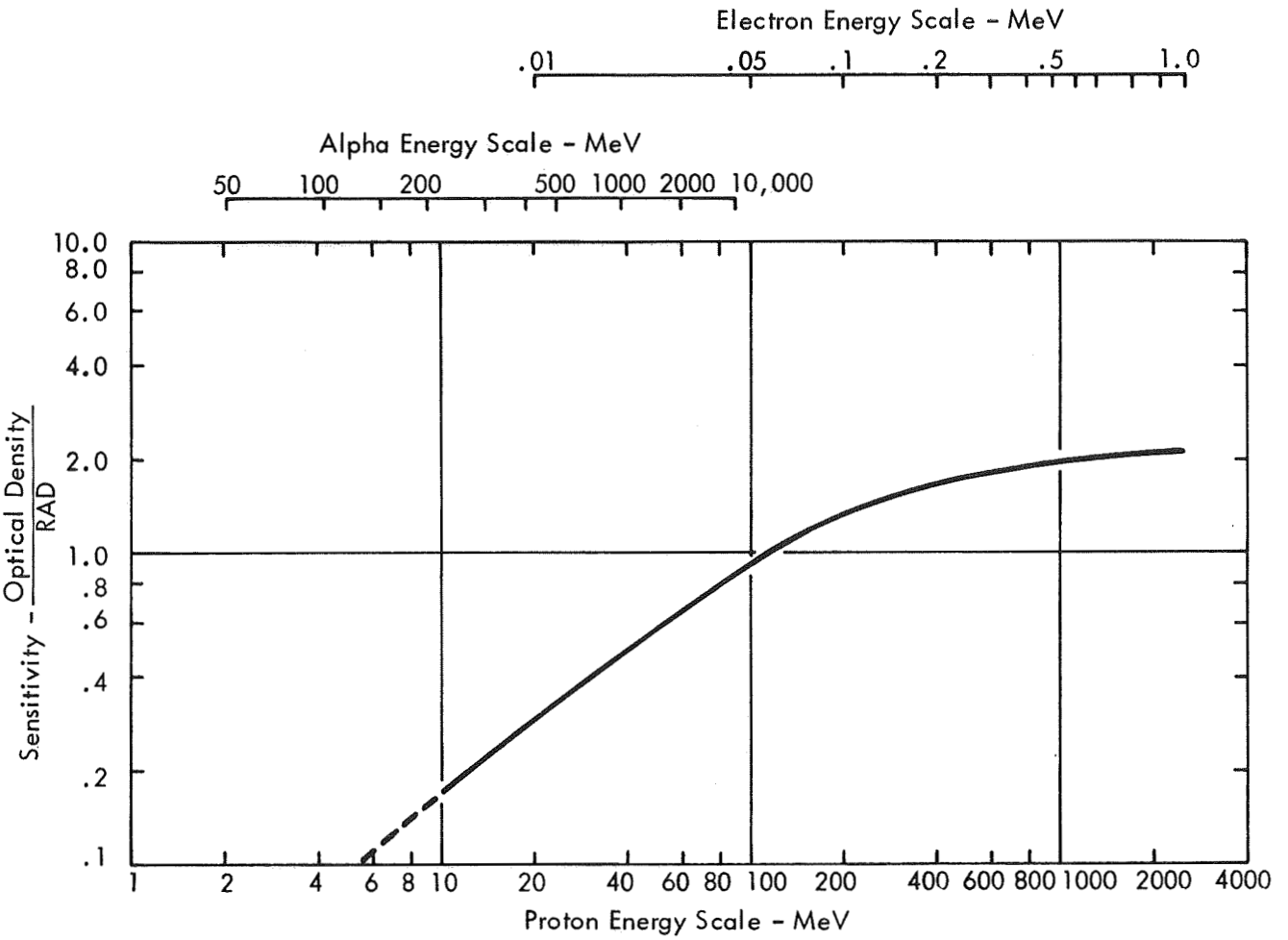

FIGURE 4.3: RADIATION SENSITIVITY OF FILM TYPE SO-166

of the damage response function for electrons at minimum LET should equal that due to cobalt-60 gamma rays. The present study uses values larger by 5 to 10 percent. The slight discrepancy is not significant herein.

4.4 Bremsstrahlung Response Functions

The fogging induced by photons (bremsstrahlung, x-rays, and gamma rays) is caused by the secondary electrons produced in collisions. For photon energies between 1 and 10 MeV, the response function is essentially constant and similar to the response function for minimum ionizing electrons. However, for photons below 1 MeV the response function is strongly peaked due to the K absorption edges of the silver halide grains.

Experimental data showing the photon-induced fogging density as a function of energy are not available for the films of interest to Skylab. The only such data available for Skylab films are for the effect of cobalt-60 gamma rays at 1.25 MeV. These data are used as normalizing points.

At lower energies the relative sensitivity of Ilford Line Film as determined by Greening[6] is used. Figure 4.4 shows the resulting damage response function for Kodak film SO-166. For this film the peak-to-minimum ratio is about 50. For slow films the peak-to-minimum ratio should be reduced to 25 or 30.[12] The SWR-type film bremsstrahlung damage estimates may be high by 3 to 30 percent for this reason. Other studies[13] on moderate speed and fast films confirm the Greening data.

4.5 GCR Response Functions

GCR offers a difficult problem in estimating film damage. It contributes about 10 millirad per day throughout the cluster according to the results of Burrell and Wright (Section 3.3). The proton component is more damaging than trapped protons for

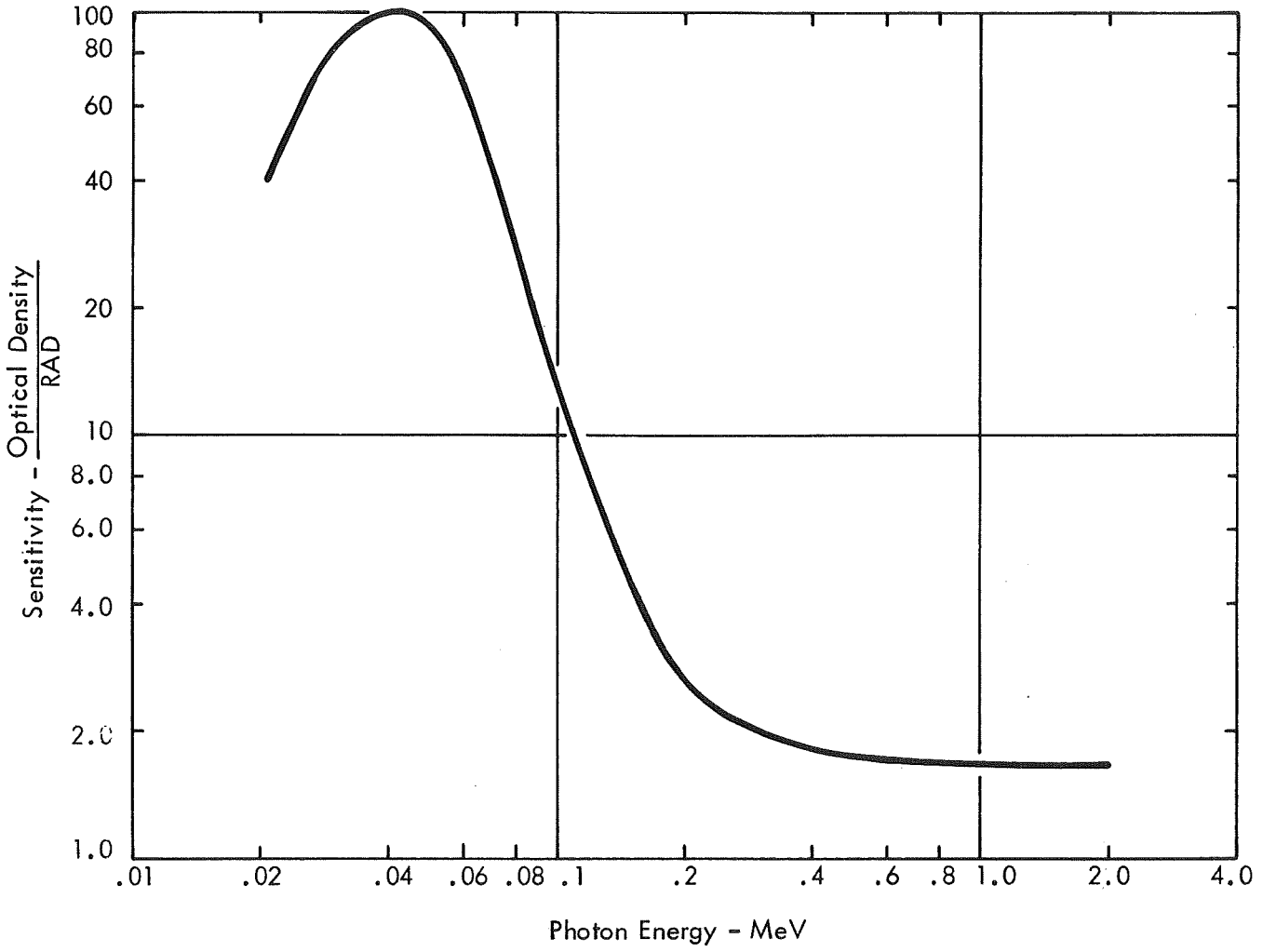

FIGURE 4.4: BREMSSTRAHLUNG SENSITIVITY OF FILM TYPE SO-166

equal doses because the spectrum is harder. The primary alpha and heavier components are probably less damaging per unit dose than trapped protons as evidenced by Figure 4.3. However, these radiations produce intense showers of secondaries which are usually more damaging to film than the primaries.

In this effort, GCR is assumed to cause the same fogging per unit dose as trapped protons do to films contained in the vaults.

5.0 ATM FILM RADIATION DAMAGE ANALYSIS

Estimates of radiation dose and radiation-induced film fogging are given for each of the 24 ATM cameras aboard the Skylab cluster. The damaging radiation components treated include trapped protons, trapped electrons, electron-produced bremsstrahlung, and galactic cosmic radiation (GCR).

Radiation transport calculations are performed for each camera in each storage and operational location in the Skylab cluster. Provision is made for the presence or absence of other nearby components over the course of the eight month flight. These results are folded together according to the ATM camera timeline of Table 5.1 in order to arrive at total radiation-induced film fogging.[14]

The arrangement of cameras in the four vaults is shown in Figures 5.1 through 5.4.[2] One detector position is chosen within the film of each camera in what is estimated to be the most exposed location. The Arabic numeral on each camera indicates load number. The letters indicate the six film-using ATM experiments; HAO, H-ALPHA 1, GSFC, AS&E, NRL-A, and NRL-B. Load 1 cameras are not shown in the vaults; they are launched in place on the ATM. The two load 4 NRL cameras are not shown because they will be resupplied by SL-4.

The return arrangement of cameras in the CSM was not available at the time computer runs were made. The assumed locations are shown in Figure 5.5. Note that mutual shielding is minimal.

The arrangement of telescopes on the ATM is shown in Figure 5.6. This scheme represents a 90 degree rotation of the equilibrium position from a previous study. Cameras are placed in the appropriate locations. The two NRL cameras are in relatively exposed places near the sun end of the ATM.

TABLE 5.1: ATM EXPERIMENT FILM LOCATION HISTORY

Item	Time Period Days	ATM Load	MDA Load	CM Load
Prelaunch	0 - 30	1	2, 3, 4	
SL 2 Manned Operation	30 - 58	1	2, 3, 4	
Return	58 - 61			1
Unmanned Operation	58 - 120	S052 & S054 2	2, 3, 4	
SL 3 Manned Operation	120 - 148	(All) 2	3, 4	2
	148 - 176	3 (All)	4	
Return	176 - 179			2, 3
Unmanned Operation	176 - 210	S052 & S054 4	4	
SL4 Manned Operation	210 - 266	(All) 4		
Return	266 - 269			4

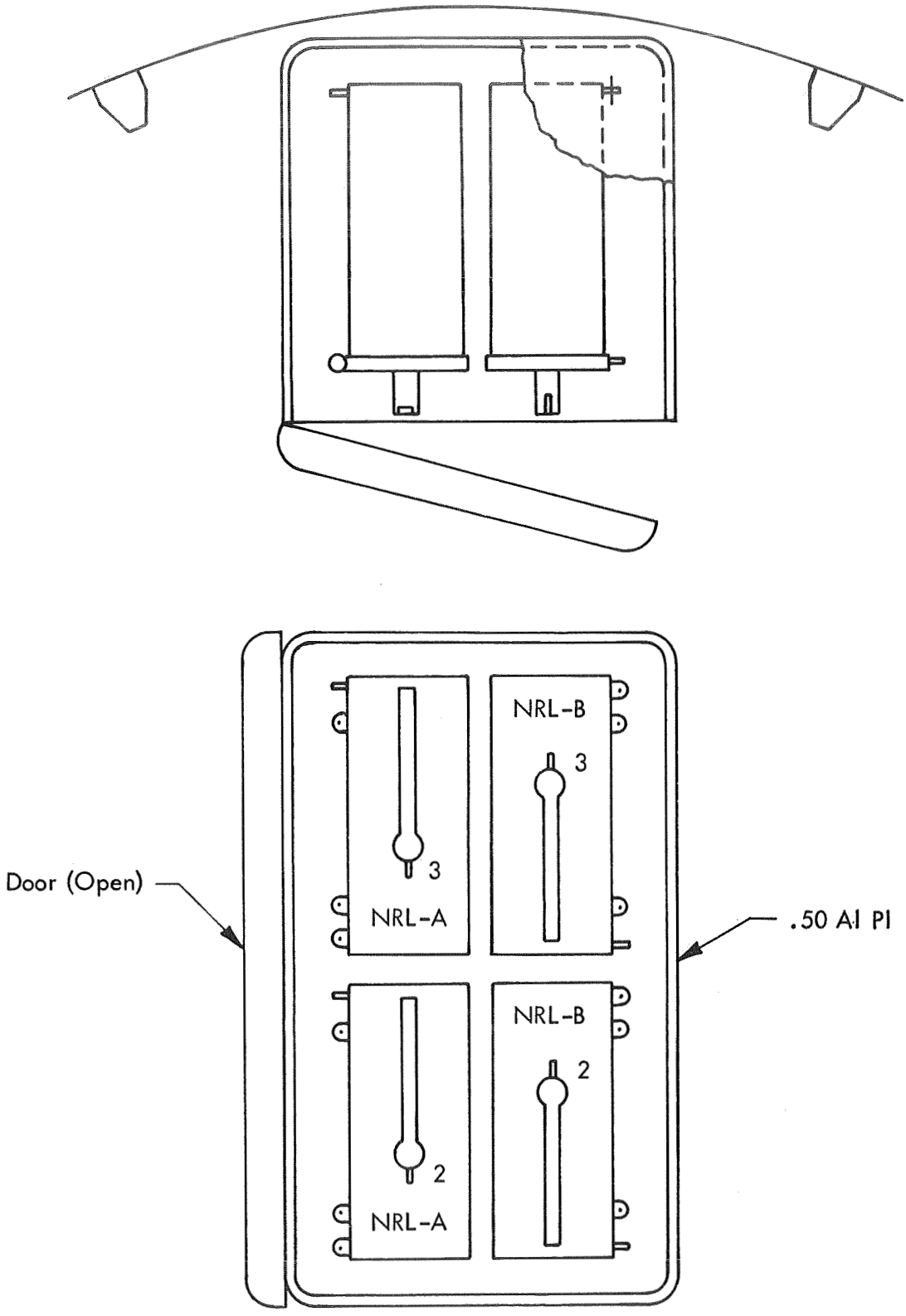

Outside Dimensions: 24.5 W x 26.8 D x 43.0 H

FIGURE 5.1: FILM VAULT NO. 1

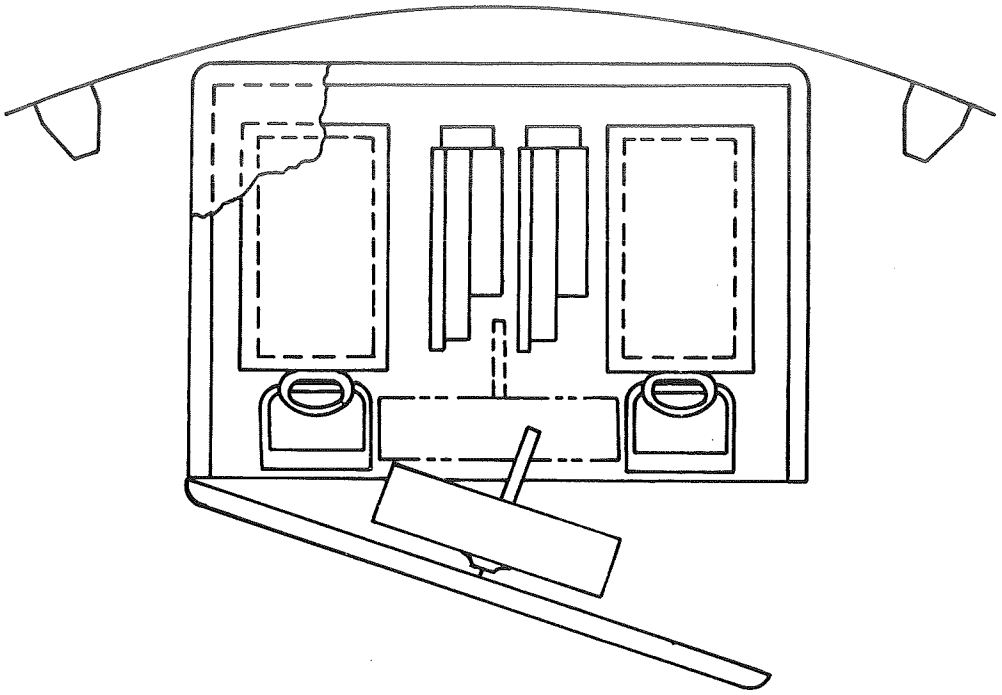

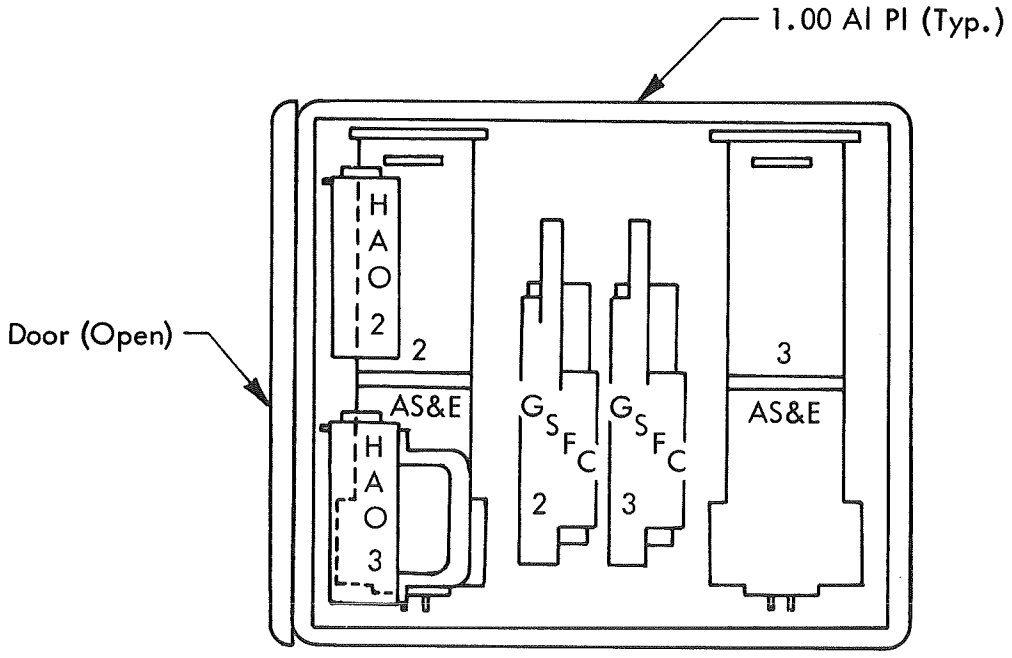

Outside Dimension: 32W x 23D x 29H

FIGURE 5.2: FILM VAULT NO. 2

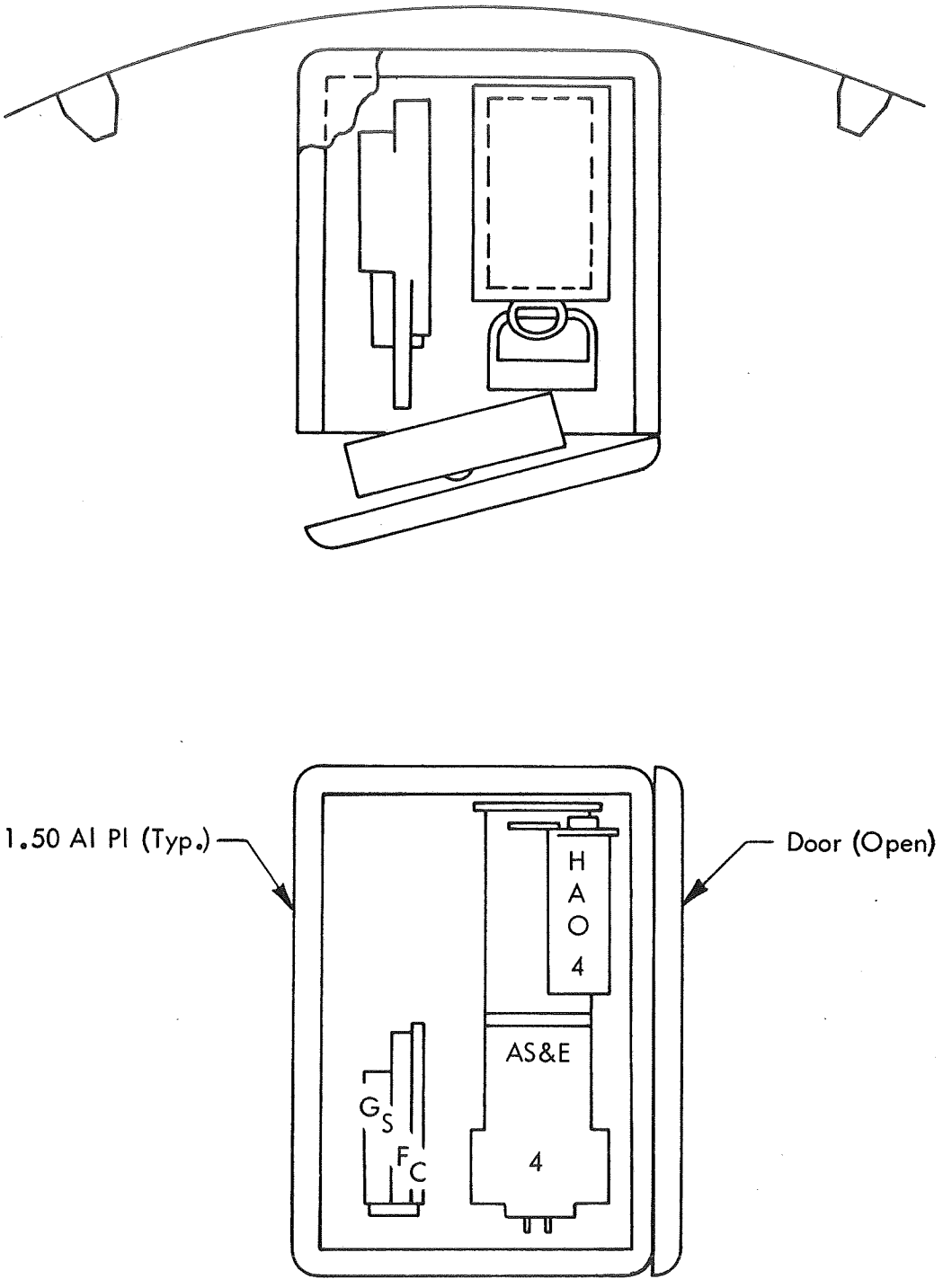

Outside Dimension: 21W x 24D x 30H

FIGURE 5.3: FILM VAULT NO. 3

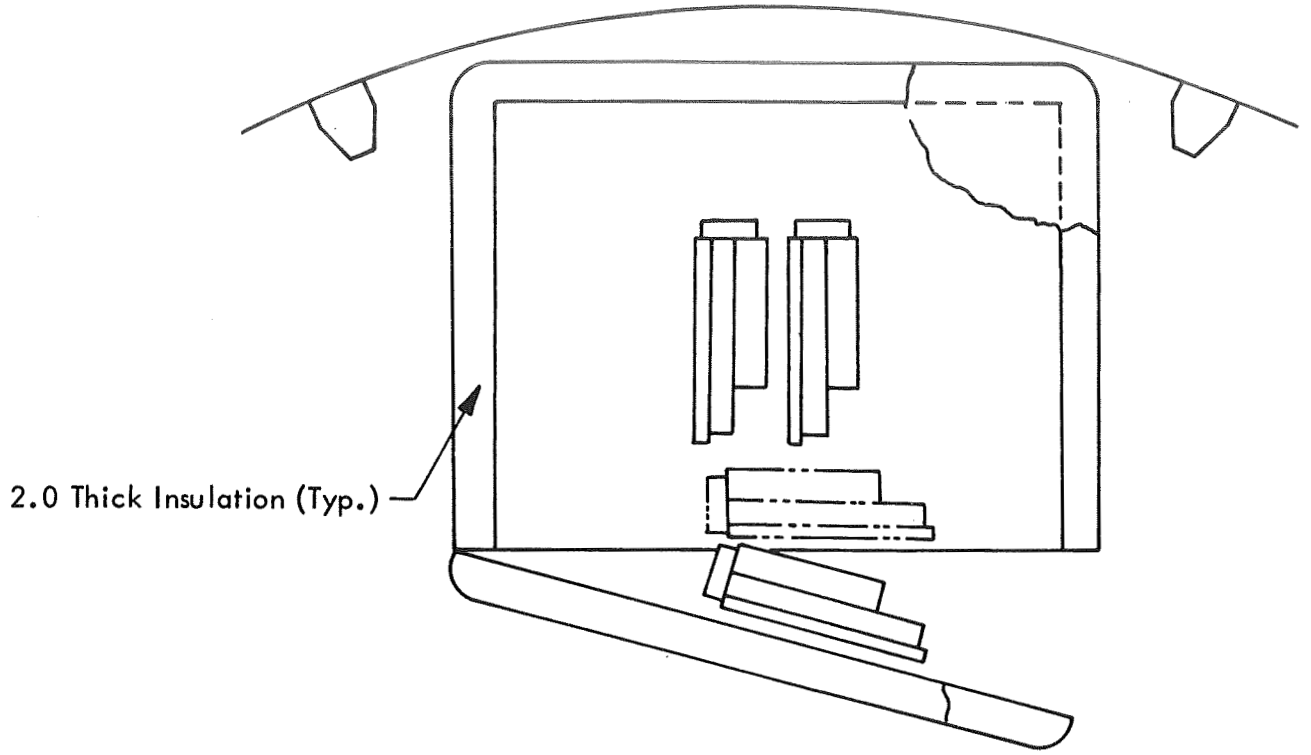

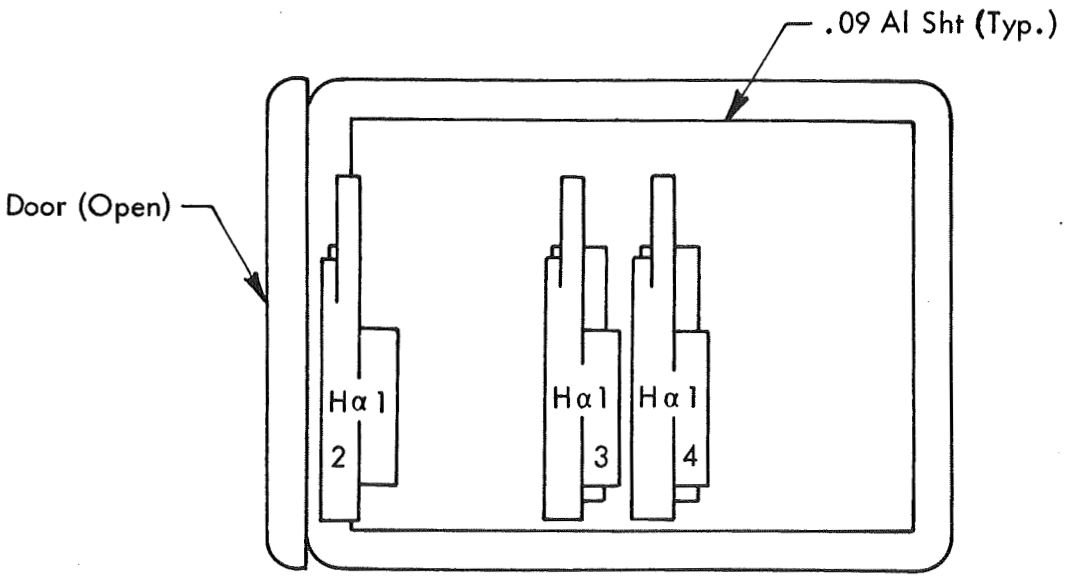

Outside Dimensions: 33.5 W x 28.0 D x 26.0 H

FIGURE 5.4: FILM VAULT NO. 4

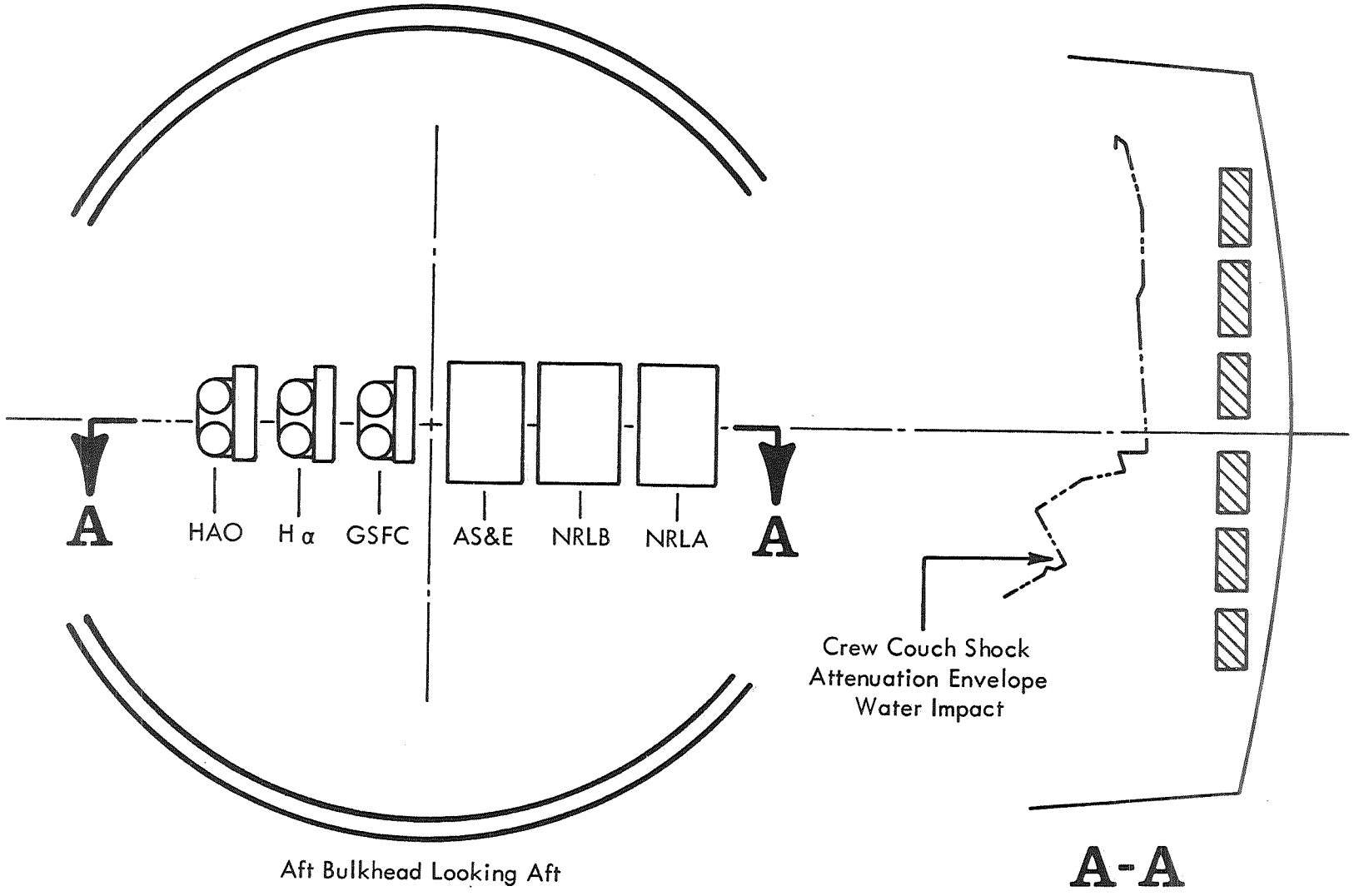

FIGURE 5.5: CM CAMERA STOWAGE

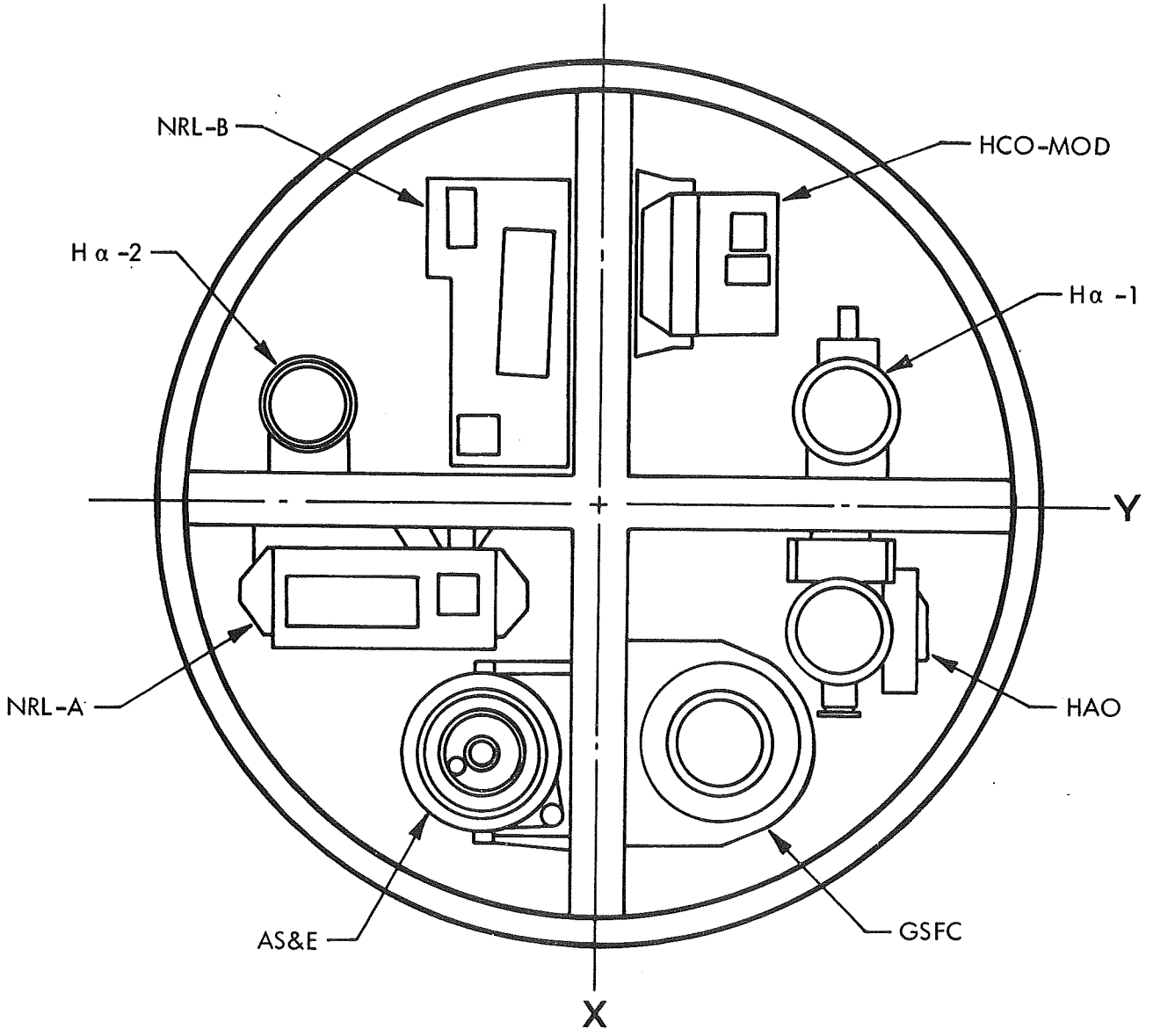

FIGURE 5.6: ATM CANISTER (SUN END)

The HAO film is Kodak 026-02 which shows the same radiation sensitivity as Kodak Pan-X 3400. The ASE film is Kodak Pan-X 3400. The GSFC film is labeled Kodak SO-212, but the emulsion and radiation response are identical to Pan-X. The H-ALPHA 1 film is Kodak SO-101 which is similar to Kodak SO-392 except for a thinner backing material. Both NRL films are Kodak 104-06 which has a radiation response identical to Kodak SWR film. As explained in Section 4, all SWR fogging results have been reduced by a factor of 3 to reflect Martin-Marietta[17] (June, 1970) and Kodak[12] (October, 1970) tests on the current product.

5.1 Dose Rates to ATM Film

The daily dose rate to each ATM film is given in Table 5.2. The GCR component, 10 mrad/day, should be added to each value as indicated in the table. A constant value is used for GCR because the data of Section 3 indicate only a 16 percent reduction within a 50 gm/cm^2 shield as compared with 1 gm/cm^2 shield. The "day" numbers at the top of each column refer to the timeline days in Table 5.1, from which camera location may be obtained. The daily dose rates range from 30 to 110 mrad/day depending upon camera type and location. During the actual mission, the cameras will be removed from the ATM to the CSM several days before that indicated in Table 5.1. This procedure will result in lower dose and film damage than indicated for each camera. Appropriate adjustments may be made with the aid of the data in Table 5.2.

The daily radiation fogging rate to each ATM film is given in Table 5.3. Again, the GCR component is listed separately and should be added to other values. The approximate range of fogging values is from 1.2×10^{-4} to 1.7×10^{-3} per day.

The relative importance of each radiation component-trapped protons, trapped electrons, bremsstrahlung, and GCR-may be estimated from the values of Table 5.4. Here, the percent of total dose rate and fogging rate, by component, is shown for

TABLE 5.2 DAILY DOSE RATE WITHOUT GCR - MRAD/DAY

	Load 1		Load 2				Load 3				
	30-58	58-61	30-58	58-120	120-148	148-179	30-58	58-120	120-148	148-176	176-179
HAO, 026-02	47.1	23.0	28.5	47.2	47.1	23.0	26.3	29.0	29.0	47.1	23.0
ASE, Pan-X	35.5	26.3	27.5	35.5	35.5	26.3	27.0	28.3	28.3	35.5	26.3
GSFC, SO-114	45.0	28.8	26.4	26.4	45.0	28.8	24.8	26.5	26.5	45.0	28.8
H-ALPHA 1, SO-101	45.8	27.9	66.2	66.2	45.8	27.9	66.3	66.3	67.1	45.8	27.9
NRL-A, 104-06	98.7	34.5	21.9	21.9	98.7	34.5	22.2	22.2	22.5	98.7	34.5
NRL-B, 104-06	66.1	28.8	22.6	22.6	66.1	28.8	23.6	23.6	23.6	66.1	28.8

	Load 4						GCR - All Loads
	30-120	120-148	148-176	176-210	210-266	266-269	
HAO, 026-02	21.2	21.2	21.3	47.2	47.1	23.0	10.
ASE, Pan-X	20.3	20.3	20.3	35.5	35.5	26.3	10.
GSFC, SO-114	22.5	22.5	22.6	22.6	45.0	28.8	10.
H-ALPHA 1, SO-101	67.2	68.0	70.5	70.5	45.8	27.9	10.
NRL-A, 104-06					98.7	34.5	10.
NRL-B, 104-06					66.1	28.8	10.

TABLE 5.3: DAILY FILM FOGGING RATE WITHOUT GCR - DAY^{-1}

	Load 1		Load 2				Load 3				
	30-58	58-61	30-58	58-120	120-148	148-179	30-58	58-120	120-148	148-176	176-179
HAO, 026-02	1.29-3	6.39-4	7.92-4	1.30-3	1.29-3	6.39-4	7.36-4	8.07-4	8.07-4	1.29-3	6.39-4
ASE, Pan-X	9.67-4	7.33-4	7.66-4	9.67-4	9.67-4	7.33-4	7.56-4	7.91-4	7.91-4	9.67-4	7.33-4
GSFC, SO-114	1.23-3	8.04-4	7.37-4	7.37-4	1.23-3	8.04-4	6.94-4	7.41-4	7.41-4	1.23-3	8.04-4
H-ALPHA 1, SO-101	1.01-3	6.11-4	1.45-3	1.45-3	1.01-3	6.11-4	1.45-3	1.45-3	1.47-3	1.01-3	6.11-4
NRL-A, 104-06	3.70-4	1.34-4	8.53-5	8.53-5	3.70-4	1.34-4	8.70-5	8.70-5	8.80-5	3.70-4	1.34-4
NRL-B, 104-06	2.48-4	1.12-4	8.77-5	8.77-5	2.48-4	1.12-4	9.17-5	9.17-5	9.17-5	2.48-4	1.12-4

	Load 4						GCR - All Loads
	30-120	120-148	148-176	176-210	210-266	266-269	
HAO, 026-02	5.97-4	5.97-4	5.98-4	1.30-3	1.29-3	6.39-4	2.79-4
ASE, PAN-X	5.69-4	5.69-4	5.70-4	9.67-4	9.67-4	7.33-4	2.79-4
GSFC, SO-114	6.28-4	6.28-4	6.30-4	6.30-4	1.23-3	8.04-4	2.79-4
H-ALPHA 1, SO-101	1.47-3	1.48-3	1.54-3	1.54-3	1.01-3	6.11-4	2.19-4
NRL-A, 104-06					3.70-4	1.34-4	3.89-5
NRL-B, 104-06					2.48-4	1.12-4	3.89-5

TABLE 5.4: PERCENT OF DAILY DOSE AND FOGGING BY COMPONENT - ATM

Dose	p	e	Brem	GCR
HAO	80.6	0.9	0.9	17.5
ASE	77.1	0.1	0.8	22.0
GSFC	80.7	0.1	0.9	18.2
H-ALPHA 1	81.0	0.1	0.9	17.9
NRL-A	85.4	4.4	1.0	9.2
NRL-B	82.4	3.6	0.9	13.1
Fogging				
HAO	72.7	1.6	8.0	17.8
ASE	73.0	0.2	4.5	22.4
GSFC	74.2	0.2	7.2	18.5
H-ALPHA 1	76.6	0.2	5.5	17.8
NRL-A	74.3	6.9	8.9	9.5
NRL-B	73.8	5.5	7.1	13.5

TABLE 5.4: PERCENT OF TOTAL DOSE AND FOGGING BY COMPONENT - LOAD 2, MDA VAULTS

Dose	p	e	Brem	GCR
HAO	73.2	0.	0.7	26.1
ASE	72.5	0.	0.7	26.7
GSFC	71.7	0.	0.7	27.5
H-ALPHA 1	85.8	0.	1.0	13.1
NRL-A	68.0	0.	0.6	31.3
NRL-B	68.7	0.	0.6	30.7
Fogging				
HAO	71.5	0.	2.5	26.0
ASE	70.6	0.	2.7	26.7
GSFC	70.2	0.	2.4	27.5
H-ALPHA 1	79.8	0.	6.7	13.1
NRL-A	67.1	0.	1.7	31.3
NRL-B	67.7	0.	1.6	30.7

TABLE 5.4: PERCENT OF TOTAL DOSE AND FOGGING BY COMPONENT - LOAD 3, MDA VAULTS

Dose	p	e	Brem	GCR
HAO	71.9	0.	0.7	27.5
ASE	72.4	0.	0.7	27.0
GSFC	70.4	0.	0.7	28.7
H-ALPHA 1	85.8	0.1	1.0	13.1
NRL-A	68.6	0.	0.6	31.0
NRL-B	69.6	0.	0.6	29.8
Fogging				
HAO	70.1	0.	2.3	27.5
ASE	70.4	0.	2.6	27.0
GSFC	69.1	0.	2.3	28.7
H-ALPHA 1	79.7	0.2	6.8	13.1
NRL-A	67.2	0.	1.6	30.9
NRL-B	68.4	0.	1.7	29.8

TABLE 5.4: PERCENT OF TOTAL DOSE AND FOGGING BY COMPONENT - LOAD 4, MDA VAULTS

Dose	p	e	Brem	GCR
HAO	67.5	0.	0.6	32.0
ASE	66.8	0.	0.6	32.8
GSFC	68.6	0.	0.6	30.8
Fogging				
HAO	66.1	0.	2.0	31.8
ASE	65.2	0.	1.9	32.9
GSFC	67.2	0.	2.0	30.8
H-ALPHA 1	79.9	0.1	6.9	13.0

cameras in the ATM and in the MDA vaults. The MDA vault data are for a fully loaded configuration. Partially loaded vault configurations will not change these values significantly. For dose rates, the proton component ranges from 67 to 86 percent; electron, from 0 to 1 percent; bremsstrahlung, from 0.6 to 1 percent; and GCR, from 9 to 33 percent. For fogging rates, the proton component ranges from 65 to 80 percent; electron, from 0 to 7 percent; bremsstrahlung, from 1.6 to 9 percent; and GCR, from 9.5 to 33 percent.

Total dose and radiation fogging estimates are obtained by folding the data of Tables 5.2 and 5.3 into the timeline of Table 5.1. These estimates are given in Table 5.5. Total doses range from 1.3 to 17.3 rad. The total radiation fogging values are discussed below.

The NRL cameras offered a particular challenge at the beginning of the present study. The tolerance value for radiation-induced fogging had been lowered to 0.05. Results from a previous study showed that the new tolerance would be difficult to meet. Steps were taken to alleviate the NRL film problem, including:

- o resupply of load 4, eliminating 180 days of MDA storage,
- o move load 2 from the thin-walled vault 4 to vault 1,
- o increase vault 1 wall thickness to 0.5 inches aluminum.

The recomputed fogging values were still over tolerance for loads 2, 3, and 4. However, Murray Cleare and Ken Huff[12] of the Eastman Kodak Company rechecked the cobalt-60 sensitivity of SWR film in late 1970. Their new measurements, communicated in July 1971, show that the radiation sensitivity of this product has fallen by a factor of 3 since the 1967 tests. This result also confirms the Martin-Marietta tests of early 1970.[17] As a result of increased protection, load 4 resupply, and - particularly - reduced radiation sensitivity, the NRL film's computed radiation fogging is well below the specified tolerance level in the eight NRL cameras.

TABLE 5.5: TOTAL DOSE AND RADIATION FOGGING WITH GCR

	Dose - Rad				Fogging Density			
	Load 1	Load 2	Load 3	Load 4	Load 1	Load 2	Load 3	Load 4
HAO	1.63	7.18	6.15	9.73	.045	.198	.171	.270
ASE	1.30	6.19	5.79	8.55	.036	.171	.161	.237
GSFC	1.57	5.93	5.83	8.96	.044	.165	.163	.249
H-ALPHA 1	1.60	9.52	10.6	17.3	.035	.208	.232	.378
NRL A	3.08	7.19	6.89	6.12	.012	.028	.027	.023
NRL B	2.16	6.18	6.12	4.29	.008	.024	.024	.017

The specified fogging density tolerance level for the other ATM films is 0.200. The proton dose rates to Pan-X type films in storage (HAO, AS&E, GSFC) have generally declined, but the inclusion of electrons and bremsstrahlung, coupled with a 23 percent increase in sensitivity due to using a more exact computational technique, has increased radiation damage to these films. For the H-ALPHA 1 film, decreased shielding and increased sensitivity as shown by the Martin-Marietta data[17] also combine to increase film damage.

Load 1 damage increases are generally due to increased sensitivity. For other loads, the increased sensitivity is partially compensated by better MDA shielding except for H-ALPHA 1 cameras.

The over-tolerance values shown for several load 4 cameras in Table 5.6 merit special attention. For the HAO load 4 camera, the dose rate in storage and on the ATM is now lower than in a previous study. The number of days in orbit has been reduced by 16. Yet the total dose is higher (9.70 vs 9.56 rad) due to 34 days on the spar during unmanned operation and an additional 28 days on the spar during SL-4. The radiation fog rose from .203 to .270 primarily due to increased film sensitivity.

For the AS&E load 4 camera, the same considerations apply. The total dose fell from 9.89 to 8.53 rad; yet the radiation fog rose from .210 to .237, primarily due to increased film sensitivity.

For the GSFC load 4 camera, the dose rate in storage fell while the dose rate on the spar rose. The total dose fell from 9.24 to 8.94 rad. The radiation fog increased from .196 to .249, primarily due to increased film sensitivity.

TABLE 5.6: COMPARISON OF LOAD 4 RESULTS FOR HAO, AS&E, AND GSFC

	1970 Values			Present Values		
	Dose Rate Rad/Day	Days	Dose Rad	Dose Rate Rad/Day	Days	Dose Rad
HAO	.0234	100	2.34	.0212	118	2.50
	.0237	28	.66	.0213	28	.60
	.0238	96	2.28	.0472	34	1.60
	.0629	28	1.76	.0471	56	2.64
			7.04			7.34
	GCR	252	2.52	GCR	236	2.36
			9.56			9.70
	Fog = .203			Fog = .270		
AS&E	.0269	100	2.69	.0203	118	2.40
	.0270	28	.76	.0203	28	.57
	.0270	96	2.59	.0355	34	1.21
	.0475	28	1.33	.0355	56	1.99
			7.37			6.17
	GCR	252	2.52	GCR	236	2.36
			9.89			8.53
	Fog = .210			Fog = .237		
GSFC	.0250	100	2.50	.0225	118	2.66
	.0250	28	.70	.0226	28	.63
	.0251	96	2.41	.0226	34	.77
	.0396	28	1.11	.0450	56	2.52
			6.72			6.58
	GCR	252	2.52	GCR	236	2.36
			9.24			8.94
	Fog = .196			Fog = .249		

The computed fogging for HAO load 1 is 0.045, up from 0.036 in the June, 1970 report[8] due to increased sensitivity. The computed value for HAO load 2 is 0.198, up from 0.145 a year ago. Most of the uncompensated increase is due to an additional 62 days dwell time on the ATM spar including unmanned operation; a smaller part is due to use of the Apollo Block II CSM geometry model which has slightly less protection than the simple model used earlier. The computed value for HAO load 3 is 0.171, up slightly from the previous estimate of 0.155, due to bremsstrahlung and electrons. HAO load 4 is over tolerance at 0.270, up from 0.203 a year ago. Half the uncompensated increase is due to 34 days on the spar during unmanned operation plus 56 rather than 28 days on the spar during SL-4. Most of the remaining increase is due to bremsstrahlung and electrons.

The ASE load 1 radiation fogging estimate rose from 0.028 to 0.036, primarily due to increased film sensitivity. The ASE load 2 estimate rose from 0.149 to 0.171 due partly to unmanned operation and higher CSM levels. The ASE load 3 estimate rose slightly from 0.153 to 0.161. The ASE load 4 estimate rose from 0.210 (over tolerance) to 0.237, partly due to 62 days additional stay time on the ATM spar during SL-4 and unmanned operation.

The GSFC load 1 radiation fogging estimates rose from 0.023 to 0.044 due to miscellaneous causes. The GSFC load 2 estimates rose from 0.133 to 0.165, partly due to the new CSM model plus inclusion of the electron and bremsstrahlung components. The GSFC load 3 estimates rose from 0.136 to 0.163. The GSFC load 4 estimates rose from 0.196 to 0.249, partly due to longer stay time on the ATM spar.

The four H-Alpha 1 cameras exhibit greatly increased fogging level estimates compared to the previous study. Three loads are now over tolerance. The reasons for the dramatic increase in H-Alpha 1 film damage estimates are detailed below.

Previous estimates were based upon Chrysler data[18] which indicated the ratio of SO-392 fogging to SO-375 fogging is 2.3 for cobalt-60 gamma rays. The present estimates use recent Martin-Marietta data[17] giving a ratio of 3.1, an increase of 35 percent in film sensitivity. Table 5.7 compares previous estimates, previous estimates corrected for higher radiation sensitivity, and present estimates. Note that the previous results are approximately a factor of two lower than the present results even with the new film sensitivity taken into account.

The H-Alpha 1, load 1 results indicate that the revised ATM configuration and inclusion of bremsstrahlung, raises fogging levels by 0.02 for a 28 day dwell time on the spar. This information implies that 0.07 to 0.11 of the fogging density increase takes place in the MDA vaults or CSM for loads 2, 3, and 4. Less than 20 percent of the increment can be attributed to bremsstrahlung; the greater part is due to the removal of two massive NRL load 2 cameras and their cannisters from vault 4. This act causes greatly increased dose and fogging rates in the thin-walled vault over a 90 to 146 day period for H-Alpha 1 camera loads 2, 3, and 4.

The CSM dose rates are overestimated because of the simple configuration used here as sketched in Figure 5.5. The planned return configuration places the NRL cameras against the flat (ablative shield) side with 25 pound pound bags strapped on top. The other ATM cameras are packed into a locker whose minimum wall thickness is .050 inches aluminum. Other film magazines are placed atop the ATM cameras. Thus, the actual configuration provides more shielding and the dose rates should be at least 20 percent lower than the CSM dose rates quoted in this section. The reduction is most significant to load 2 films which will be stored in the CSM over a 28 day period. CSM storage should provide equal or better shielding than the MDA vaults.

TABLE 5.7: COMPARISON OF H-ALPHA 1 RADIATION FOGGING ESTIMATES

Load	Previous Study	Previous Study - New Film Sensitivity	Present Study
1	.012	.016	.035
2	.088	.119	.208
3	.088	.119	.232
4	.162	.219	.378

5.2 Status of the Radiation Hazard to ATM Film

1. All ATM load 1 fogging estimates are below specified tolerance limits by factors of 4 to 6.

2. The load 2, 3, and 4 NRL fogging estimates are below specified tolerance limits by factors of 1.8 to 3. This conclusion is based upon resupply of load 4 and relocation of load 2 to MDA vault 1.

3. The HAO, ASE, and GSFC fogging estimates for loads 2 and 3 are slightly below specified tolerance limits with safety margins ranging from 1 to 20 percent. These margins are significantly smaller than computational uncertainties (factor of two).

4. The HAO, ASE, and GSFC fogging estimates for load 4 are above specified tolerance limits by 19 to 35 percent.

5. The H-Alpha 1 fogging estimates for loads 2, 3, and 4 are above specified tolerance limits by 4 to 90 percent. Part of all of the excess fogging may be eliminated by putting massive components in vault 4.

6. Significant, unanticipated changes in the radiation sensitivities of several film types have occurred over a four year period. Samples of film to be flown aboard Skylab should be periodically sampled up to the procurement date.

6.0 OWS FILM RADIATION DAMAGE ANALYSES

All Skylab films not specifically assigned to the ATM will be termed "OWS films" in this report because they are usually stored in the OWS vault when not in use. Detailed time lines, operational modes, and radiation fogging tolerance criteria were not available to Lockheed during the present study. Therefore, daily dose and fogging rates at several locations are given. The user may combine these data with his own timeline in order to compute total radiation damage to individual experiment films.

The results of the OWS vault study are given in Section 6.1. Results for the T027 and S190 operational locations are given in Sections 6.2 and 6.3, respectively.

6.1 OWS Vault Analysis

A sketch of the OWS aluminum vault is shown in Figure 6.1. The center-hinged doors are removed for clarity. The top is 0.25 inches thick and the bottom is 3.4 inches thick. The side walls, back, and doors are stepped so that, in conjunction with several internal dividers, varying amounts of shielding surround groups of drawers. Drawers A and G are protected by at least 0.25 inches aluminum. Drawers B, C, D, H, and I are protected by at least 1.9 inches aluminum. Drawer J is protected by at least 2.9 inches aluminum. Drawers E, F, K, and L are protected by at least 3.4 inches aluminum.

The drawer contents are shown in Figure 6.2 a-e. Above each sketch is a label showing the mission, drawer, minimum shield thickness, and drawer height. The location of individual film magazines is shown inside the drawer. Each magazine has three labels. The first indicates the experiment for which it is intended; the second, the film identification; and the third, the number of days in orbit. The latter value is not necessarily equal to the number of days in the vault.

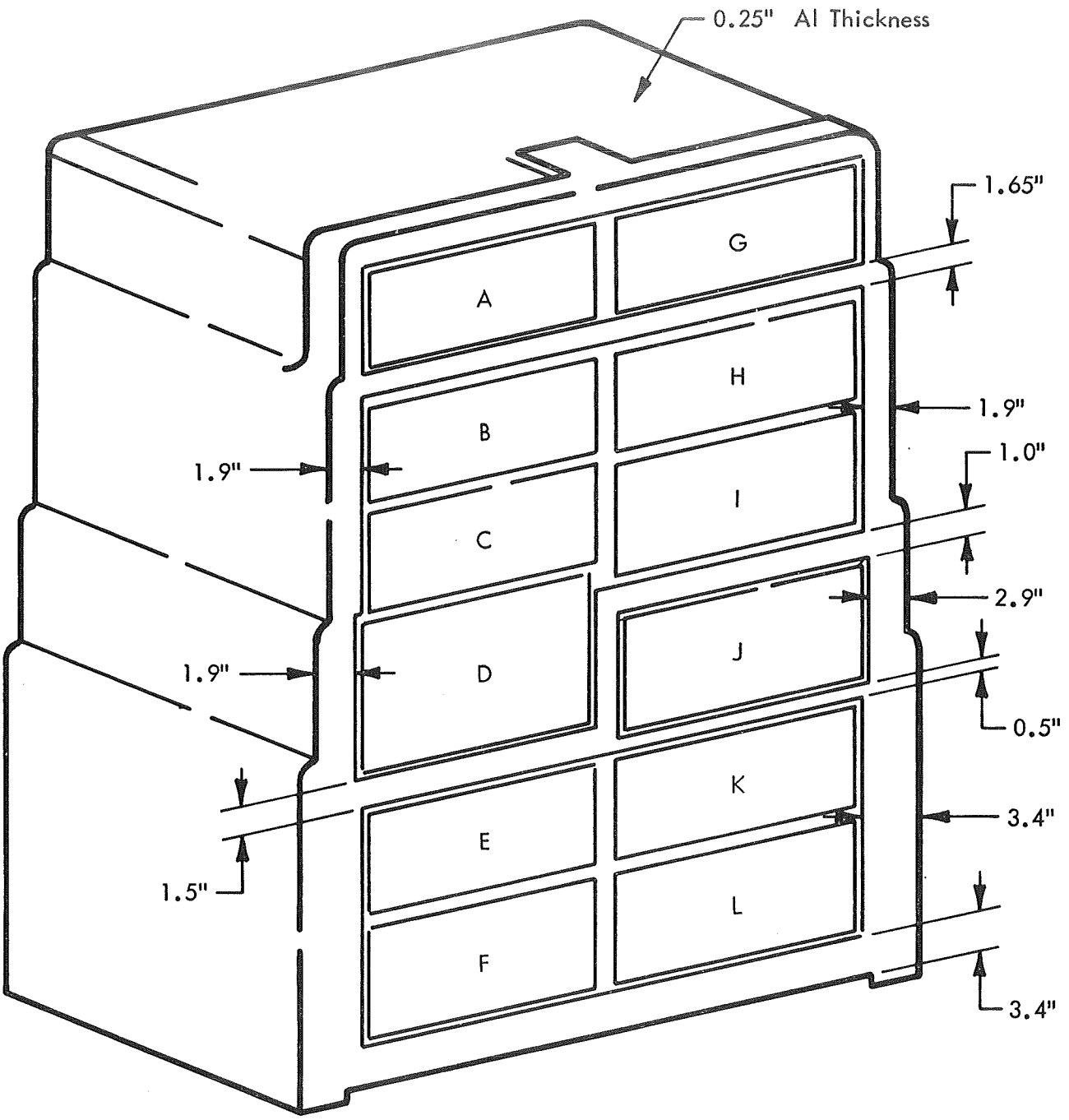

FIGURE 6.1: OWS VAULT CONFIGURATION

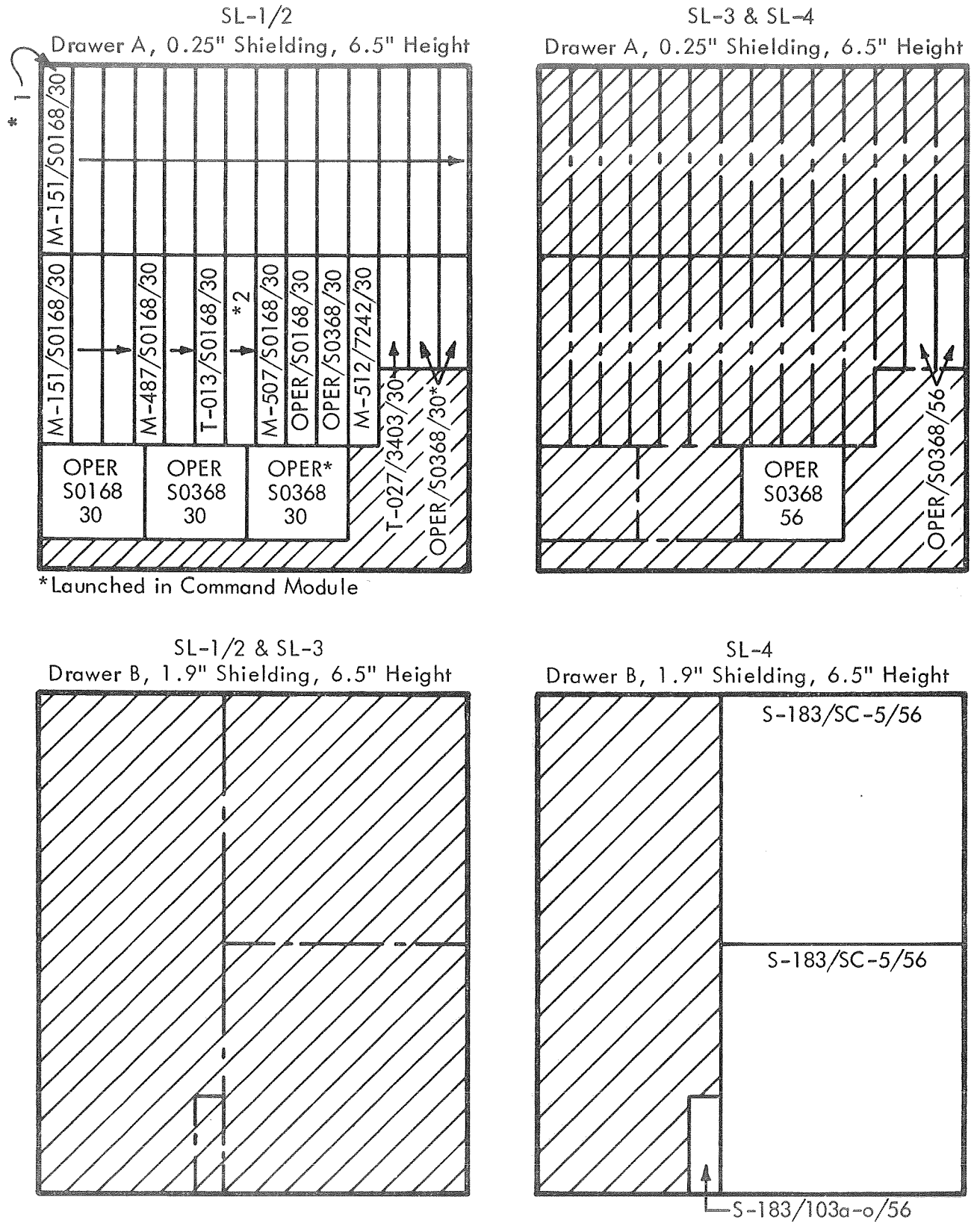

FIGURE 6.2a: MAGAZINE ARRANGEMENT

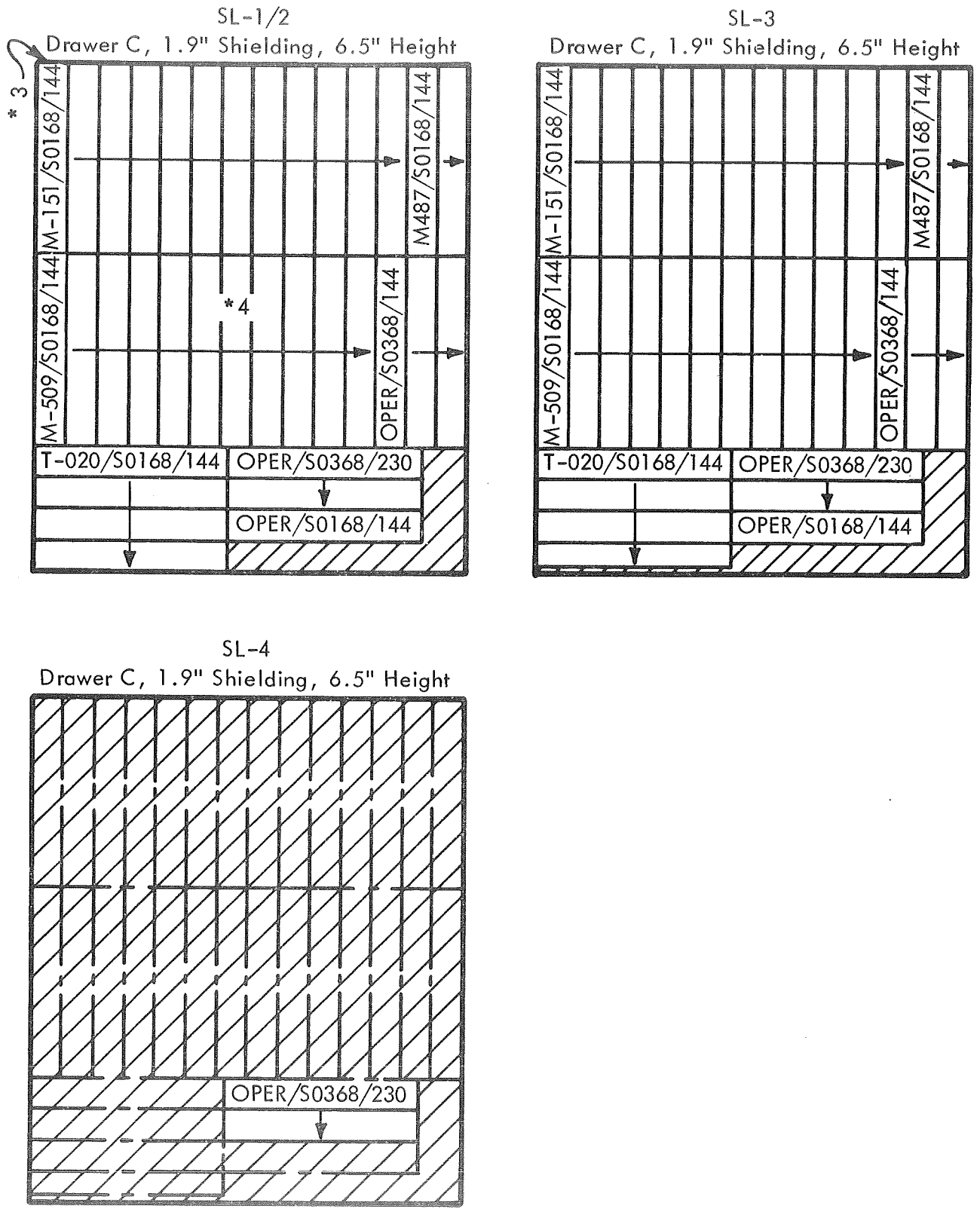

FIGURE 6.2b: MAGAZINE ARRANGEMENT

SL-1/2
Drawer D, 1.9" Shielding, 8.0" Height

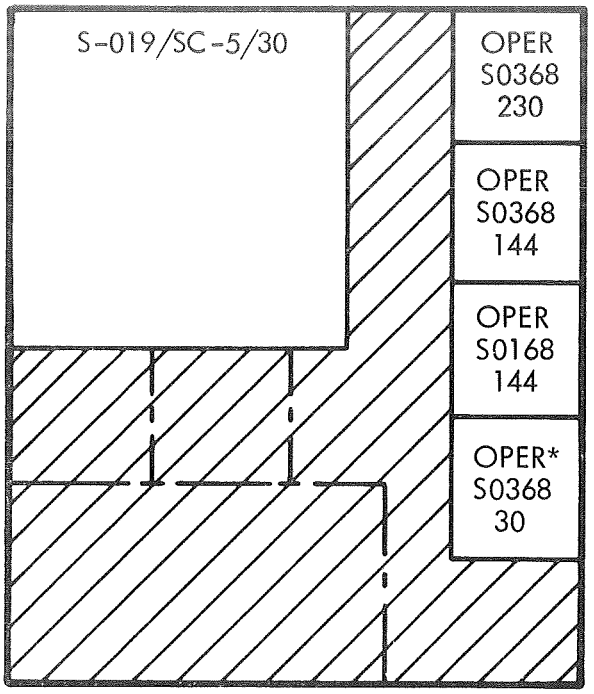

*PIO Film

SL-3
Drawer D, 1.9" Shielding, 8.0" Height

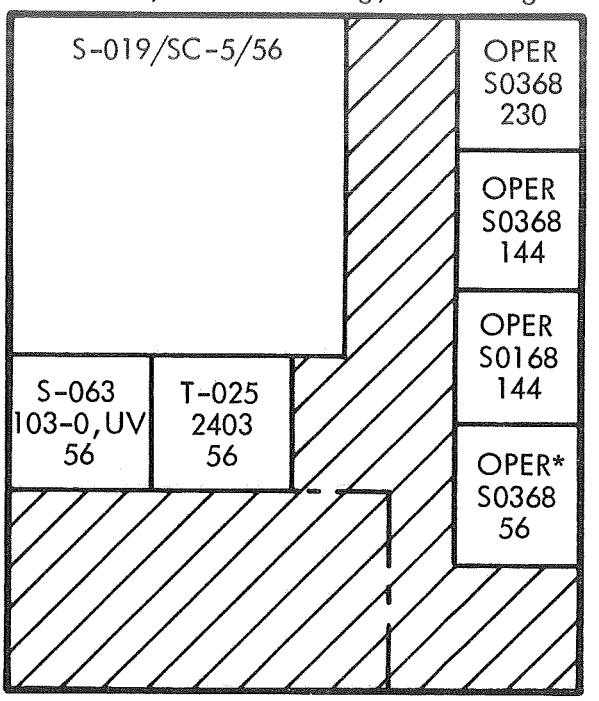

*PIO Film

SL-4
Drawer D, 1.9" Shielding, 8.0" Height

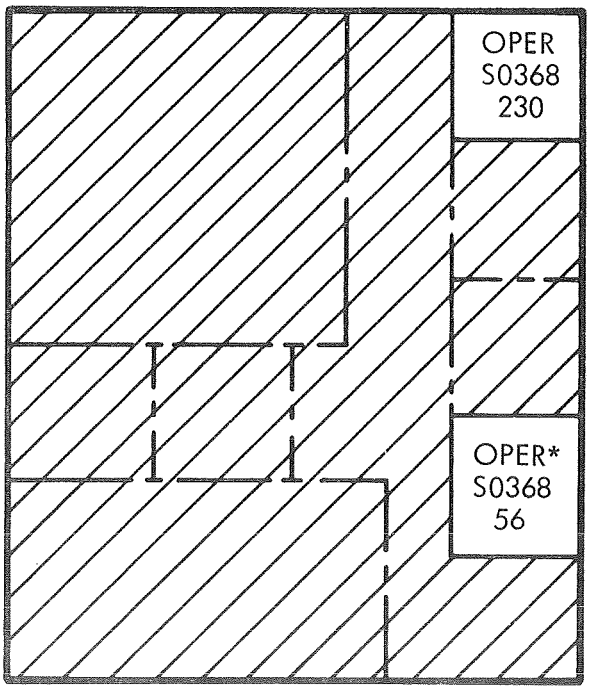

*PIO Film

FIGURE 6.2c: MAGAZINE ARRANGEMENT

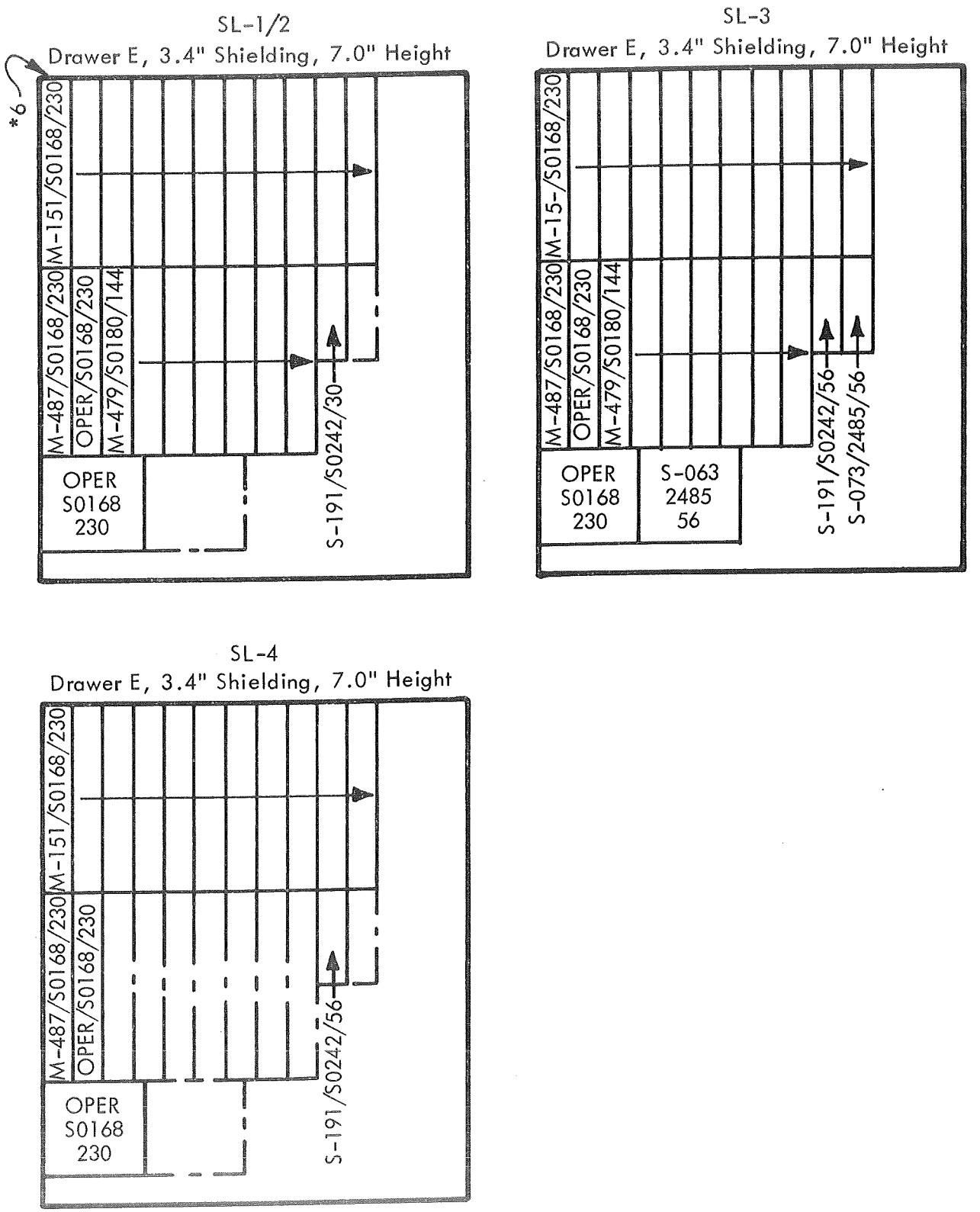

FIGURE 6.2d: MAGAZINE ARRANGEMENT

SL-1/2,
Drawer F, K, & L
3.4" Shielding, 7.0" Height

S-190 S0242 30 *7F	S-190 S0246 30 *10K 11L	S-190 3401 30 *8F
S-190 S0180 30	S-190 S0246 30	S-190 3401 30 *9F

SL-3, & SL-4
Drawer F, K, & L
3.4" Shielding, 7.0" Height

S-190 S0242 56 *7F	S-190 S0246 56 *10K 11L	S-190 3401 56 *8F
S-190 S0180 56	S-190 S0246 56	S-190 3401 56 *9F

SL-1/2, SL-3, & SL-4
Drawer J, 2.9" Shielding, 8.0" Height

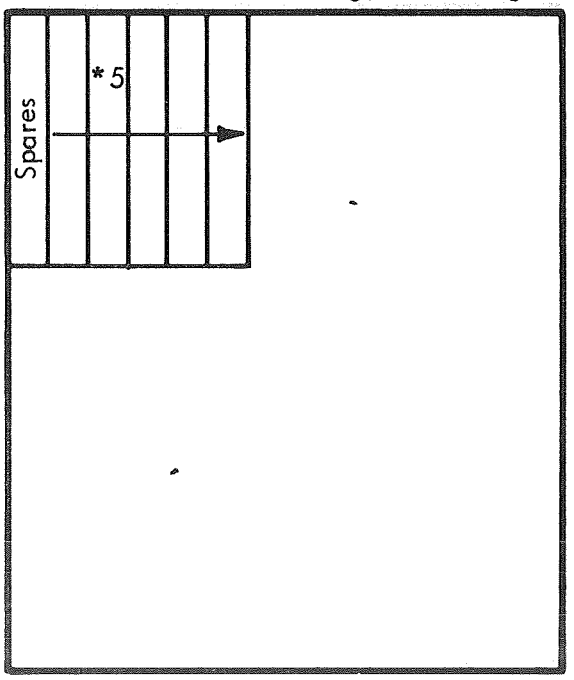

FIGURE 6.2e: MAGAZINE ARRANGEMENT

Seven different types of film magazines, cassettes, and canisters are modeled and reproduced in sufficient quantity to fill the requirements shown in Figure 6.2. Canisters K and M for experiments S019 and S183, respectively, are assumed to be identical. Canister L for S020 is omitted because it will not remain in the vault very long. A large block of nuclear emulsion for S009 is omitted for the same reason.

Magazine type B for experiments M151, M487, M508, M509, T013, T020, and others has .078" magnesium walls. Other magazines are made of aluminum.

The numbered asterisks in Figure 6.2 identify the eleven detector locations studied. Detectors are located 0.1" from the film outer surface. A number of runs were made in order to simulate vault loading during major mission segments.

Daily dose rates, excluding GCR, at the 11 detector positions are shown in Table 6.1. The first column shows dose rates in an empty vault. Subsequent columns identify Mission SL 1/2, S1 (first unmanned storage period), SL3, S2 (second unmanned storage period), and SL4. Approximately 10 mrad/day should be added to each value to account for the GCR contribution. The blank spaces in Table 6.1 indicate that the associated film magazine is not present during that mission segment.

Film locations within the vault and film types assigned to experiments are not yet frozen. To illustrate this point, it might be noted that many of the film locations were changed before the geometry model was completed. Moderately accurate dose rate estimates may be derived for new configurations from Table 6.1.

Film fogging estimates for various films in new configurations are more difficult to estimate without extensive data. For this reason, net radiation fogging density change values for 8 black and white films and 4 color films are given in Table 6.2. For the color films, net density changes are given in 4 spectral regions; visible, red, green, and blue.

TABLE 6.1: OWS VAULT DOSE RATE - RAD/DAY

(without GCR)

OWS Vault	Empty Vault	SL 1/2	S1	SL3	S2	SL4
1	7.24-2	5.66-2				
2	6.06-2	2.38-2				
3	2.07-2	1.71-2	1.72-2	1.72-2		
4	2.28-2	1.15-2	1.19-2	1.18-2		
5	1.23-2	9.12-3				
6	1.08-2	8.87-3	8.94-3	8.87-3	9.15-3	9.15-3
7	1.19-2	9.27-3		9.27-3		9.40-3
8	1.11-2	7.87-3		7.87-3		7.97-3
9	1.12-2	6.44-3		6.42-3		6.55-3
10	1.10-2	7.69-3		7.69-3		7.79-3
11	1.07-2	7.82-3		7.82-3		7.90-3

TABLE 6.2: OWS VAULT - RADIATION FOGGING RATE - DENSITY/DAY
(without GCR)

S0166(2485)

Detector	Empty Vault	SL 1/2	S1	SL3	S2	SL4
1	5.32-2	3.70-2				
2	4.47-2	1.74-2				
3	1.56-2	1.30-2	1.31-2	1.30-2		
4	1.71-2	9.27-3	9.58-3	9.52-3		
5	9.82-3	7.37-3				
6	8.74-3	7.21-3	7.27-3	7.21-3	7.43-3	7.43-3
7	9.55-3	7.55-3		7.55-3		7.66-3
8	8.93-3	6.46-3		6.46-3		6.54-3
9	9.02-3	5.38-3		5.37-3		5.47-3
10	8.87-3	6.31-3		6.31-3		6.39-3
11	8.69-3	6.42-3		6.42-3		6.49-3

2403

Detector	Empty Vault	SL 1/2	S1	SL3	S2	SL4
1	2.53-2	1.72-2				
2	2.13-2	8.14-3				
3	7.28-3	6.06-3	6.12-3	6.09-3		
4	8.00-3	4.35-3	4.49-3	4.46-3		
5	4.60-3	3.46-3				
6	4.10-3	3.38-3	3.41-3	3.38-3	3.49-3	3.49-3
7	4.48-3	3.54-3		3.54-3		3.59-3
8	4.19-3	3.03-3		3.03-3		3.07-3
9	4.23-3	2.53-3		2.52-3		2.57-3
10	4.16-3	2.96-3		2.96-3		3.00-3
11	4.08-3	3.01-3		3.01-3		3.04-3

SC 5

Detector	Empty Vault	SL 1/2	S1	SL3	S2	SL4
1	1.13-2	7.92-3				
2	9.47-3	3.54-3				
3	3.13-3	2.60-3	2.62-3	2.61-3		
4	3.44-3	1.81-3	1.88-3	1.86-3		
5	1.93-3	1.44-3				
6	1.71-3	1.41-3	1.42-3	1.41-3	1.45-3	1.45-3
7	1.87-3	1.47-3		1.47-3		1.49-3
8	1.75-3	1.26-3		1.26-3		1.27-3
9	1.76-3	1.04-3		1.04-3		1.06-3
10	1.74-3	1.23-3		1.23-3		1.24-3
11	1.70-3	1.25-3		1.25-3		1.26-3

SO-246

Detector	Empty Vault	SL 1/2	S1	SL3	S2	SL4
1	9.35-3	6.55-3				
2	7.85-3	2.98-3				
3	2.65-3	2.20-3	2.22-3	2.21-3		
4	2.91-3	1.55-3	1.60-3	1.59-3		
5	1.65-3	1.23-3				
6	1.46-3	1.20-3	1.21-3	1.20-3	1.24-3	1.24-3
7	1.60-3	1.26-3		1.26-3		1.28-3
8	1.49-3	1.08-3		1.08-3		1.09-3
9	1.51-3	8.94-4		8.91-4		9.09-4
10	1.48-3	1.05-3		1.05-3		1.07-3
11	1.45-3	1.07-3		1.07-3		1.08-3

TABLE 6.2 (Continued)

Detector	Plux-X(3401) Empty Vault	SL 1/2	S1	SL3	S2	SL4	Pan-X(3400) Empty Vault	SL 1/2	S1	SL3	S2	SL4
1	7.03-3	4.90-3					1.98-3	1.42-3				
2	5.91-3	2.30-3					1.66-3	6.45-4				
3	2.06-3	1.71-3	1.73-3	1.72-3			5.72-4	4.74-4	4.79-4	4.77-4		
4	2.26-3	1.22-3	1.26-3	1.26-3			6.28-4	3.33-4	3.45-4	3.42-4		
5	1.30-3	9.72-4					3.55-4	2.65-4				
6	1.15-3	9.50-4	9.58-4	9.51-4	9.80-4	9.80-4	3.14-4	2.58-4	2.61-4	2.59-4	2.67-4	2.67-4
7	1.26-3	9.95-4		9.96-4		1.01-3	3.43-4	2.70-4		2.71-4		2.74-4
8	1.18-3	8.51-4		8.52-4		8.62-4	3.21-4	2.31-4		2.31-4		2.34-4
9	1.19-3	7.09-4		7.08-4		7.21-4	3.24-4	1.91-4		1.91-4		1.95-4
10	1.17-3	8.32-4		8.32-4		8.42-4	3.19-4	2.26-4		2.25-4		2.28-4
11	1.15-3	8.47-4		8.47-4		8.55-4	3.12-4	2.30-4		2.30-4		2.32-4

Detector	SO-392						SWR (104-06)					
1	1.62-3	1.16-3					2.75-4	2.00-4				
2	1.36-3	5.29-4					2.30-4	9.00-5				
3	4.69-4	3.89-4	3.92-4	3.91-4			7.93-5	6.57-5	6.63-5	6.63-5		
4	5.15-4	2.72-4	2.82-4	2.80-4			8.73-5	4.60-5	4.73-5	4.73-5		
5	2.90-4	2.17-4					4.90-5	3.63-5				
6	2.57-4	2.11-4	2.13-4	2.11-4	2.18-4	2.18-4	4.33-5	3.57-5	3.60-5	3.57-5	3.67-5	3.67-5
7	2.81-4	2.21-4		2.21-4		2.24-4	4.73-5	3.73-5		3.73-5		3.77-5
8	2.62-4	1.89-4		1.89-4		1.91-4	4.44-5	3.17-5		3.17-5		3.21-5
9	2.65-4	1.56-4		1.56-4		1.59-4	4.47-5	2.62-5		2.61-5		2.67-5
10	2.61-4	1.84-4		1.84-4		1.87-4	4.40-5	3.10-5		3.10-5		3.14-5
11	2.55-4	1.88-4		1.88-4		1.90-4	4.30-5	3.15-5		3.15-5		3.18-5

TABLE 6.2 (Continued)

S0168 Visible

Detector	Empty Vault	SL 1/2	S1	SL3	S2	SL4
1	1.88-2	1.30.2				
2	1.58-2	6.09-3				
3	5.44-3	4.52-3	4.56-3	4.54-3		
4	5.97-3	3.23-3	3.34-3	3.31-3		
5	3.42-3	2.57-3				
6	3.04-3	2.51-3	2.53-3	2.51-3	2.59-3	2.59-3
7	3.32-3	2.63-3		2.63-3		2.66-3
8	3.11-3	2.25-3		2.25-3		2.28-3
9	3.14-3	1.87-3		1.87-3		1.90-3
10	3.09-3	2.20-3		2.20-3		2.22-3
11	3.03-3	2.23-3		2.23-3		2.26-3

S0168 Red

Empty Vault	SL 1/2	S1	SL3	S2	SL4
2.15-2	1.48-2				
1.81-2	6.94-3				
6.20-3	5.16-3	5.21-3	5.18-3		
6.81-3	3.69-3	3.81-3	3.79-3		
3.91-3	2.94-3				
3.48-3	2.87-3	2.89-3	2.87-3	2.96-3	2.96-3
3.80-3	3.00-3		3.01-3		3.05-3
3.55-3	2.57-3		2.57-3		2.60-3
3.59-3	2.14-3		2.14-3		2.18-3
3.53-3	2.51-3		2.51-3		2.54-3
3.46-3	2.56-3		2.56-3		2.58-3

S0168 Green

1.47-2	1.03-2				
1.24-2	4.79-3				
4.27-3	3.54-3	3.58-3	3.56-3		
4.69-3	2.52-3	2.61-3	2.59-3		
2.68-3	2.00-3				
2.38-3	1.96-3	1.98-3	1.96-3	2.02-3	2.02-3
2.60-3	2.05-3		2.05-3		2.08-3
2.43-3	1.75-3		1.75-3		1.78-3
2.45-3	1.46-3		1.46-3		1.48-3
2.41-3	1.71-3		1.71-3		1.7313
2.36-3	1.74-3		1.74-3		1.76-3

S0168 Blue

1.30-2	9.11-3				
1.09-2	4.23-3				
3.76-3	3.12-3	3.15-3	3.14-3		
4.13-3	2.22-3	2.29-3	2.28-3		
2.36-3	1.76-3				
2.09-3	1.72-3	1.74-3	1.72-3	1.78-3	1.78-3
2.29-3	1.80-3		1.80-3		1.83-3
2.14-3	1.54-3		1.54-3		1.56-3
2.16-3	1.28-3		1.28-3		1.30-3
2.12-3	1.51-3		1.51-3		1.53-3
2.08-3	1.53-3		1.53-3		1.55-3

TABLE 6.2 (Continued)

S0368 Visible

Detector	Empty Vault	SL 1/2	S1	SL3	S2	SL4
1	9.35-3	6.55-3				
2	7.85-3	2.98-3				
3	2.65-3	2.20-3	2.22-3	2.21-3		
4	2.91-3	1.55-3	1.60-3	1.59-3		
5	1.65-3	1.23-3				
6	1.46-3	1.20-3	1.21-3	1.20-3	1.24-3	1.24-3
7	1.60-3	1.26-3		1.26-3		1.28-3
8	1.49-3	1.08-3		1.08-3		1.09-3
9	1.51-3	8.94-4		8.91-4		9.09-4
10	1.48-3	1.05-3		1.05-3		1.07-3
11	1.45-3	1.07-3		1.07-3		1.08-3

S0368 Red

Empty Vault	SL 1/2	S1	SL3	S2	SL4
5.60-3	3.93-3				
4.70-3	1.83-3				
1.64-3	1.36-3	1.37-3	1.37-3		
1.80-3	9.69-4	1.00-3	9.95-4		
1.03-3	7.70-4				
9.13-4	7.53-4	7.59-4	7.53-4	7.77-4	7.77-4
9.98-4	7.88-4		7.88-4		8.00-4
9.33-4	6.74-4		6.74-4		6.83-4
9.43-4	5.61-4		5.60-4		5.71-4
9.27-4	6.59-4		6.58-4		6.67-4
9.08-4	6.70-4		6.70-4		6.77-4

S0368 Green

1	4.96-3	3.48-3				
2	4.16-3	1.62-3				
3	1.45-3	1.20-3	1.21-3	1.21-3		
4	1.59-3	8.55-4	8.84-4	8.78-4		
5	9.07-4	6.80-4				
6	8.06-4	6.64-4	6.70-4	6.65-4	6.85-4	6185-4
7	8.81-4	6.95-4		6.96-4		7.06-4
8	8.23-4	5.95-4		5.95-4		6.02-4
9	8.32-4	4.95-4		4.93-4		5.03-4
10	8.18-4	5.81-4		5.81-4		5.88-4
11	8.01-4	5.91-4		5.91-4		5.97-4

S0368 Blue

4.06-3	2.87-3				
3.41-3	1.33-3				
1.18-3	9.83-4	9.92-4	9.88-4		
1.30-3	6.97-4	7.22-4	7.17-4		
7.41-4	5.55-4				
6.58-4	5.42-4	5.46-4	5.42-4	5.59-4	5.59-4
7.19-4	5.67-4		5.67-4		5.75-4
6.72-4	4.85-4		4.85-4		4.91-4
6.79-4	4.03-4		4.02-4		4.10-4
6.68-4	4.74-4		4.73-4		4.80-4
6.54-4	4.82-4		4.82-4		4.87-4

TABLE 6.2 (Continued)

S0180 Visible

Detector	Empty Vault	SL 1/2	S1	SL3	S2	SL4
1	8.08-3	5.64-3				
2	6.78-3	2.61-3				
3	2.33-3	1.93-3	1.95-3	1.94-3		
4	2.56-3	1.37-3	1.42-3	1.41-3		
5	1.46-3	1.09-3				
6	1.29-3	1.07-3	1.08-3	1.07-3	1.10-3	1.10-3
7	1.41-3	1.12-3		1.12-3		1.13-3
8	1.32-3	9.54-4		9.55-4		9.66-4
9	1.34-3	7.94-4		7.92-4		8.07-4
10	1.31-3	9.33-4		9.32-4		9.44-4
11	1.29-3	9.49-4		9.49-4		9.58-4

S0180 Red

Empty Vault	SL1/2	S1	SL3	S2	SL4
1.13-2	7.95-3				
9.49-3	3.58-3				
3.18-3	2.63-3	2.66-3	2.65-3		
3.49-3	1.85-3	1.91-3	1.90-3		
1.97-3	1.47-3				
1.74-3	1.43-3	1.44-3	1.43-3	1.48-3	1.48-3
1.90-3	1.50-3		1.50-3		1.52-3
1.78-3	1.28-3		1.28-3		1.30-3
1.80-3	1.06-3		1.06-3		1.08-3
1.77-3	1.25-3		1.25-3		1.27-3
1.73-3	1.27-3		1.27-3		1.29-3

S0180 Green

4.06-3	2.87-3				
3.41-3	1.33-3				
1.18-3	9.83-4	9.92-4	9.88-4		
1.30-3	6.97-4	7.22-4	7.17-4		
7.4-14	5.55-4				
6.58-4	5.42-4	5.46-4	5.42-4	5.59-4	5.59-4
7.19-4	5.67-4		5.67-4		5.75-4
6.72-4	4.85-4		4.85-4		4.91-4
6.79-4	4.03-4		4.02-4		4.10-4
6.68-4	4.74-4		4.73-4		4.80-4
6.54-4	4.82-4		4.82-4		4.87-4

S0180 Blue

3.47-3	2.45-3				
2.91-3	1.13-3				
1.01-3	8.37-4	8.45-4	8.42-4		
1.11-3	5.93-4	6.13-4	6.09-4		
6.30-4	4.71-4				
5.59-4	4.60-4	4.64-4	4.61-4	4.75-4	4.75-4
6.11-4	4.82-4		4.82-4		4.89-4
5.71-4	4.12-4		4.12-4		4.17-4
5.77-4	3.42-4		3.41-4		3.48-4
5.67-4	4.03-4		4.02-4		4.07-4
5.56-4	4.09-4		4.09-4		4.13-4

TABLE 6.2 (Continued)

S0121 Visible

Detector	Empty Vault	SL 1/2	S1	SL3	S2	SL4
1	5.60-3	3.93-3				
2	4.70-3	1.83-3				
3	1.64-3	1.36-3	1.37-3	1.37-3		
4	1.80-3	9.69-4	1.00-3	9.95-4		
5	1.03-3	7.70-4				
6	9.13-4	7.53-4	7.59-4	7.53-4	7.77-4	7.77-4
7	9.98-4	7.88-4		7.88-4		8.00-4
8	9.33-4	6.74-4		6.74-4		6.83-4
9	9.43-4	5.61-4		5.60-4		5.71-4
10	9.27-4	6.59-4		6.58-4		6.67-4
11	9.08-4	6.70-4		6.70-4		6.77-4

S0121 Red

Empty Vault	SL 1/2	S1	SL3	S2	SL4
4.24-3	3.00-3				
3.59-3	1.39-3				
1.24-3	1.03-3	1.04-3	1.03-3		
1.36-3	7.30-4	7.56-4	7.51-4		
7.76-4	5.81-4				
6.89-4	5.68-4	5.72-4	5.68-4	5.85-4	5.85-4
7.53-4	5.94-4		5.94-4		6.03-4
7.04-4	5.08-4		5.08-4		5.14-4
7.11-4	4.22-4		4.21-4		4.29-4
6.99-4	4.96-4		4.96-4		5.02-4
6.85-4	5.05-4		5.05-4		5.10-4

S0121 Green

1	3.24-3	2.29-3				
2	2.72-3	1.06-3				
3	9.41-4	7.81-4	7.89-4	7.85-4		
4	1.03-3	5.52-4	5.72-4	5.68-4		
5	5.87-4	4.39-4				
6	5.21-4	4.29-4	4.33-4	4.29-4	4.43-4	4.43-4
7	5.69-4	4.49-4		4.49-4		4.56-4
8	5.32-4	3.84-4		3.84-4		3.88-4
9	5.38-4	3.19-4		3.18-4		3.24-4
10	5.29-4	3.75-4		3.75-4		3.80-4
11	5.18-4	3.81-4		3.81-4		3.85-4

S0121 Blue

1.68-2	1.17-2				
1.41-2	5.45-3				
4.86-3	4.04-3	4.08-3	4.07-3		
5.35-3	2.88-3	2.98-3	2.96-3		
3.06-3	2.29-3				
2.72-3	2.24-3	2.26-3	2.24-3	2.31-3	2.31-3
2.97-3	2.34-3		2.35-3		2.38-3
2.78-3	2.01-3		2.01-3		2.03-3
2.80-3	1.67-3		1.67-3		1.70-3
2.76-3	1.96-3		1.96-3		1.98-3
2.70-3	1.99-3		1.99-3		2.01-3

6.2 T027 Analysis

The T027 experiment is to be extended on an 18 foot boom through the Scientific Airlock (SAL). The camera is mounted adjacent to the optics housing on the end of the boom. The experiment is modeled on the sunside SAL. A second geometry model simulates the experiment and boom withdrawn into the SAL with the door closed for temporary storage.

The exposed location of the T027 camera causes it to be subjected to high radiation levels unless it is retracted at certain times. Experimental constraints and crew availability may preclude frequent retraction so an auxiliary shield is placed around four sides of the camera (excluding lens and optics housing sides) for partial protection. The shield layers from inside to outside are lead, aluminum, and polyethylene. Several shield configurations are considered.

The T027 film type is Kodak 2485, a change from Kodak 3403 as indicated in Figure 6.2a, Drawer A, of the OWS vault.

The daily dose rates and radiation fogging rates on the boom and withdrawn into the SAL are given in Table 6.3. Fogging rates pertinent to T027 are given for Kodak 2485 and 3403 films. The SWR fogging rate is included so that approximate estimates may be made for other SAL experiments using slower film. Note that GCR is not included in this table.

An experiment timeline is not available for purposes of estimating total film fogging. An example will be worked to illustrate the method that may be used in conjunction with a timeline.

Assume the total T027 film magazine time in orbit is 29 days, of which 26 days are spent in the film vault. Let a fraction of a day be spent on the boom, and the remainder

TABLE 6.3: DOSE AND FOGGING RATES FOR T027 FILM

(without GCR)

Shield-Inches Pb	Al	Poly	On Boom p	e	Brem	Total	Dose Rate - Rad/Day	Within SAL p	e	Brem	Total
0	0	0	2.30-1	8.59-2	3.10-3	3.19-1		6.64-2	4.95-5	7.95-4	6.73-2
0	0	.1	2.11-1	3.19-2	2.11-3	2.45-1		6.50-2	4.95-5	7.83-4	6.58-2
1/32	.15	0	1.61-1	1.63-3	1.20-3	1.64-1					
1/16	.3	0	1.32-1	8.83-4	1.02-3	1.34-1		5.42-2	4.95-5	4.97-4	5.47-2
1/16	.3	.1	1.29-1	8.76-4	9.39-4	1.30-1		5.35-2	4.95-5	4.55-4	5.40-2
							SO-166 (2485) Fog				
0	0	0	1.25-1	1.65-1	4.66-2	3.37-1	Day^{-1}	4.42-2	9.08-5	4.71-3	4.90-2
0	0	.1	1.15-1	6.12-2	3.17-2	2.08-1		4.34-2	9.08-5	4.66-3	4.82-2
1/32	.15	0	9.42-2	2.93-3	1.01-2	1.07-1					
1/16	.3	0	8.03-2	1.60-3	9.88-3	9.16-2		3.68-2	9.08-5	2.65-3	3.96-2
1/16	.3	.1	7.85-2	1.59-3	9.50-3	8.96-2		3.63-2	9.08-5	2.65-3	3.91-2
							3403 Fog				
0	0	0	5.84-2	9.18-2	2.57-2	1.76-1	Day^{-1}	2.06-2	5.02-5	2.60-3	2.33-2
0	0	.1	5.36-2	3.41-2	1.75-2	1.05-1		2.02-2	5.02-5	2.57-3	2.28-2
1/32	.15	0	4.37-2	1.61-3	5.56-3	5.09-2					
1/16	.3	0	3.73-2	8.83-4	5.33-3	4.35-2		1.72-2	5.02-5	1.46-3	1.87-2
1/16	.3	.1	3.65-2	8.77-4	5.24-3	4.26-2		1.69-2	5.02-5	1.46-3	1.84-2
							Pan X 3400 Fog				
0	0	0	5.00-3	4.39-3	1.34-3	1.07-2	Day^{-1}	1.68-3	2.46-6	1.36-4	1.82-3
0	0	.1	4.59-3	1.63-3	9.13-4	7.14-3		1.65-3	2.46-6	1.34-4	1.79-3
1/32	.15	0	3.70-3	8.03-5	2.90-4	4.07-3					
1/16	.3	0	3.13-3	4.37-5	2.78-4	3.45-3		1.39-3	2.46-6	7.64-5	1.47-3
1/16	.3	.1	3.05-3	4.34-5	2.74-4	3.37-3		1.37-3	2.46-6	7.63-5	1.45-3
							SWR Fog				
0	0	0	7.27-4	5.06-4	1.53-4	1.39-3	Day^{-1}	2.38-4	2.86-7	1.54-5	2.54-4
0	0	.1	6.67-4	1.88-4	1.04-4	9.59-4		2.33-4	2.86-7	1.53-5	2.48-4
1/32	.15	0	5.27-4	9.30-6	3.28-5	5.70-4					
1/16	.3	0	4.47-4	5.10-6	3.16-5	4.83-4		1.96-4	2.86-7	8.70-6	2.05-4
1/16	.3	.1	4.37-4	5.03-6	2.78-5	4.70-4		1.93-4	2.86-7	8.67-6	2.02-4

of a three day period in the SAL. Assume the boom stay time encounters several proton pulses totaling 30 percent of the daily average, and that the same fraction applies to electrons. Finally, assume the boom-mounted camera is unshielded.

The radiation environment in the vault should be similar to that of detector 2. Thus, fogging to Kodak 2485 in the vault due to trapped radiation would approximate:

$26 \times .0174$ (from Table 6.2) $= 0.425$.

Fogging on the boom is:

$0.3 \times .339$ (from Table 6.3) $= 0.102$.

Fogging in the SAL is:

$2.7 \times .0490$ (from Table 6.3) $= 0.132$

The total without GCR is 0.686.

GCR fogging may be approximated by assuming the fogging per unit dose is equal to that for trapped protons. At vault detector 2 a dose of 0.0238 rad produces a fog of 0.0174 in Kodak 2485, with trapped protons dominating. The GCR dose rate is .010 rads/day. For 29 days, the GCR fogging is approximately:

$$29 \times \frac{.0174}{.0238} \times .010 = 0.212$$

The total fog is then 0.898.

Moving the T027 magazines to Drawer E (detector 6) would reduce the OWS vault, trapped radiation fog from 0.425 to: $26 \times .00721 = 0.187$. The total fog would then be 0.660.

If the SAL residence time is reduced by two days and the vault time (Drawer E) increased by two days, the fog would be reduced by:

$$2 \times (.049 - .00721) = .0836$$

The total fog would then be 0.577.

The minimum fog achievable is for 29 days in Drawer E:

$$29 \times (.00721) + .212 \text{ (GCR)} = 0.421.$$

Half the minimum achievable fog is due to GCR whose radiation response function is uncertain.

6.3 S190 Analysis

The S190 experiment contains six cameras mounted at an optically flat window within the MDA. Three cameras are mounted along the top of the window (CSM end) and three are mounted along the bottom. Relative to an observer within the MDA, film fogging is computed for the lower left, lower center, and upper center cameras. The dose rates to these films are, respectively, 0.0606, 0.0693, and 0.0555 rad per day. At their storage location within the OWS vault (detectors 7 through 11) the dose rates range from 0.00642 to 0.00940 rad per day according to Table 6.1. The GCR dose rate of 0.010 rad per day should be added to these values.

The daily fogging rates at the MDA window are given in Table 6.4.

TABLE 6.4: DOSE AND FOGGING RATES AT S190 OPERATING LOCATION
(without GCR)

	Lower Left				Lower Center				Upper Center			
Dose Rate - Rad/Day	6.06-2				5.93-2				5.55-2			
Fogging Rate - Day^{-1}	Visible	Red	Green	Blue	Visible	Red	Green	Blue	Visible	Red	Green	Blue
SO-166 (2485)	3.92-2				3.85-2				3.62-2			
2403	1.83-2				1.79-2				1.68-2			
* SO-246	6.96-3				6.83-3				6.41-3			
* Plus-X 3401	5.20-3				5.10-3				4.79-3			
Pan-X 3400	1.50-3				1.47-3				1.38-3			
* SO-180	5.99-3	8.46-3	3.04-3	2.60-3	5.88-3	8.30-3	2.98-3	2.55-3	5.52-3	7.78-3	2.80-3	2.40-3
* SO-121	4.16-3	3.18-3	2.43-3	1.24-2	4.08-3	3.12-3	2.39-3	1.21-2	3.83-3	2.93-2	2.24-3	1.14-2

* Proposed for use.

7.0 PROTON SPECTROMETER

The Proton Spectrometer (PS) is designed to detect energetic protons and electrons, and to give a measure of the spectral characteristics of each component. The instrument is unusual in that it is sensitive to protons with energies up to 400 MeV, whereas most earlier measurements cut off at 100 to 200 MeV. Film damage in heavily shielded regions such as the OWS vault is due largely to protons whose initial energy lies between 200 and 400 MeV. The object of this effort is to determine whether PS data taken early in the mission can be used to correct preflight dose and damage estimates.

Proton environment data is provided by J. J. Wright and M. O. Burrell.[3] A 235 n.mi. circular orbit inclined at 50 degrees was selected. The starting point is 0 degrees latitude, 0 degrees longitude. The initial direction is approximately northeast. The position is calculated at intervals of 62.4 seconds over a time period of 6 days, 10 hours. Proton flux data for this orbit is shown in Section 3. At each point, several parameters are calculated and punched on cards if the proton flux above 50 MeV is greater than 3 protons/cm^2 - sec. A total of 701 points satisfy the criterion.

Each punched card contains the following data.

- Time - T
- Altitude - H
- Latitude - Θ
- Longitude - ϕ
- Three components of the magnetic field vector in earth spherical coordinate system - B_r, B_θ, B_ϕ
- Proton flux above 50 MeV - $\underline{\Phi}$ (> 50)
- Proton spectral parameter - E'

The integral proton flux above energy E is:

$$\Phi\ (> E) = \Phi\ (> 50) \exp(-E/E')$$

This expression is differentiated to permit evaluation of the proton flux, differential in energy, at 9 energies ranging from 20 to 400 MeV. The intermediate energies are chosen to provide equal logarithmic energy intervals, thus approximating the 8 energy bin format of the PS.

The approach outlined below examines the possibility of correlating the measured environment with the Vette model environment. It provides no corrections for uncertainties in radiation transport techniques, geometry models, and film damage functions. Furthermore, it does not test the validity of the isotropic flux assumption used in the transport calculations, though it could be extended to include and correct that assumption.

A large part of the radiation-induced film damage is expected to be caused by protons in the South Atlantic magnetic anomaly. The protons are confined to pitch angles which lie within 30 degrees of the plane perpendicular to magnetic field lines. This distribution comprises 34 percent of the total solid angle about a point. The PS has an acceptance cone with a 22.5 degree half angle, which corresponds to 3.8 percent of the total solid angle. It is necessary to correlate the PS axis with the local field line direction and flux intensity in order to account for proton anisotropy and instrument directionality.

A newly written computer program, FOPSO (Flux Observed by Proton Spectrometer in Orbit), performs several manipulations on the environment data. The vector components of B are transformed from an earth-rotating spherical to a Cartesian coordinate system. A second transformation is applied to convert to an arbitrary celestial Cartesian coordinate system which is fixed relative to distant stars.

The direction of the PS axis in this celestial coordinate system is changing by less than one degree per day due to the earth revolving about the sun once per year. A time-dependent transformation accounts for this correction. The above assumption neglects pitch, roll, and yaw drifts of the Skylab.

The cosine of the angle between the PS axis and the field line B is computed from the scalar product of unit vectors along these directions. A table look-up then determines the fraction of the omnidirectional proton flux within the acceptance cone of the PS, assuming azimuthal symmetry about the field line. The pitch angle distribution is represented by a gaussian with deviation equal to 7.5 degrees, according to the data of Heckman and Nakano[7] for an altitude of 364 km.

Appropriate integrals over time and energy are performed to yield total and PS-intercepted proton flux, differential in energy, as well as total and PS-intercepted flux in 8 energy bins.

Results

The Skylab orbit encounters protons in the South Atlantic anomaly. A check was made to determine the adequacy of the magnetic field model in this region. The basic representation used in the study is a 48 term spherical harmonic expansion for 1960. A partial recalculation was made with a 100 term expansion for 1965. The PS responses agree within 3 percent. It is concluded that no improvement would result by going to a higher order spherical harmonic expansion of the geomagnetic field.

The effect of initial pointing direction upon PS response during a 6 day, 10 hour period is shown in Figure 7.1. The coordinates are latitude and longitude of the initial orientation in the arbitrary celestial system described above. A southward drift of one degree per day is assumed.

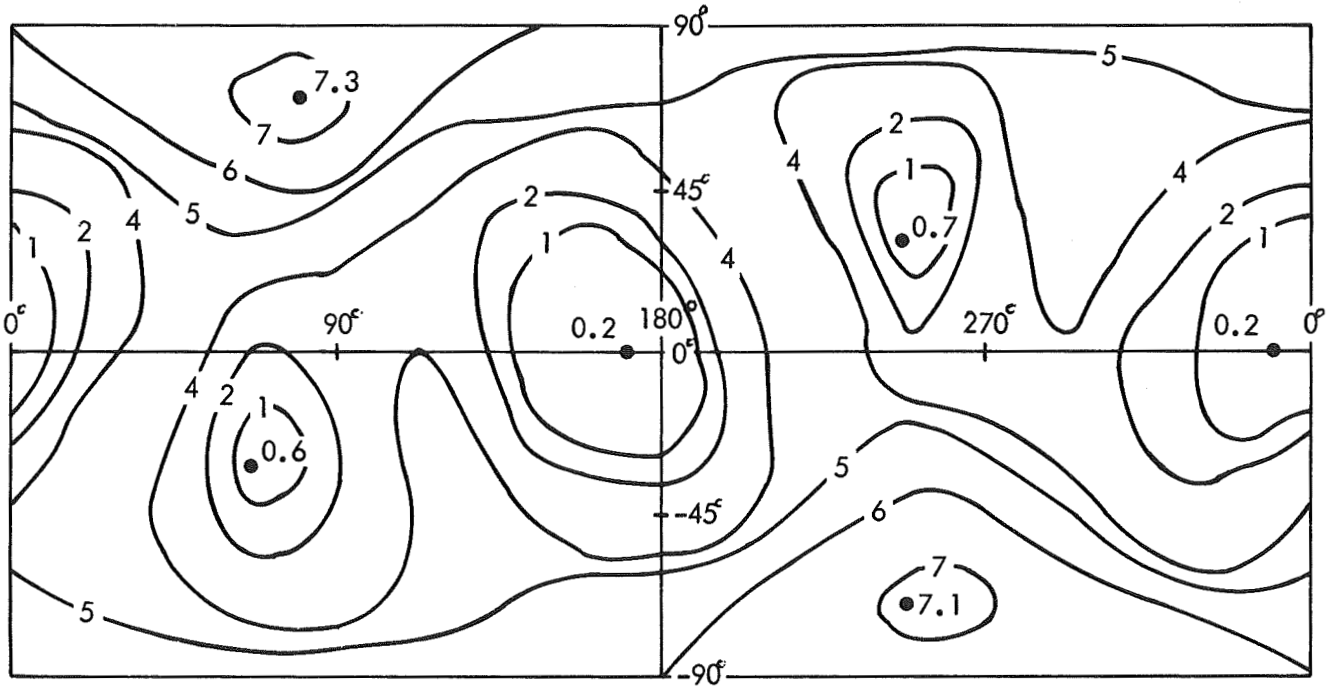

Coordinates are latitude and longitude in an arbitrary celestial system. A one degree per day southward drift is assumed. Values are counts in units of 10^7.

FIGURE 7.1: CONTOUR MAP OF PROTON SPECTROMETER TOTAL COUNTS DURING A 6.5 DAY PERIOD AS A FUNCTION OF INITIAL POINTING DIRECTION

At the south pole, longitude is incremented by 180 degrees and the drift is continued in a northward direction.

Approximately 400 cases have been processed. Based upon these data, contour lines of PS total counts from 20 to 400 MeV are shown. The total flux in this interval is 86.0×10^7 protons/cm^2.

Computed response of the instrument varies from 0.25 percent to 8.4 percent of the total environment during the 6-1/2 day period. Expected cluster drift from the desired orientation is not presently available, but could be as large as 30 degrees between attitude corrections. Such a drift could change PS response significantly. It therefore appears necessary to correlate PS orientation with its response during anomaly passes.

Can the PS response, correlated with cluster orientation, be used to correct preflight dose predictions? Additional information is necessary to answer this question. In lightly shielded locations such as a boom-mounted camera outside the Scientific Airlocks, incident protons below 100 MeV dominate. In heavily shielded locations such as part of the OWS vault (3.4" Al), incident protons between 200 to 400 MeV dominate. The proton spectrum within the acceptance cone of the PS as a function of initial pointing direction will be compared to the omnidirectional spectrum in order to provide guidance in answering the above question.

The top curve in Figure 7.2 shows the omnidirectional flux from 20 to 400 MeV corresponding to 86.0×10^7 protons/cm^2. The other curves show the spectrum entering the acceptance cone for five initial pointing directions. Three curves, labeled 7.3, 4.0, and 2.3×10^7 p/cm^2, exhibit the same spectral shape possessed by the omnidirectional flux. At 1.2 and 0.23×10^7 p/cm^2, the spectrum is softer. The relative number of protons in eight energy intervals is shown in Figure 7.3 for the two extreme cases. Note that the numbers of protons above 275 MeV which enter one nappe of the acceptance cone per unit area differs greatly in the two cases.

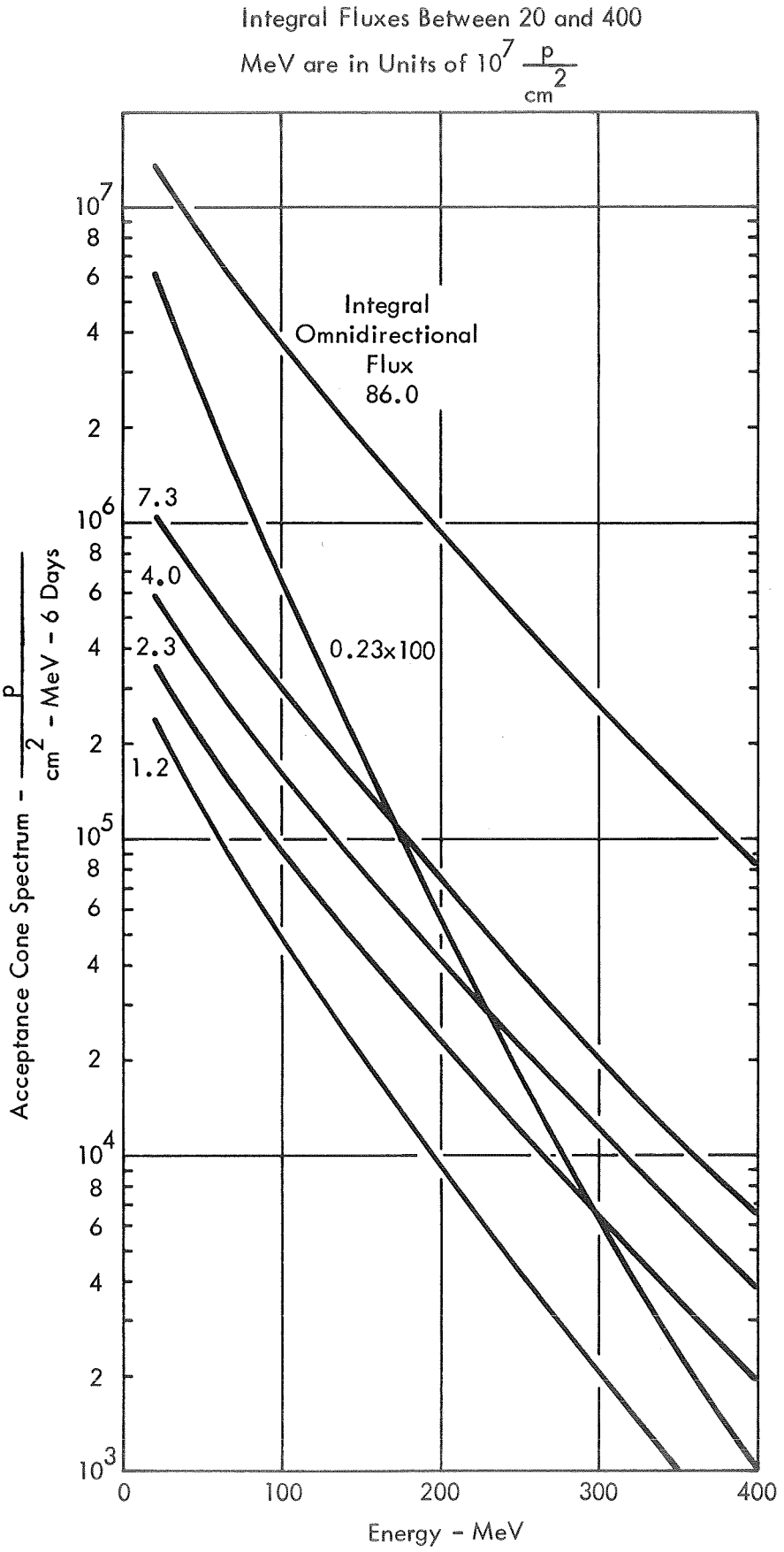

FIGURE 7.2: PROTON SPECTRUM ENTERING THE ACCEPTANCE CONE OF THE PROTON SPECTROMETER

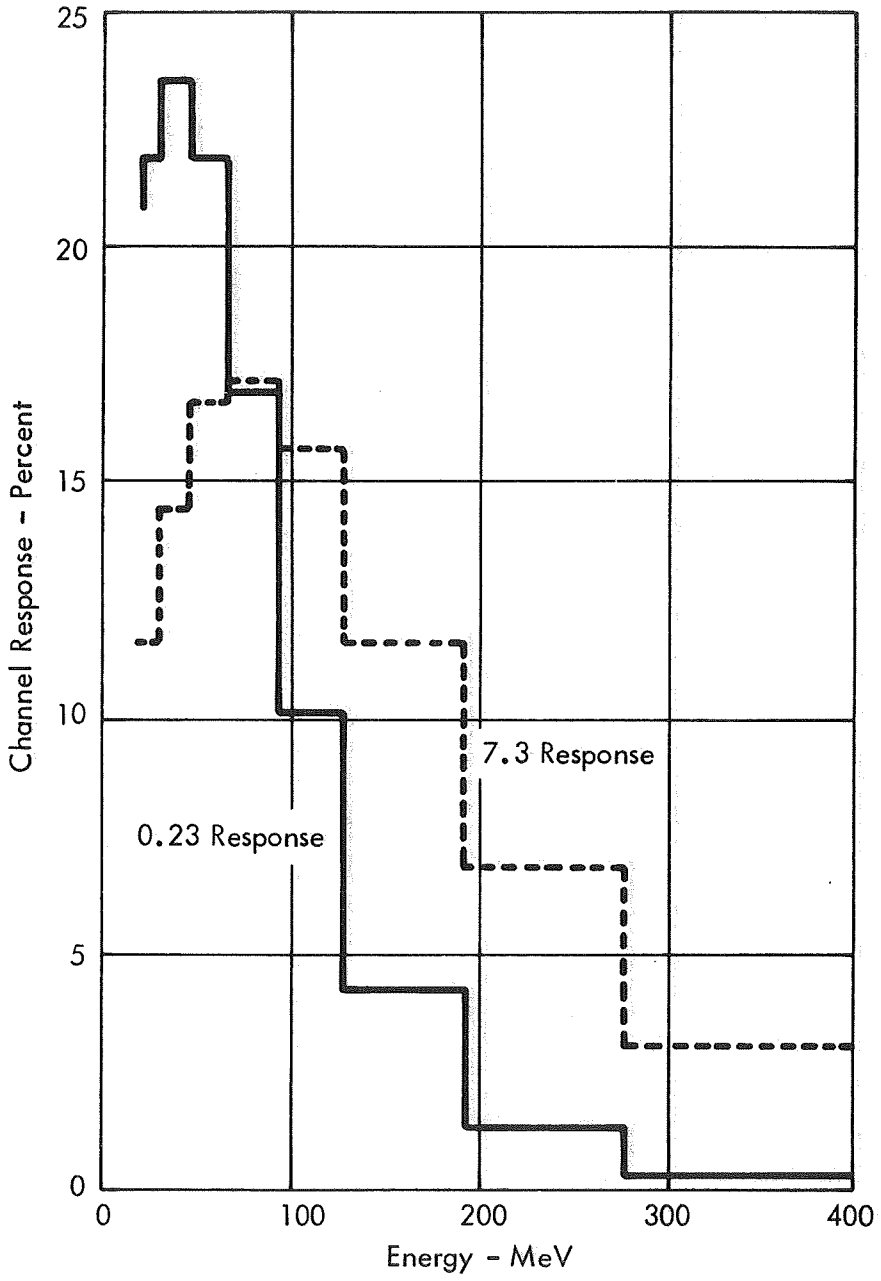

FIGURE 7.3: SPECTRAL SHAPE FOR TWO INITIAL POINTING DIRECTIONS

- Hard spectrum

  2.9% of $7.3 \times 10^7 = 2.1 \times 10^6$ protons

- Soft spectrum

  0.2% of $0.23 \times 10^7 = 4.6 \times 10^3$ protons

Dr. Vette's warning against using results from his trapped radiation belt environment models to prove hypotheses concerning the trapped radiation belts should be kept in mind in analyzing the results presented above. The radiation belt models probably give good estimates of the trapped proton omnidirectional flux below 200 MeV in the Skylab orbit as evidenced by insensitivity to the magnetic field representation and good (20 percent) agreement at peak fluxes with preliminary results of a recent Air Force experiment.[3] However, data above 200 MeV are sparse and computed results should be regarded with caution.

Two approximations are peculiar to the present analysis. Both arise from the necessity of converting omnidirectional flux to flux differential in angle. First, an energy-independent pitch angle distribution is chosen. The distribution is a Gaussian of the form $f(X) = \exp(-x^2/\sigma^2)$, where X is the angle from the plane perpendicular to the local field line and σ is 7.4 degrees from the work of Heckman and Nakano[7] at 364 km. Second, the east-west asymmetry is neglected. This asymmetry is due to the fact that protons moving east in the South Atlantic mirroring region have their guiding centers at higher altitudes and are less attenuated by the atmosphere. At 364 km, the eastward-traveling flux above 60 MeV is a factor of 2.3 larger than the westward-traveling flux, and the ratio is strongly dependent upon energy. The effect should be markedly less at 436 km (235 n.mi.) because the atmospheric scale height is 62 km.

The first approximation above tends to steepen the gradient of the proton flux contours in Figure 7.1. The second approximation is more serious. It leads to a false near-symmetry about the origin and distorts the spectrum somewhat for the 6-1/2 day period sampled.

Conclusions

With the above cautions in mind, several conclusions may be drawn.

1. Over the eight month duration of the mission, all orientations of the PS axis with respect to the field lines in high flux regions will be well sampled. A good omni-directional spectrum may then be derived from the data.

2. For sample periods less than approximately two months, corrections to the proton flux environment model will require correlations between local field lines and PS attitude, as well as position.

3. For sample periods less than one month, an additional condition is necessary before the desired analysis may be performed, i.e., the PS axis must be aligned nearly perpendicular to local field lines during several passes through the high-flux region. This condition may be met by fortuitous happenstance, by deliberate cluster reorientation, or by sampling over a longer time period.

4. Care should be used in interpreting experimental spectra which may be distorted by the east-west asymmetry. The two low-energy bins (20 - 45 MeV) should not exhibit this effect because the gyroradius of these protons is small. The two high-energy bins (190 - 400 MeV) should see minimal east-west asymmetry because the PS samples both nappes of the acceptance cone above 200 MeV. The four intermediate-energy bins may exhibit the east-west effect noticeably.

5. PS data taken during the first week or two of the SL-1 mission may be used to correct preflight estimates of film damage provided that favorable cluster attitude is achieved and a detailed data analysis is performed in near-real-time.

APPENDIX

An experimental study of radiation effects to 13 Skylab candidate film types has been conducted by Mr. Richard R. Adams, Langley Research Center, NASA. Mr. Adams' results were not available in time to be incorporated into the present study. A portion of his data are included in this Appendix at the request of the Contracting Officer's Representative for the benefit of the Skylab film-using community. As Mr. Adams notes, these data are preliminary in nature.

LET.	EMULSION NUMBER	TARGET SPEED	Co-60 RADS AIR		PROTON RADS AIR		2850°K LIGHT		PROCESSING			
			MIN	MAX	MIN	MAX	ADDED FILTER	LOG E (mcs)	CHEM	TIME (min)	TEMP (°F)	COMMENTS
B	101-01-24	N/A	.270	21.1	.078	206	N/A	N/A	D-19 (1:1)	4.0	68	D.W. presoak
C	2485-25-1M	ASA-5000	.035	1.39	.039	10.2	C-5900	$\bar{2}$.97	D-19	12.0	75	N_2-Burst, 3 sec/8 sec
D	103a-0(UV)	N/A	.174	8.36	.078	206	C-5900	.152	D-19	4.0	68	N_2-Burst, 1 sec/10 sec Cyclohexane, Borax
E	2484-097-Z	Determine by test	.070	2.79	.065	53.2	C-5900	$\bar{2}$.97	D-19	5.0	75	N_2-Burst, 1 sec/10 sec
G	3401-352-2	AEI-64	.261	18.1	.157	103	C-5900	.143	D-19	8.0	68	N_2-Burst, 1 sec/10 sec
L	026-02-02	AEI-20	1.57	70.0	.392	360	C-5900	.143	D-19	8.0	68	N_2-Burst, 1 sec/10 sec
M	3414	AEI-1.6	17.8	306	7.01	3240	C-5900	1.50	D-19	8.0	68	N_2-Burst, 1 sec/10 sec
COLOR:												
A	5256-726-31B	ASA-64	2.11	118	.784	554	C-5900	.014	ME-2A	3.4 FPM	98	MSC, High Speed
F	SO-242-5-1	AEI-2	10.6	455	3.05	1860	C-5900	1.50	ME-4	15 FPM	98	MSC, Houston
H	SO-168-007-31Z	ASA-160	.783	42.3	.235	277	C-5900	$\bar{1}$.75	ME-4	93 FPM	98	MSC, RAM
I	SO-168-007-31Z	ASA-320	.783	42.3	.235	277	C-5900	$\bar{1}$.49	ME-4	63 FPM	98	MSC, RAM
J	SO-168-007-31Z	ASA-500	.783	42.3	.235	277	C-5900	$\bar{1}$.37	ME-4	52 FPM	98	MSC, RAM
K	2443-9-1	AEI-10 (thru#12	1.83	85.1	.392	443	C-5900 Wrat #12	.706	EA-5	9 FPM	113	MSC, 1811M

SUMMARY TABLE

SUMMARY

The attached data represents the preliminary results of an investigation conducted by the Langley Research Center in response to a request by the Marshall Space Flight Center (S&E-ASTN-DIR-70-445) in support of Skylab. The photographic effects of ionizing radiation have been determined for 13 OWS candidate film types listed in the summary table.

The data is considered representative of those samples tested under identical exposure, processing, and readout conditions within the limitations outlined below. The test films, obtained from the most readily available sources, were not necessarily representative of the manufacturers best product, since in many cases their previous history is unknown.

Gamma-ray exposures were made at about 1 rad (in air) per hour on the Langley Co-60 Sensitometer and are considered to be accurate to within ±10%, although a photographic comparison against the Eastman Kodak Co-60 facility agreed to better than ±5%.

Proton exposures were made using the external beam of the Harvard University Cyclotron* and the medical collimator. Proton doses are considered to be accurate to ±8% or ±0.05 rads in air, whichever is greater, and have been corrected for slight beam intensity non-uniformity.

Light exposures were made using the Langley Sensitometer at an exposure time of 1/10 second. "Simulated Daylight" is interpreted as 2850 degree Kelvin tungsten light modulated by a Corning 5900 filter polished to a thickness of 4.50 millimeters. Photopic intensity measurements of the light source were repeatable to the equivalent of 1/6 of an f/stop and are considered accurate to within 1/3 of an f/stop at this writing. Intensities were varied by the use of calibrated apertures rather than neutral density filtration.

Color film types A,F,H,I,J, and K were processed by the Manned Spacecraft Center Photographic Division as specified. All remaining black-and-white emulsions were sensitometrically processed at Langley using commercially prepared D-19 developer and a 3½ gallon sink-line tank system with nitrogen agitation as specified.

Color film densities were read using a McBeth TD-203 densitometer located in the Langley Photographic Branch through a 4 millimeter aperture and "Status A" filters. Repeatability between successive readings was noted to be within 0.02 density units. A comparison taken between density readings on a test strip at MSC and Langley agreed to within 0.04 density units except for those readings through the blue filter pack at densities greater than unity, where the Langley readings were up to 0.07 density units lower than those of MSC.

---

* Owned by the U.S. Office of Naval Research and operated by the Department of Physics, Harvard University.

Black-and-white densities were read on a McBeth TD-102 densitometer through a 2 millimeter aperture and a 106 filter. Repeatability between successive readings was again within 0.02 density units and accuracy is considered to be 0.04 density units at this writing.

Smooth curves were sketched through plotted points with the above limitations in mind where at all possible.

DISCUSSION OF RESULTS

The discussion which follows is the result of a "quick-look" approach to the attached preliminary data, the object being to point out general overall trends between film types and suggest a rationale for these trends. Final data analysis will result in a tightening of the conservative error limits used here which hopefully will accentuate the noted trends while exposing other less obvious ones which may contribute to Langleys primary objective of reducing the photographic effects of ionizing space radiation.

It has been found in all cases (with the possible exception of SO-242, discussed later) that of the three radiation types studied, the Co-60 gamma-rays were the most effective per unit dose in producing damage and the 55 MeV protons the least. This is consistent with previous observations[1] which are explained in terms of a localized increased dose saturation effect as the radiation LET increases.

The "single hit" theory predicts a unity slope at low net densities for the radiation response curves (log net density versus log rads in air) and have been drawn as such within the limitations discussed in the summary for all types except D, K, L, and M. Types K, L, and M depart measurably from the above toward greater slope and have been drawn accordingly, the rationale being that for these slower emulsions the conservative error limitations imposed at this writing were exceeded by a trend toward a "multiple hit" phenomenon[2]. The response curve slope of type D was found to be less than unity which possibly can be attributed to fogging of adjacent grains by the non-directional nature of fluorescence produced by radiation excitation of the UV overcoat. This is further supported by a measureable difference in slope between the Co-60 gamma-ray curve and the proton curves, while for all other types no such slope differential was noted.

---

[1]Herz, R.H. "The Photographic Action of Ionizing Radiations" Wiley Interscience - 1969, pp 179-186

[2]Huff, K.E., Cleare, H.M. "Effects of Proton Exposure on Several Kodak Black-and-white Films" Eastman Kodak Internal Paper, 1968

Another general tendency, although less apparent, has been noted and that is that the difference in dose required to produce the same photographic effect for the three radiation types studied increased with increasing film sensitivity, which might be expected from considerations of realtive grain size, distance between grains, and localized saturation as previously mentioned.

The anomoly noted in SO-242 mentioned above has not been clearly explained at this time. It should be mentioned, however, that processing difficulties left severe damage to the film in localized areas. It was noted that the Dmax measured between proton exposures was often considerably greater than that of the unexposed control. This appears to be the rule rather than the exception for reversal-processed emulsions.

Light exposures were not attempted on type 101-01 due to the extreme sensitivity of the emulsion to pressure and abrasion and the questionable value of daylight exposures for this film type anyway.

The data for type 2443 was only partially read using the blue filter pack since the Langley TD-203A densitometer is not equipped with a null balance feature, limiting the maximum density readable to 4.00 density units. The blue Dmax used was taken from MSC readings.

Richard R. Adams

Richard R. Adams
703-827-2466 MS/234
NASA Langley Research Center

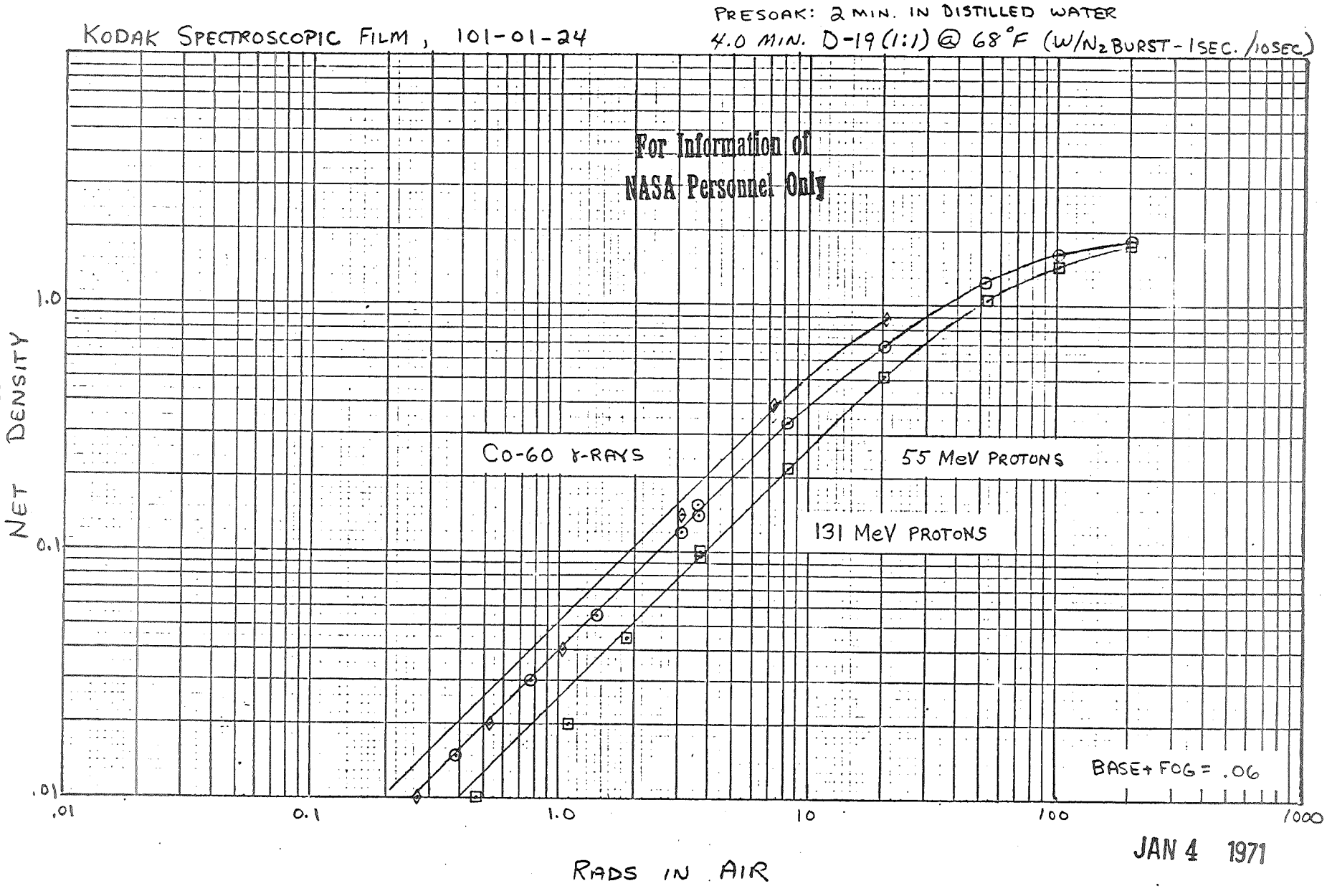
KODAK SPECTROSCOPIC FILM, 101-01-24
PRESOAK: 2 MIN. IN DISTILLED WATER
4.0 MIN. D-19 (1:1) @ 68°F (W/N2 BURST - 1SEC. /10SEC.)
For Information of
NASA Personnel Only
Co-60 γ-RAYS
55 MeV PROTONS
131 MeV PROTONS
BASE+FOG = .06
NET DENSITY
1.0
0.1
.01
.01
0.1
1.0
10
100
1000
RADS IN AIR
JAN 4 1971

KODAK HIGH SPEED RECORDING FILM, 2485-25-1M 12.0 MIN D-19 @ 75°F (W/N_2 BURST AGIT. 1SEC/10SEC)

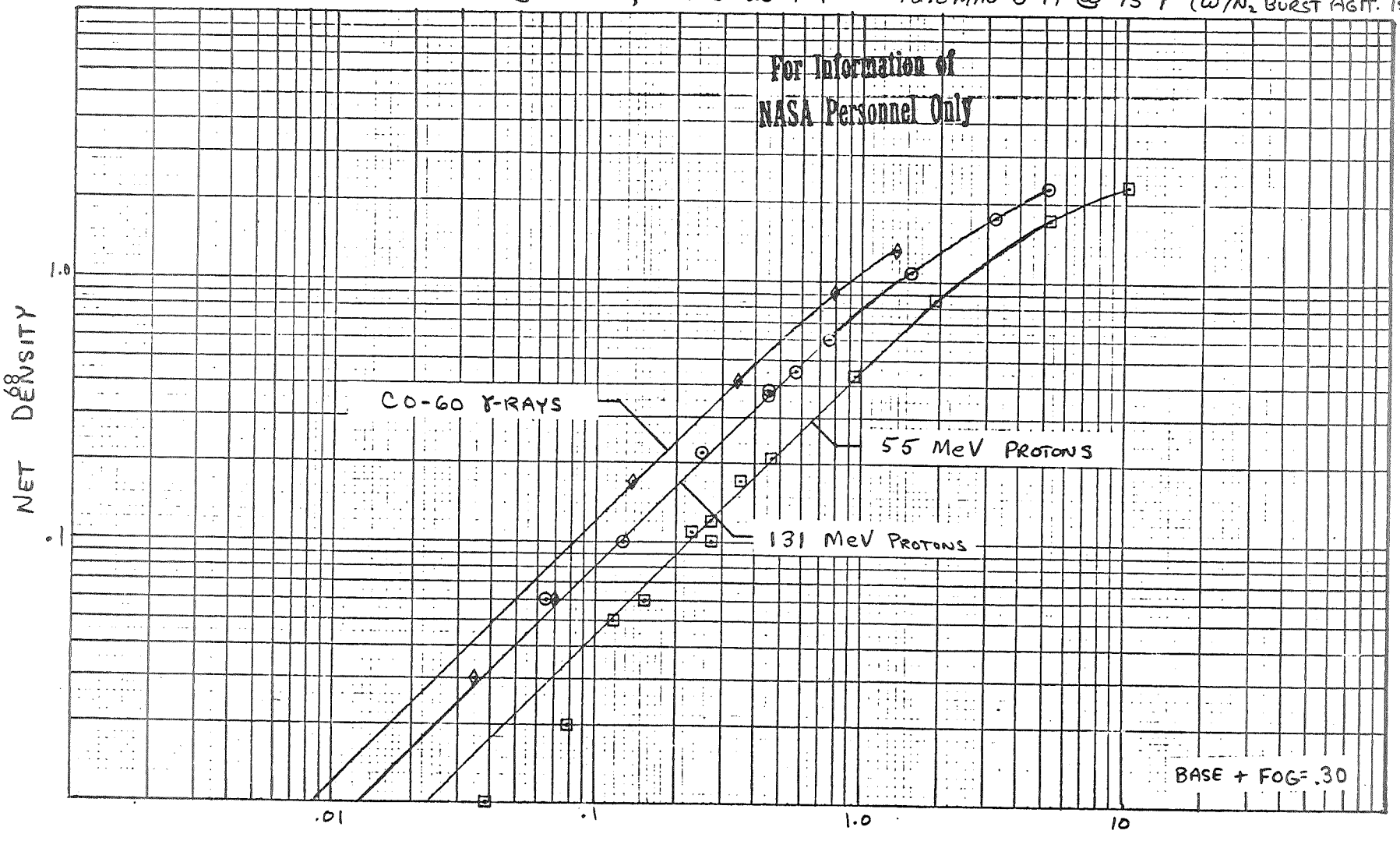

JAN 25 1971
P R Adams
LRC

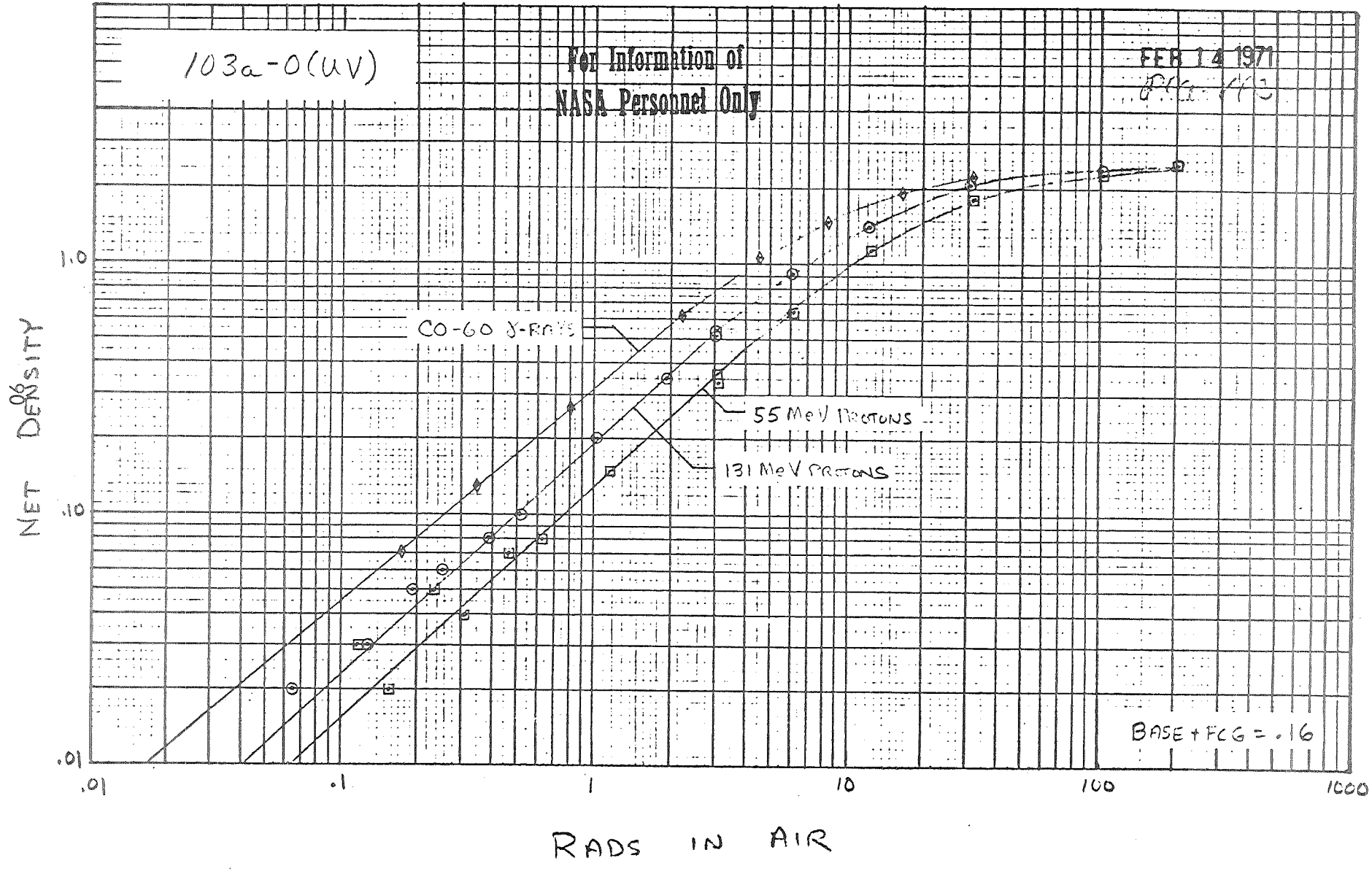
103a-0(UV)
For Information of
NASA Personnel Only
FEB 14 1971
CO-60 γ-RAYS
55 MeV PROTONS
131 MeV PROTONS
BASE + FOG = .16
NET DENSITY
1.0
.10
.01
.01
.1
1
10
100
1000
RADS IN AIR

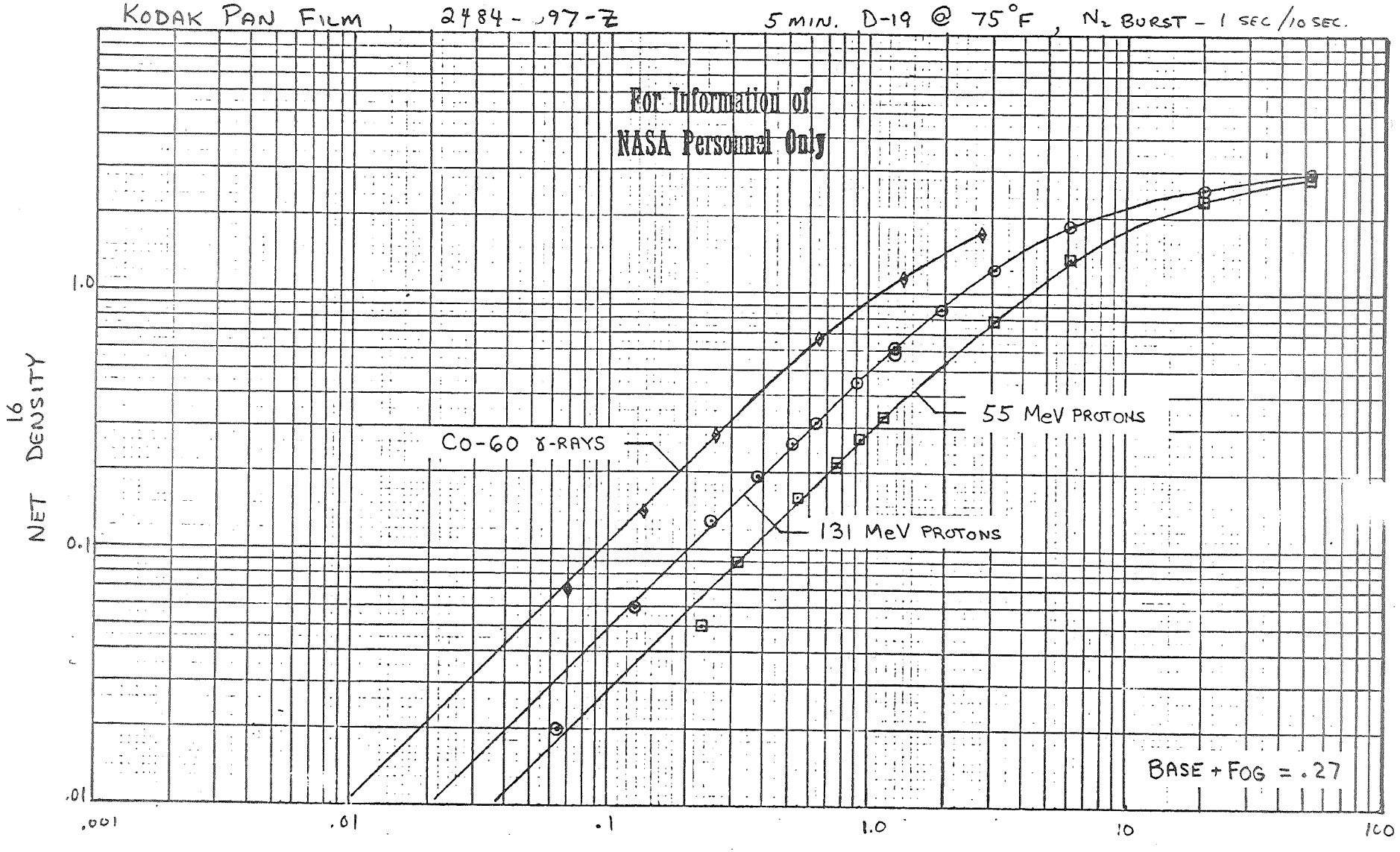

JAN 26 1971
R.P. Adams
LRC

KODAK PLUS-X AERIAL FILM, 3401-352-2

8.0 MIN. D-19 @ 68°F (w/N_2 BURST AGIT. 1 SEC/10SEC

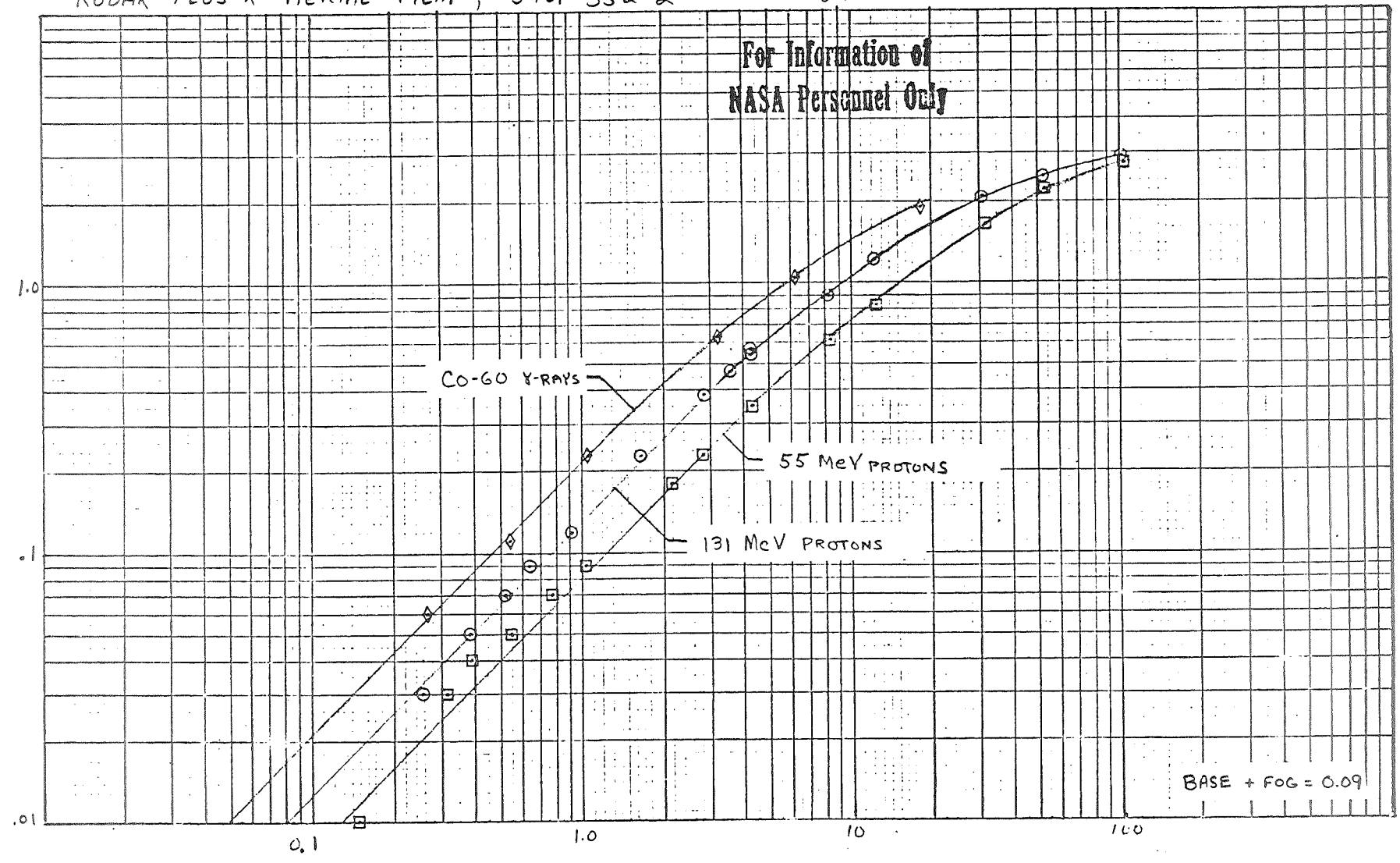

JAN 19 1971

R R Adams
LRC

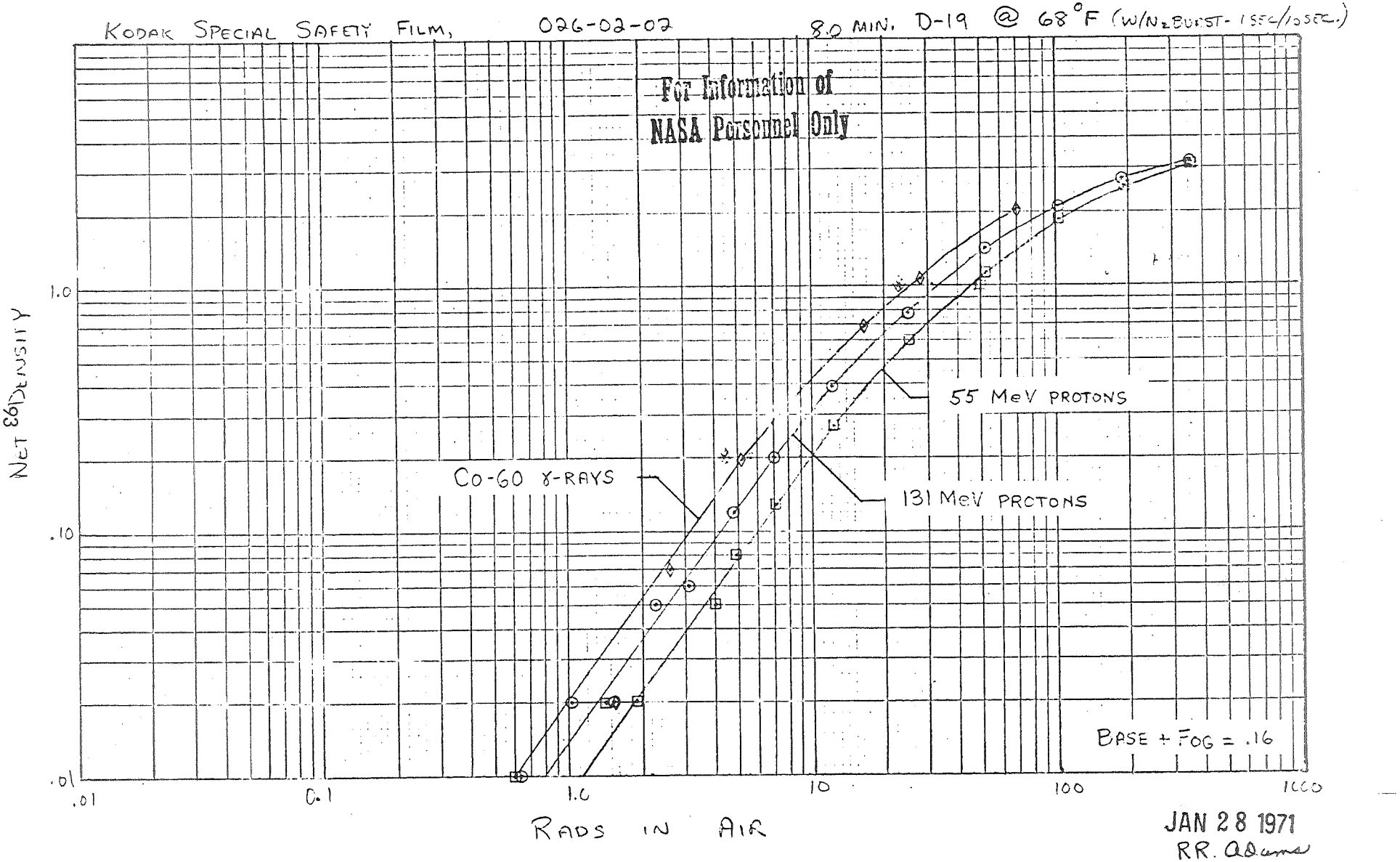
KODAK SPECIAL SAFETY FILM, 026-02-02
8.0 MIN. D-19 @ 68°F (W/N₂ BURST - 1 SEC/10 SEC.)
For Information of
NASA Personnel Only
NET ΔD DENSITY
1.0
.10
.01
.01
0.1
1.0
10
100
1000
RADS IN AIR
55 MeV PROTONS
Co-60 γ-RAYS
131 MeV PROTONS
BASE + FOG = .16
JAN 28 1971
RR. Adams
LRC

KODAK HIGH DEFINITION AERIAL FILM, 3414 8.0 MIN. D-19 @ 68°F (N_2 BURST - 1 SEC EACH 10 SEC)

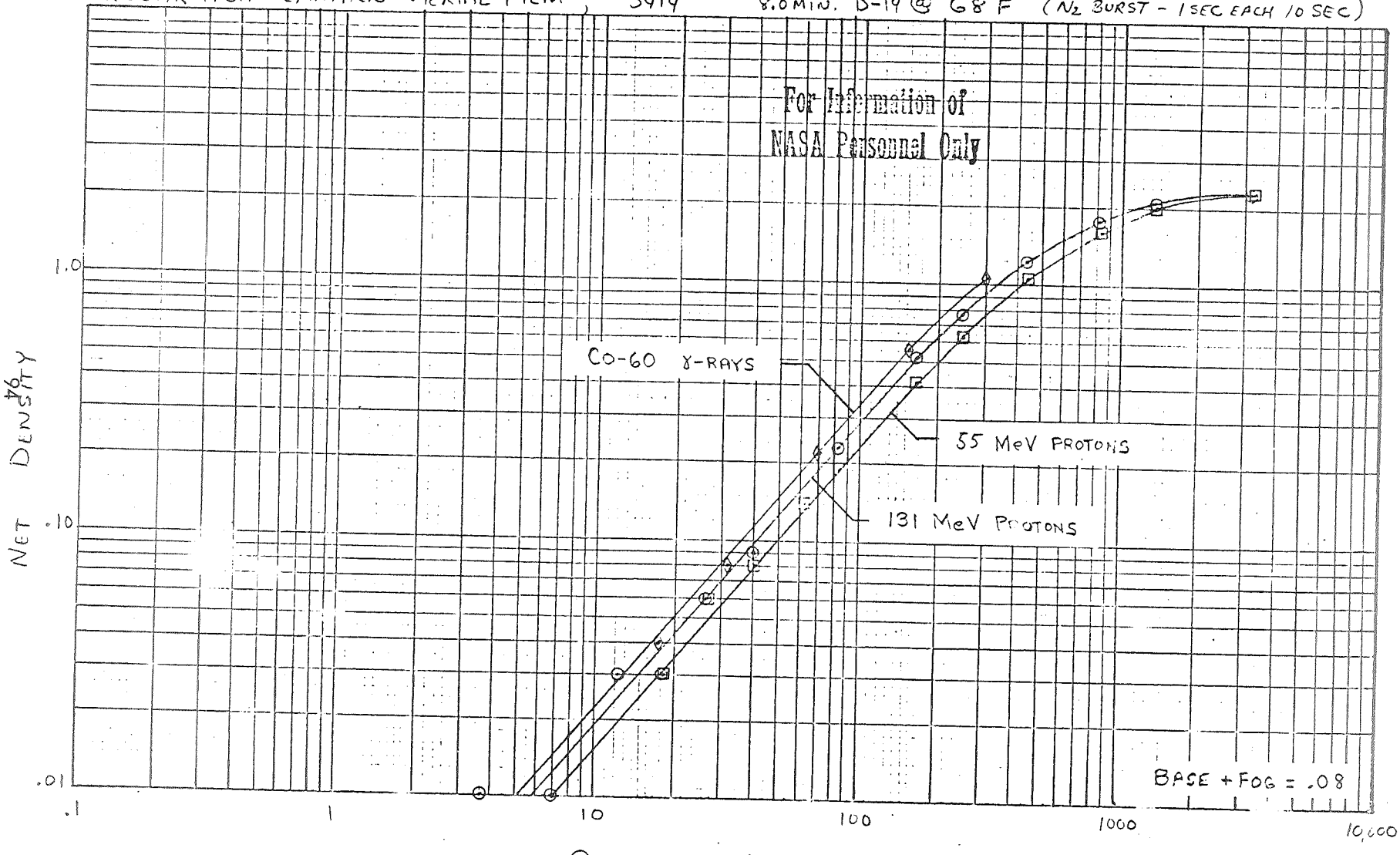

JAN 28 1971
R.R. Adams
LRC

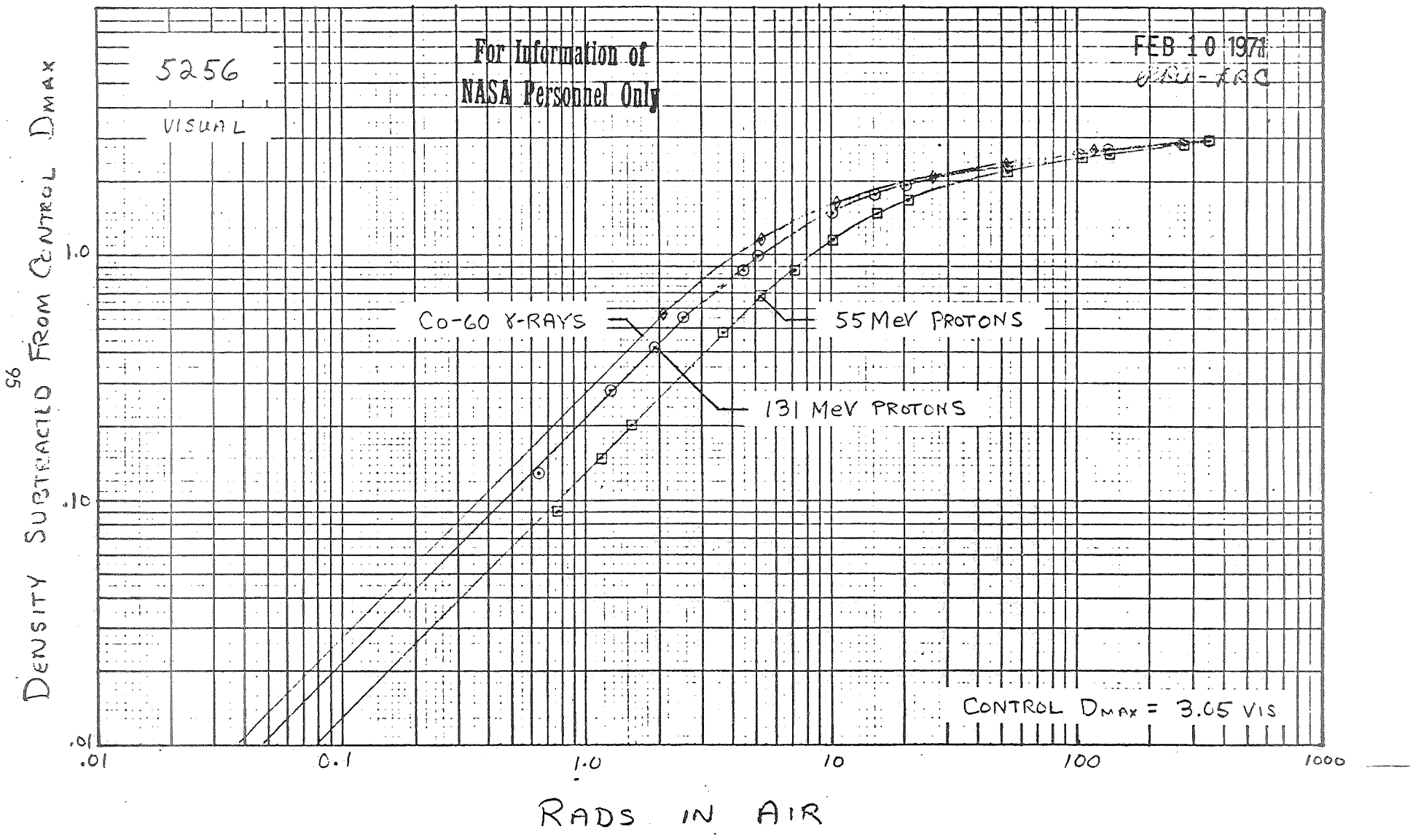
5256
VISUAL
For Information of
NASA Personnel Only
FEB 10 1971
Co-60 γ-RAYS
55 MeV PROTONS
131 MeV PROTONS
CONTROL DMAX = 3.05 VIS
DENSITY SUBTRACTED FROM CONTROL DMAX
RADS IN AIR
.01
.10
1.0
.01
0.1
1.0
10
100
1000

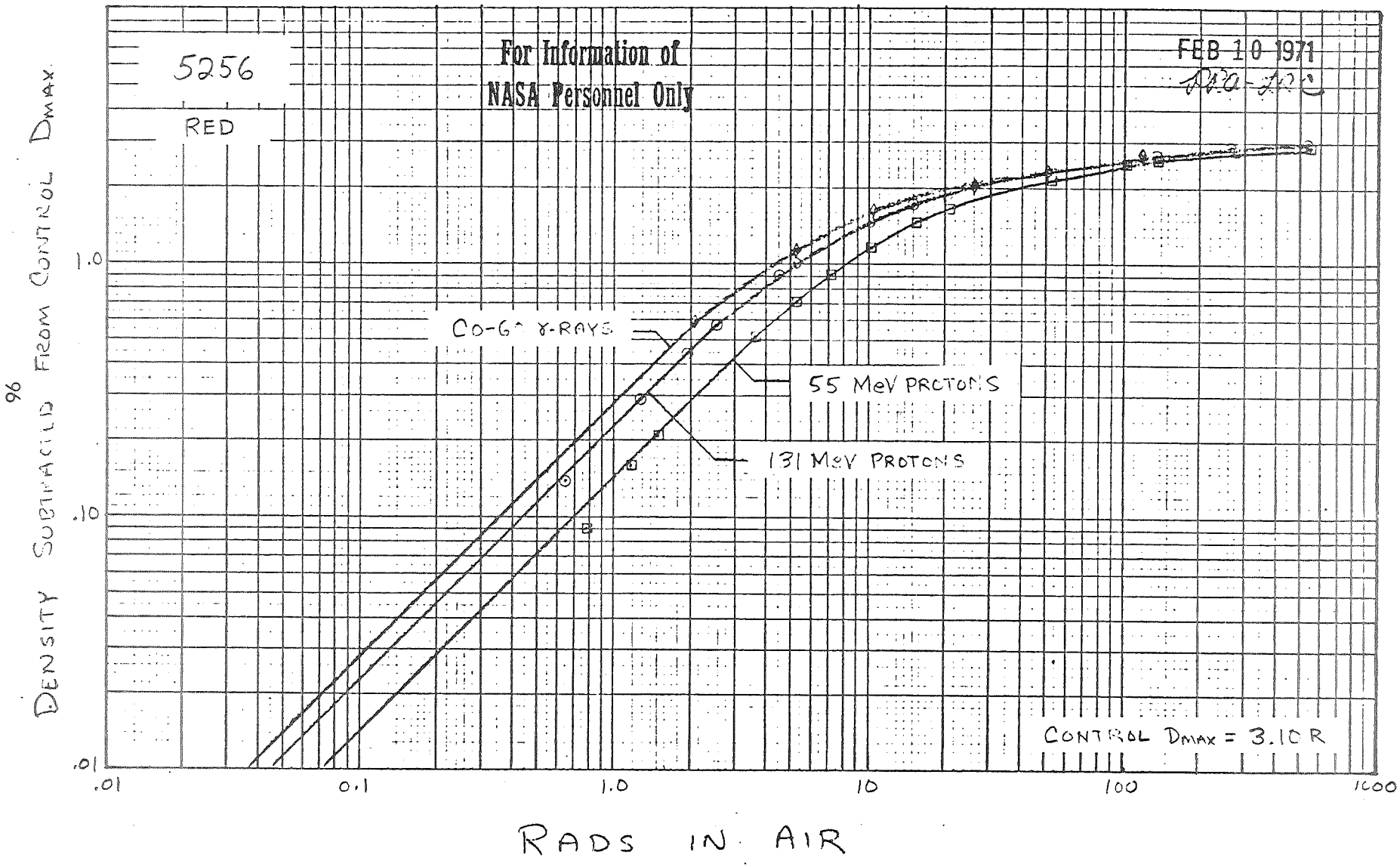
5256
RED
For Information of
NASA Personnel Only
FEB 10 1971
Co-60 γ-RAYS
55 MeV PROTONS
131 MeV PROTONS
CONTROL DMAX = 3.10 R
DENSITY SUBTRACTED FROM CONTROL DMAX
1.0
.10
.01
.01
0.1
1.0
10
100
1000
RADS IN AIR

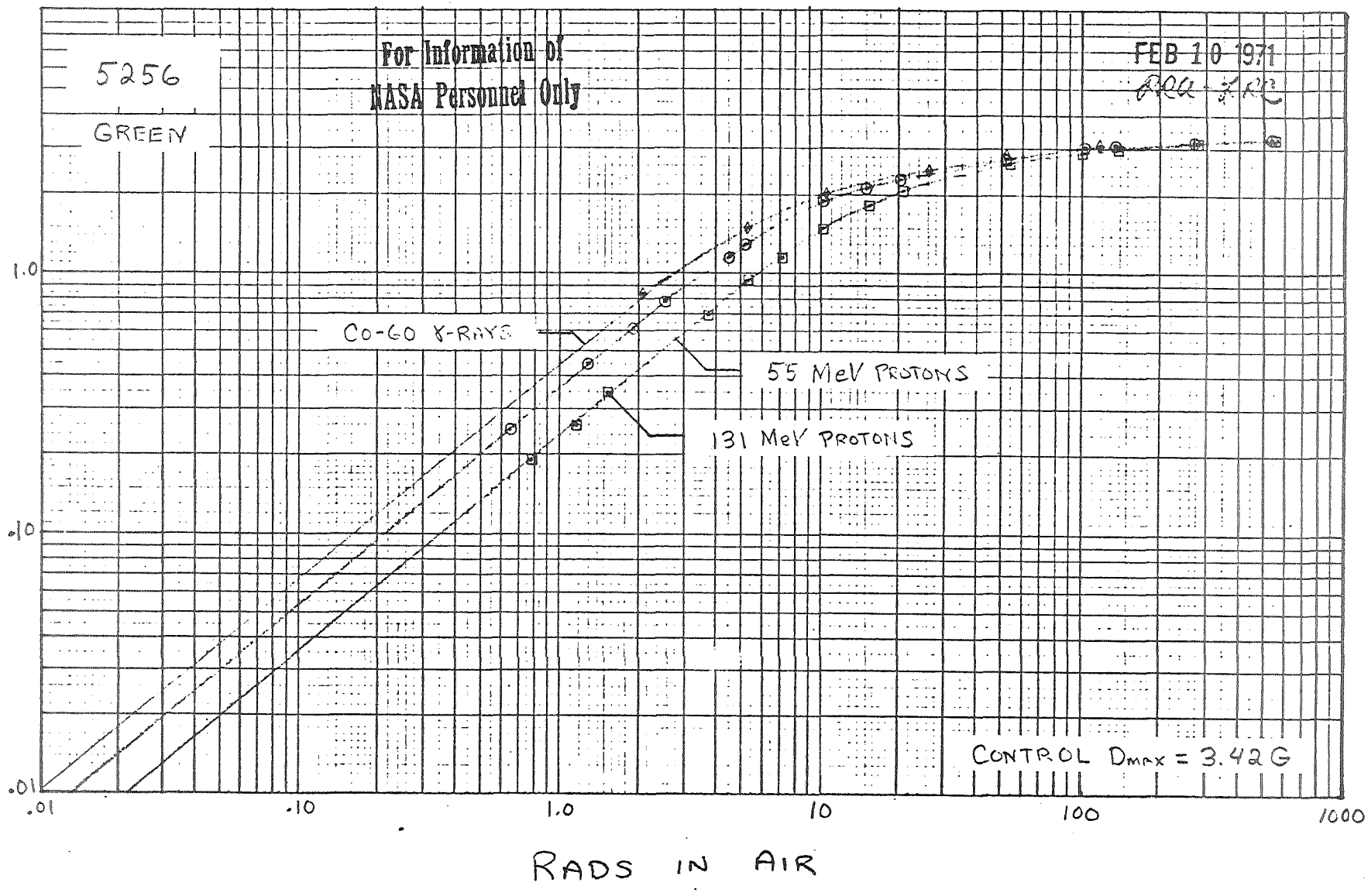
5256
GREEN
For Information of
NASA Personnel Only
FEB 10 1971
Co-60 X-RAYS
55 MeV PROTONS
131 MeV PROTONS
CONTROL Dmax = 3.42 G
DENSITY SUBTRACTED FROM CONTROL Dmax
1.0
.10
.01
.01
.10
1.0
10
100
1000
RADS IN AIR

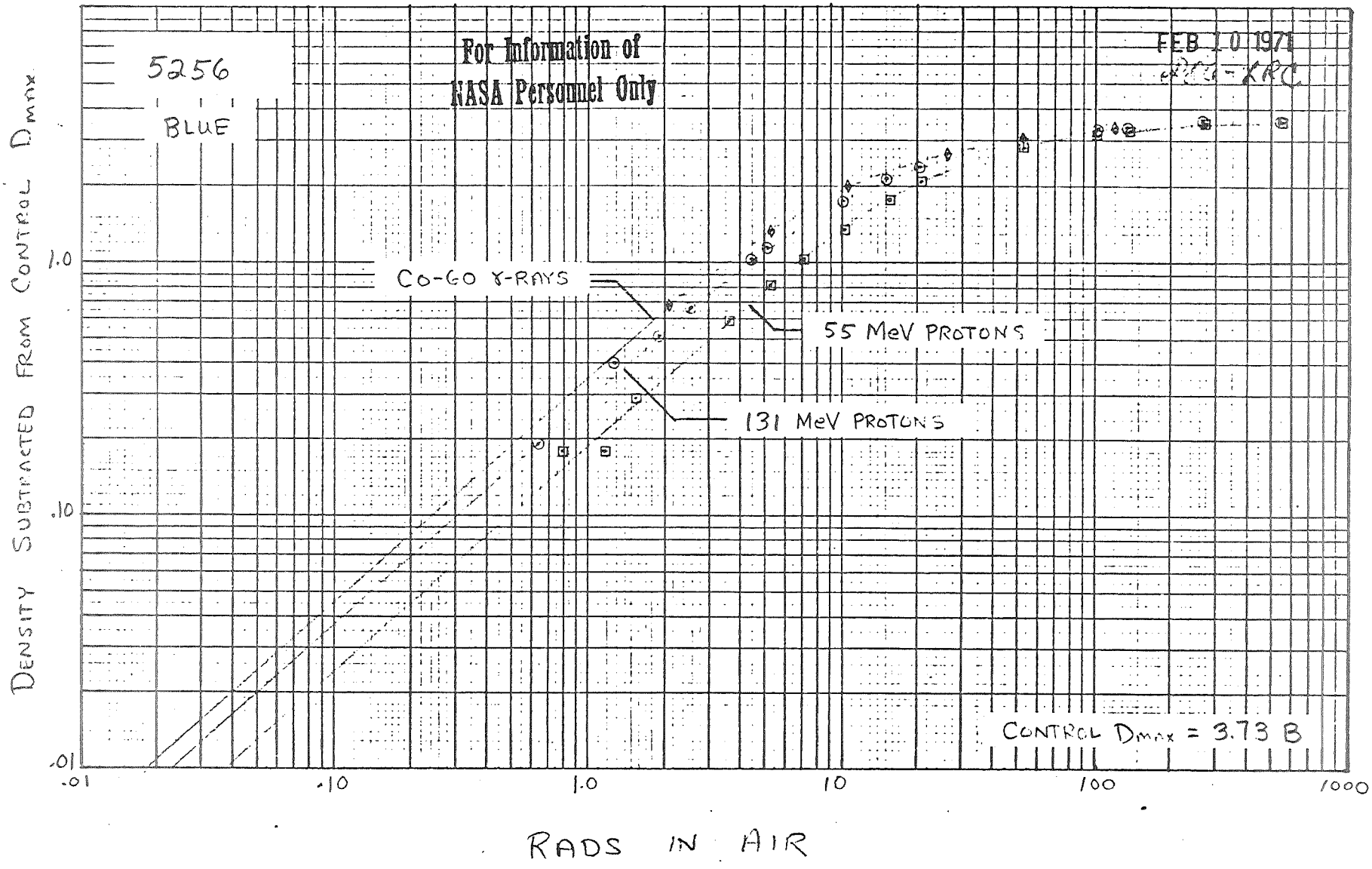
For Information of
NASA Personnel Only
5256
BLUE
FEB 10 1971
Co-60 γ-RAYS
55 MeV PROTONS
131 MeV PROTONS
CONTROL Dmax = 3.73 B
DENSITY SUBTRACTED FROM CONTROL Dmax
1.0
.10
.01
.01
.10
1.0
10
100
1000
RADS IN AIR

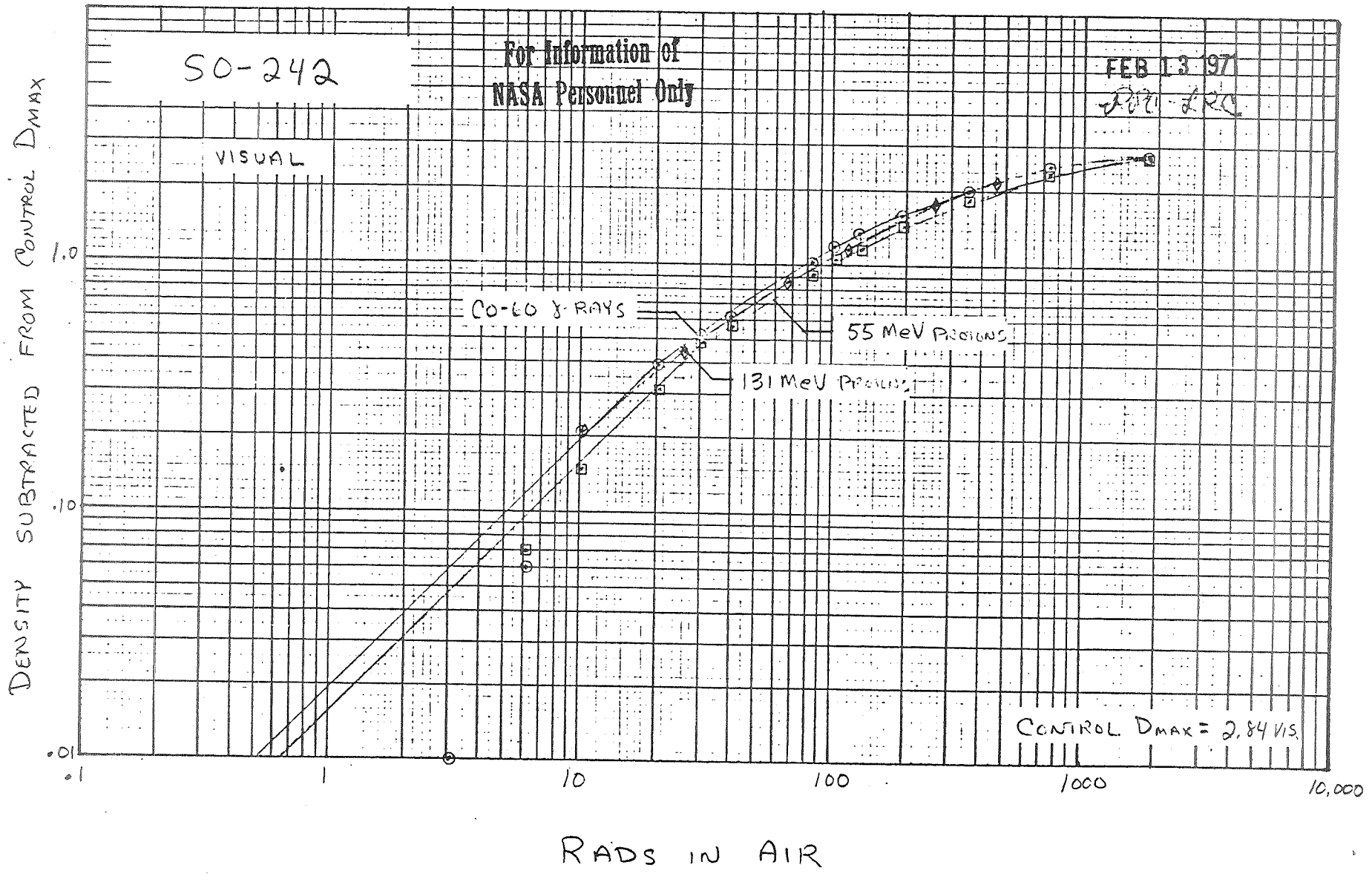
SO-242
For Information of
NASA Personnel Only
FEB 13 1971
VISUAL
CO-60 γ-RAYS
55 MeV PROTONS
131 MeV PROTONS
CONTROL DMAX = 2.84 VIS.
DENSITY SUBTRACTED FROM CONTROL DMAX
1.0
.10
.01
.1
1
10
100
1000
10,000
RADS IN AIR

66

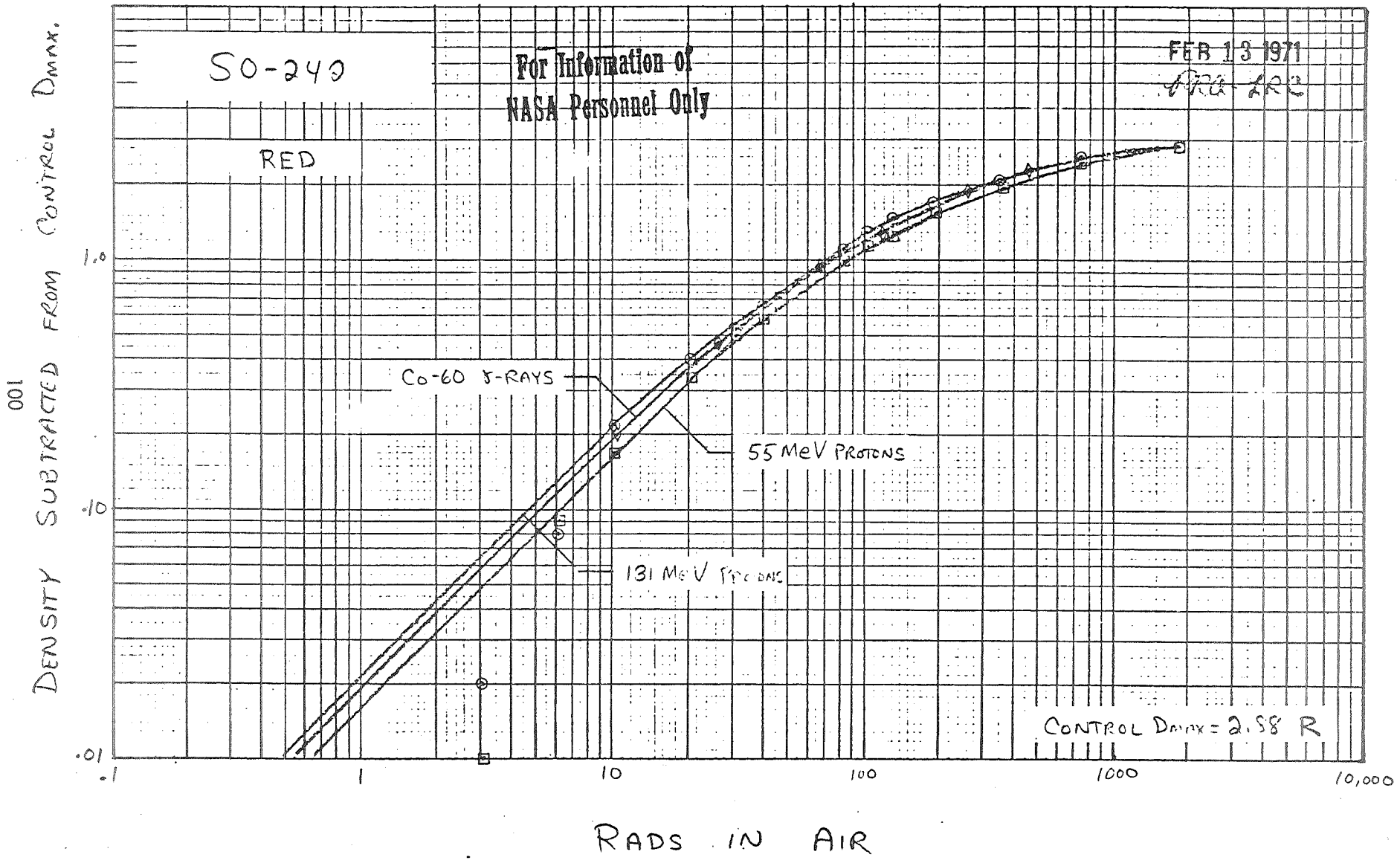
SO-249
For Information of
NASA Personnel Only
FEB 1 3 1971
RED
Co-60 γ-RAYS
55 MeV PROTONS
131 MeV PROTONS
CONTROL Dmax = 2.58 R
DENSITY SUBTRACTED FROM CONTROL Dmax.
001
1.0
.10
.01
.1
1
10
100
1000
10,000
RADS IN AIR

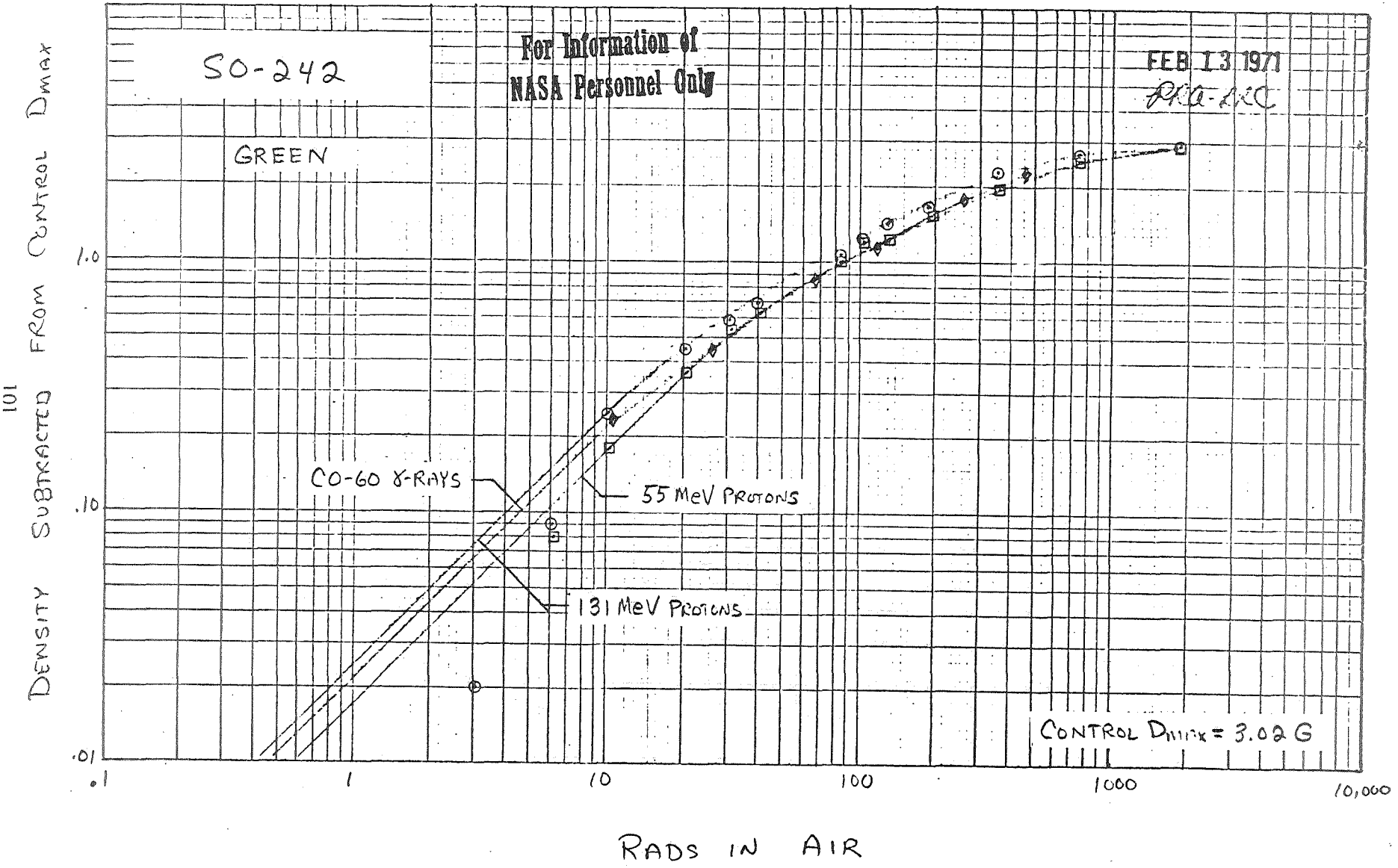
SO-242
GREEN
For Information of
NASA Personnel Only
FEB 13 1971
CO-60 X-RAYS
55 MeV PROTONS
131 MeV PROTONS
CONTROL DMAX = 3.02 G
DENSITY SUBTRACTED FROM CONTROL DMAX
1.0
.10
.01
.1
1
10
100
1000
10,000
RADS IN AIR

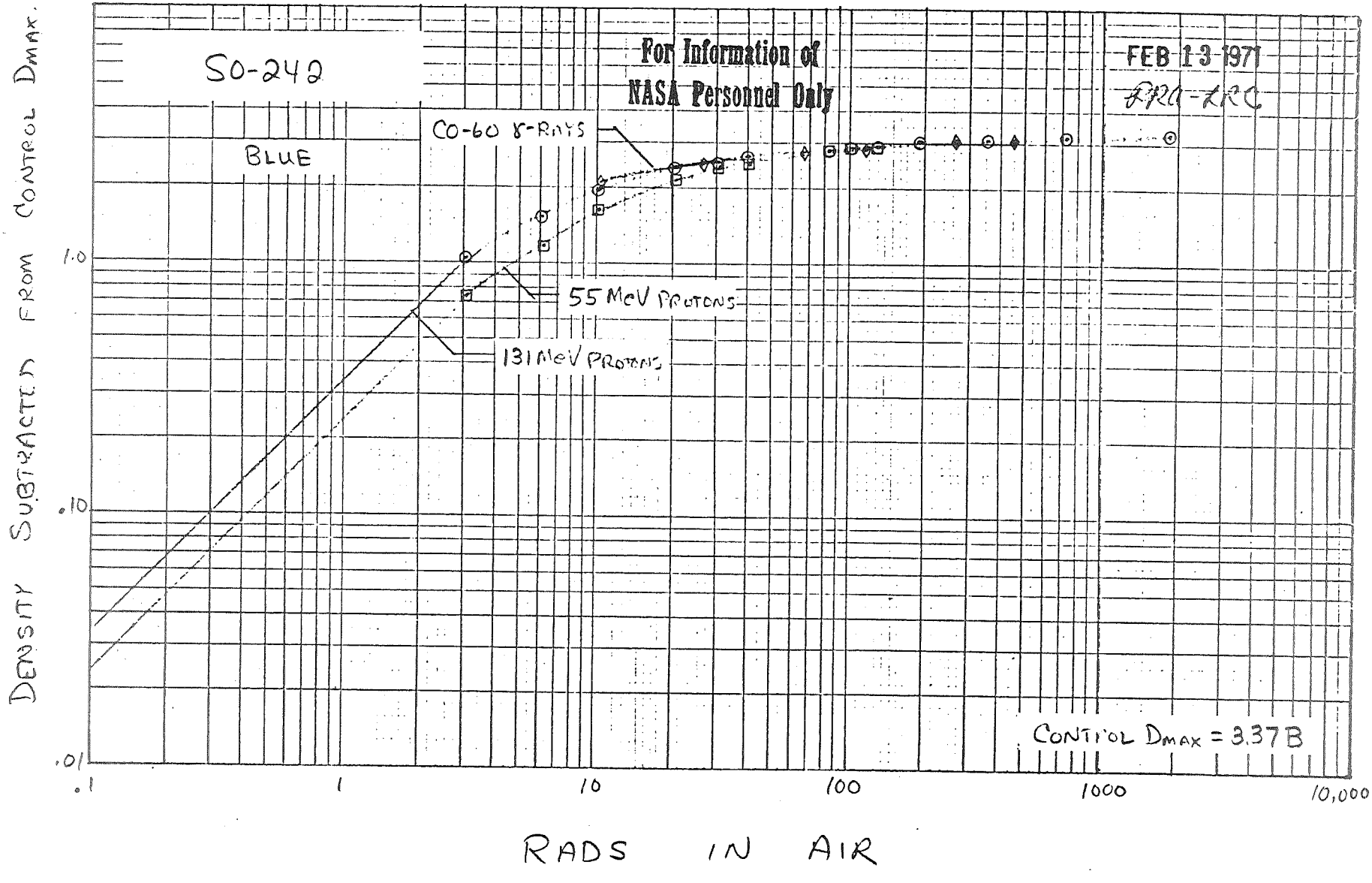
SO-242
For Information of
NASA Personnel Only
FEB 13 1971
BLUE
CO-60 γ-RAYS
55 MeV PROTONS
131 MeV PROTONS
CONTROL DMAX = 3.37 B
1.0
.10
.01
.1
1
10
100
1000
10,000
DENSITY SUBTRACTED FROM CONTROL DMAX.
RADS IN AIR

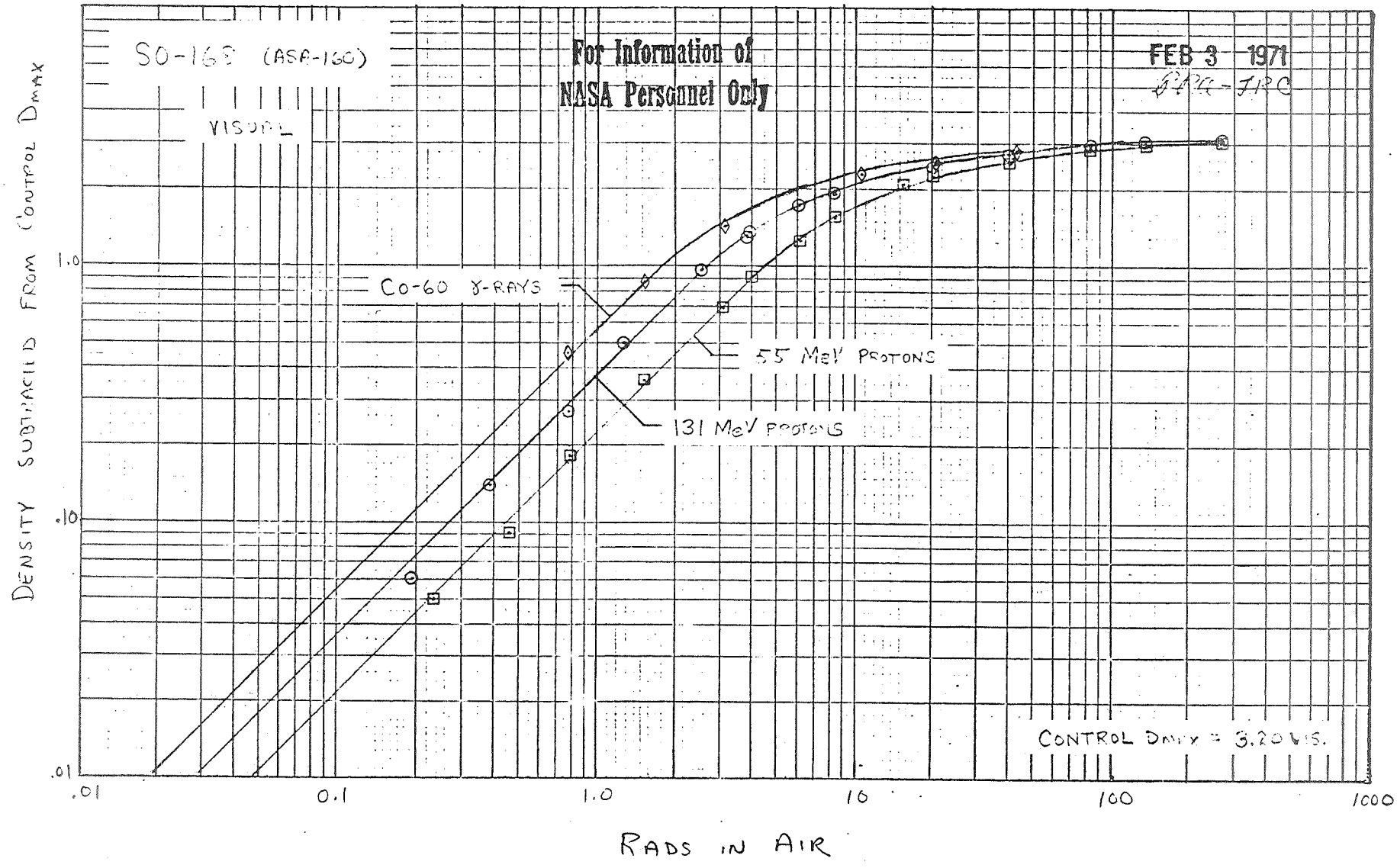
SO-168 (ASA-160)
VISUAL
For Information of
NASA Personnel Only
FEB 3 1971
GAF-IRC
Co-60 γ-RAYS
55 MeV PROTONS
131 MeV PROTONS
CONTROL Dmax = 3.20 VIS.
DENSITY SUBTRACTED FROM CONTROL Dmax
1.0
.10
.01
.01
0.1
1.0
10
100
1000
RADS IN AIR

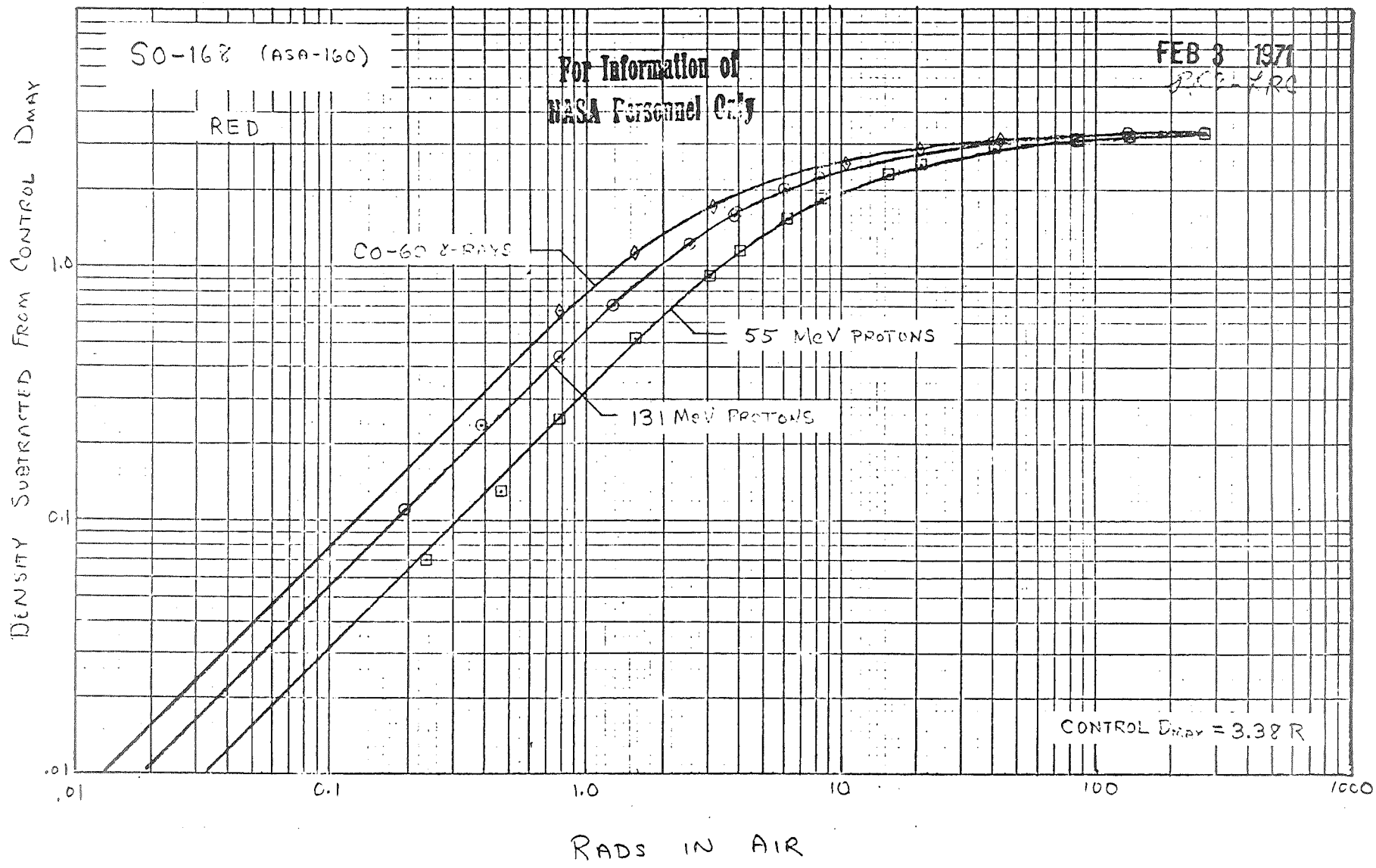
SO-168 (ASA-160)
RED
For Information of
NASA Personnel Only
FEB 3 1971
Co-60 γ-RAYS
55 MeV PROTONS
131 MeV PROTONS
CONTROL D_MAY = 3.38 R
DENSITY SUBTRACTED FROM CONTROL D_MAY
RADS IN AIR
.01
0.1
1.0
10
100
1000

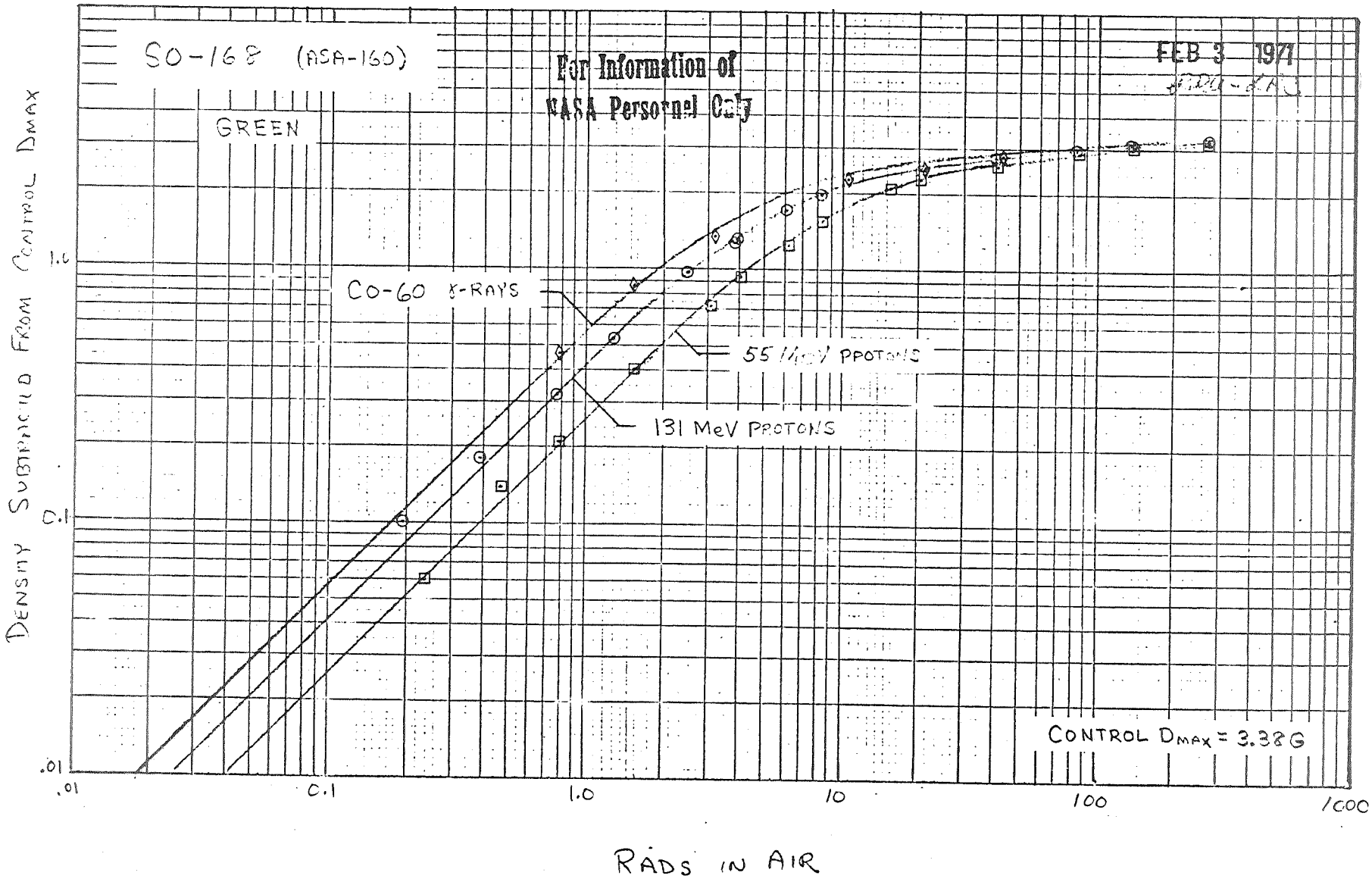
SO-168 (ASA-160)
GREEN
For Information of
NASA Personnel Only
FEB 3 1971
Co-60 X-RAYS
55 MeV PROTONS
131 MeV PROTONS
CONTROL DMAX = 3.38 G
DENSITY SUBTRACTED FROM CONTROL DMAX
1.0
0.1
.01
.01
0.1
1.0
10
100
1000
RADS IN AIR

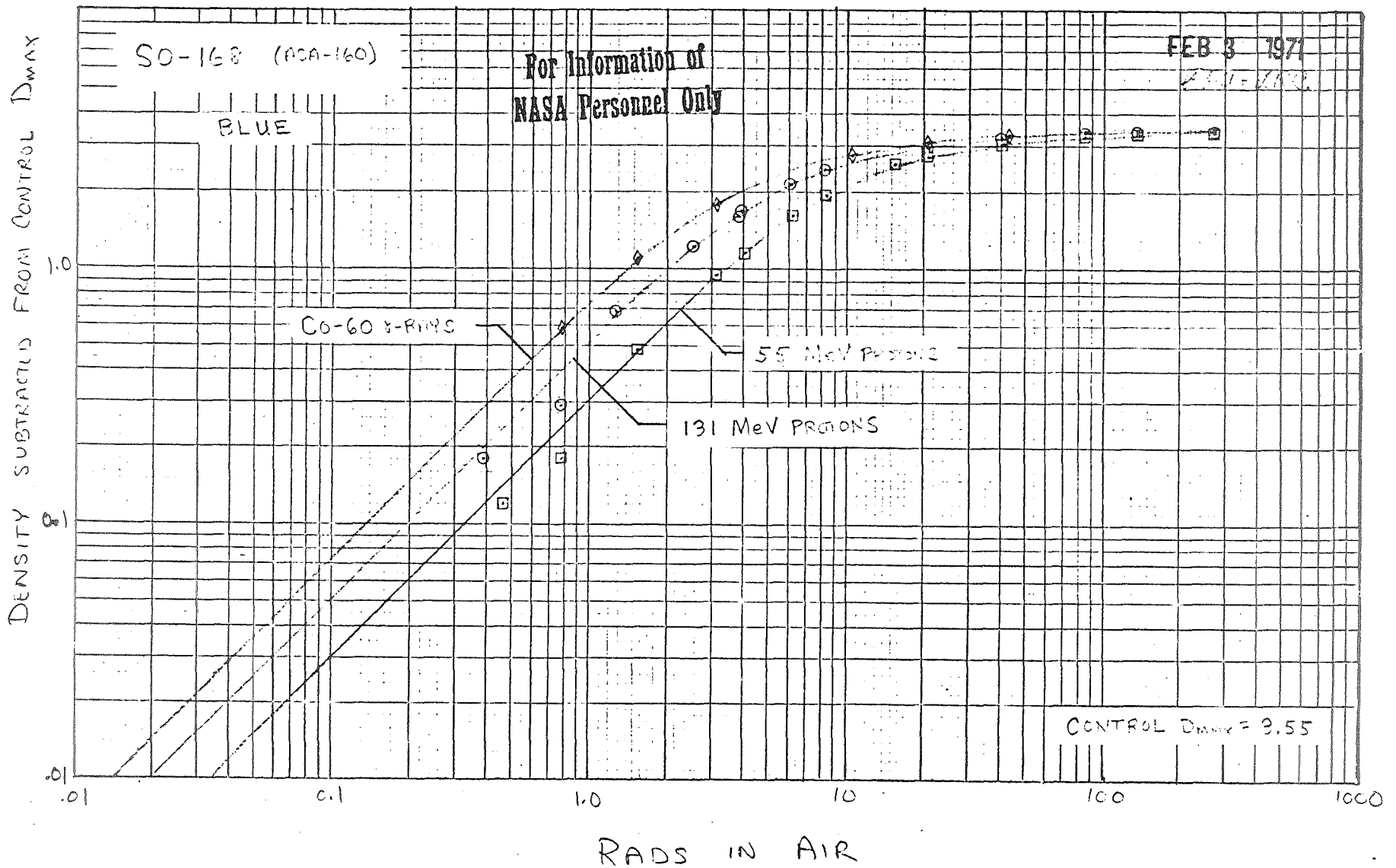
SO-168 (ACA-160)
BLUE
For Information of
NASA Personnel Only
FEB 3 1971
Co-60 γ-RAYS
55 MeV PROTONS
131 MeV PROTONS
CONTROL Dmax = 9.55
DENSITY SUBTRACTED FROM CONTROL Dmax
901
1.0
.1
.01
.01
0.1
1.0
10
100
1000
RADS IN AIR

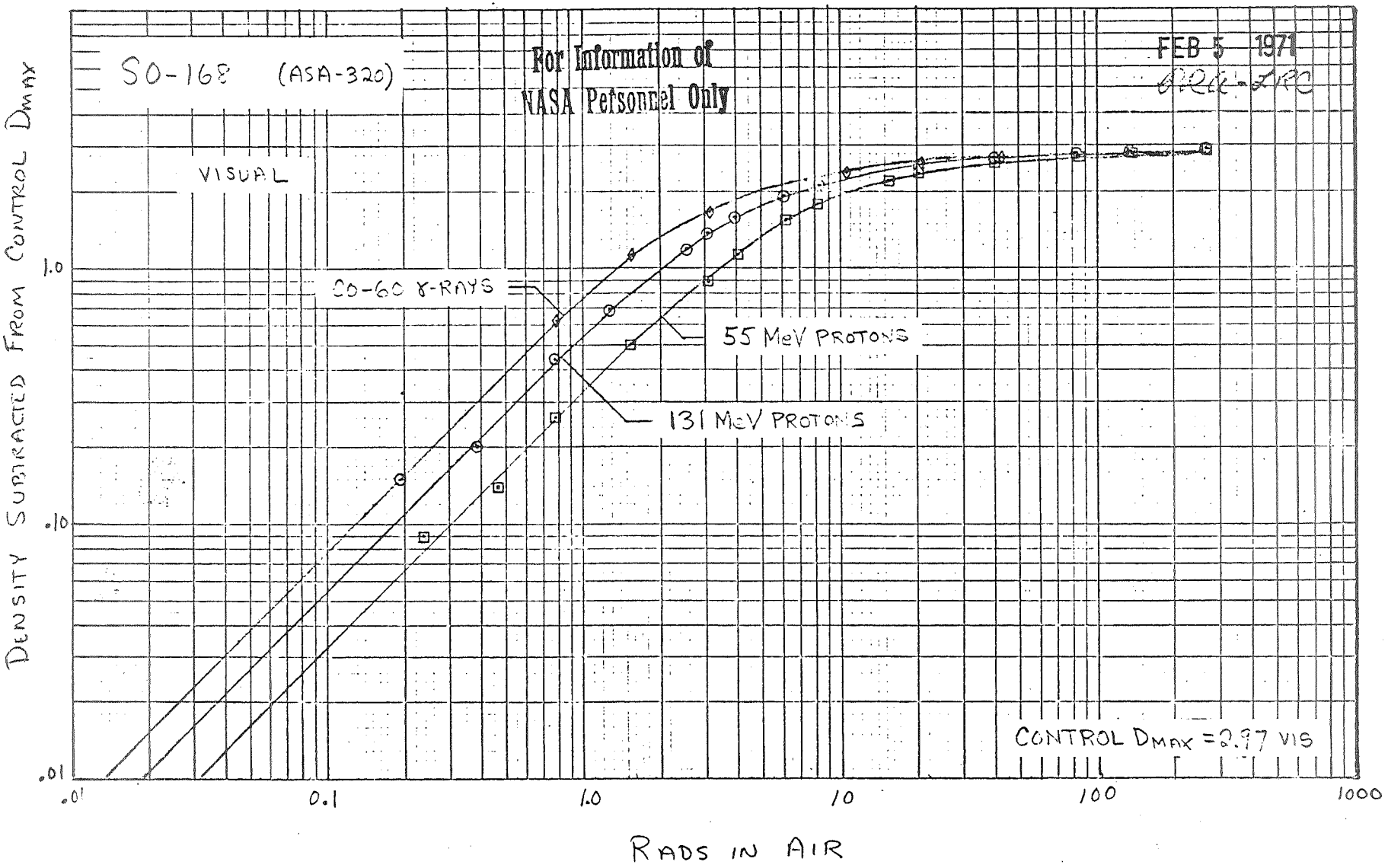
SO-168 (ASA-320)
For Information of
NASA Personnel Only
FEB 5 1971
VISUAL
CO-60 γ-RAYS
55 MeV PROTONS
131 MeV PROTONS
CONTROL DMAX = 2.97 VIS
DENSITY SUBTRACTED FROM CONTROL DMAX
1.0
.10
.01
.01
0.1
1.0
10
100
1000
RADS IN AIR

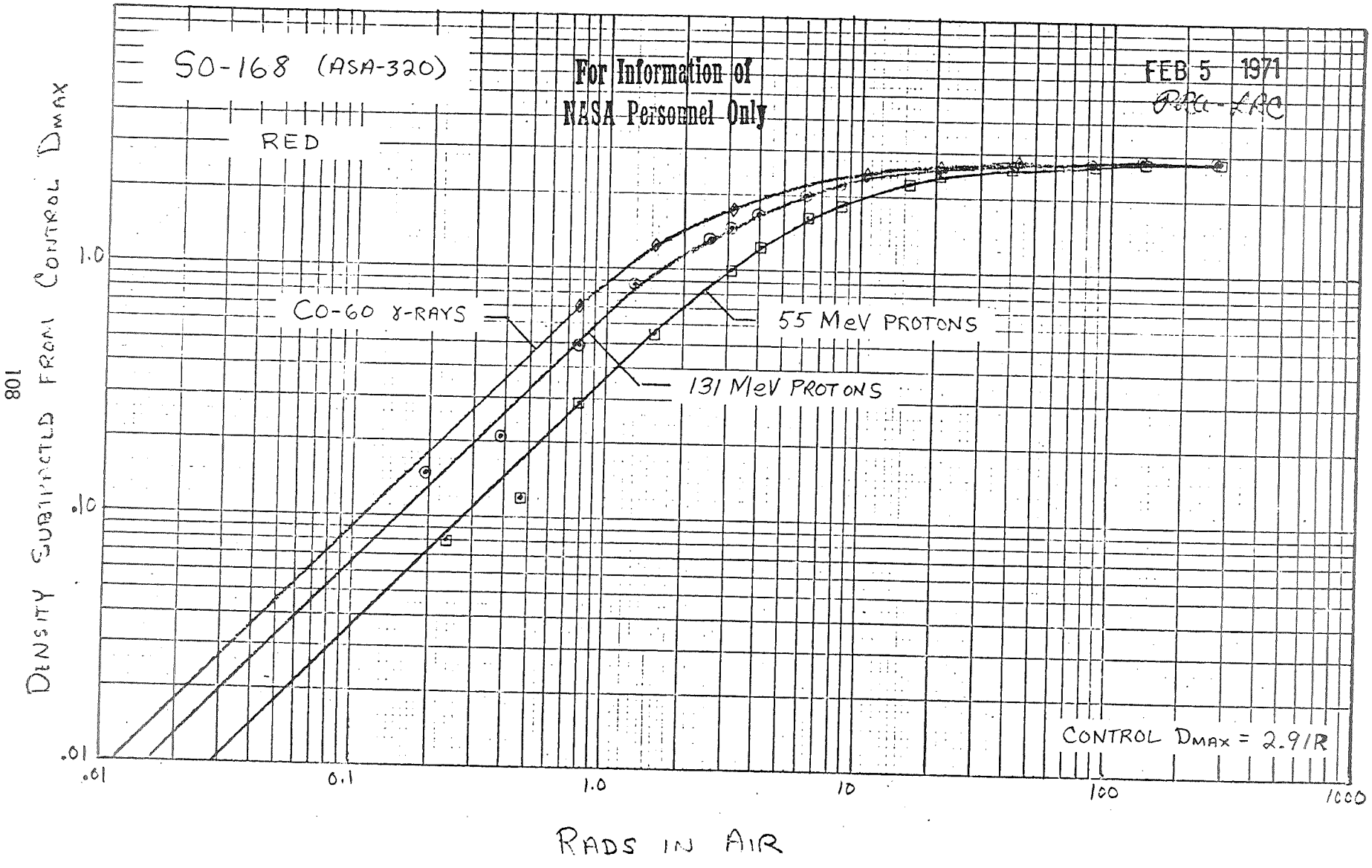
SO-168 (ASA-320)
For Information of
NASA Personnel Only
FEB 5 1971
RED
CO-60 X-RAYS
55 MeV PROTONS
131 MeV PROTONS
CONTROL DMAX = 2.91R
DENSITY SUBTRACTED FROM CONTROL DMAX
1.0
.10
.01
.01
0.1
1.0
10
100
1000
RADS IN AIR

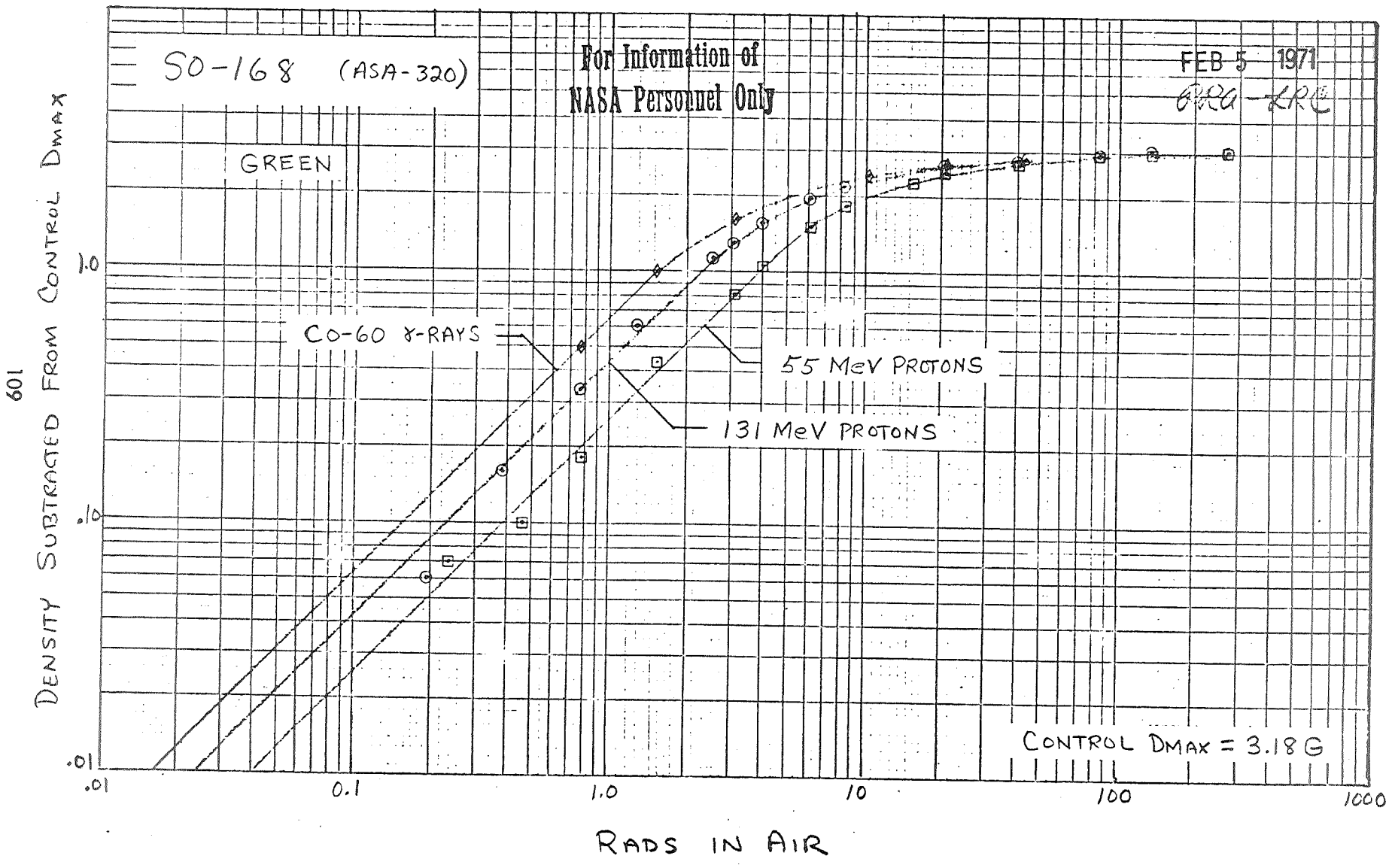
SO-168 (ASA-320)
For Information of
NASA Personnel Only
FEB 5 1971
GREEN
CO-60 X-RAYS
55 MeV PROTONS
131 MeV PROTONS
CONTROL DMAX = 3.18 G
601
DENSITY SUBTRACTED FROM CONTROL DMAX
1.0
.10
.01
.01
0.1
1.0
10
100
1000
RADS IN AIR

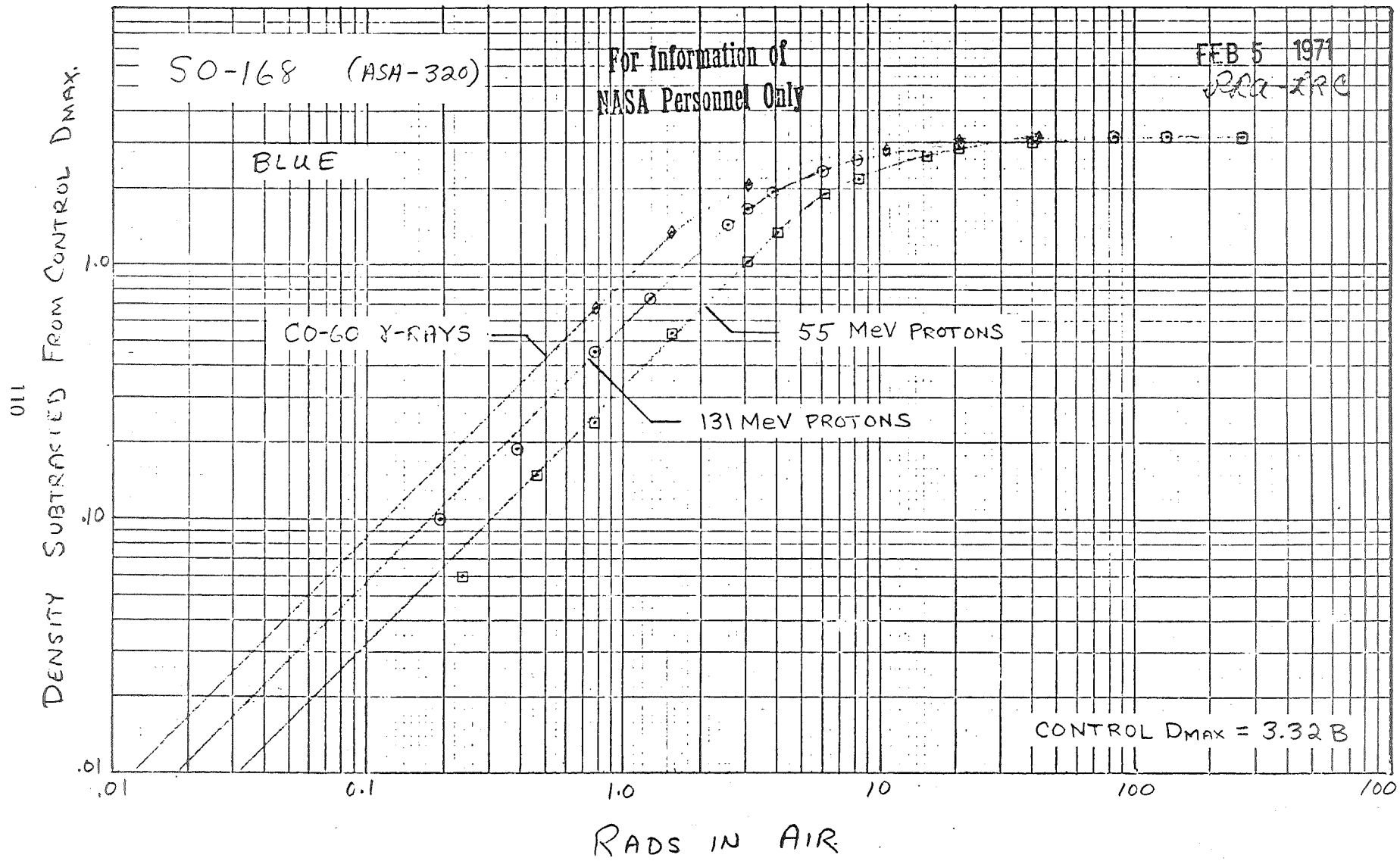
SO-168 (ASA-320)
For Information of
NASA Personnel Only
FEB 5 1971
BLUE
CO-60 γ-RAYS
55 MeV PROTONS
131 MeV PROTONS
CONTROL DMAX = 3.32 B
DENSITY SUBTRACTED FROM CONTROL DMAX.
RADS IN AIR
.01
.10
1.0
.01
0.1
1.0
10
100
100

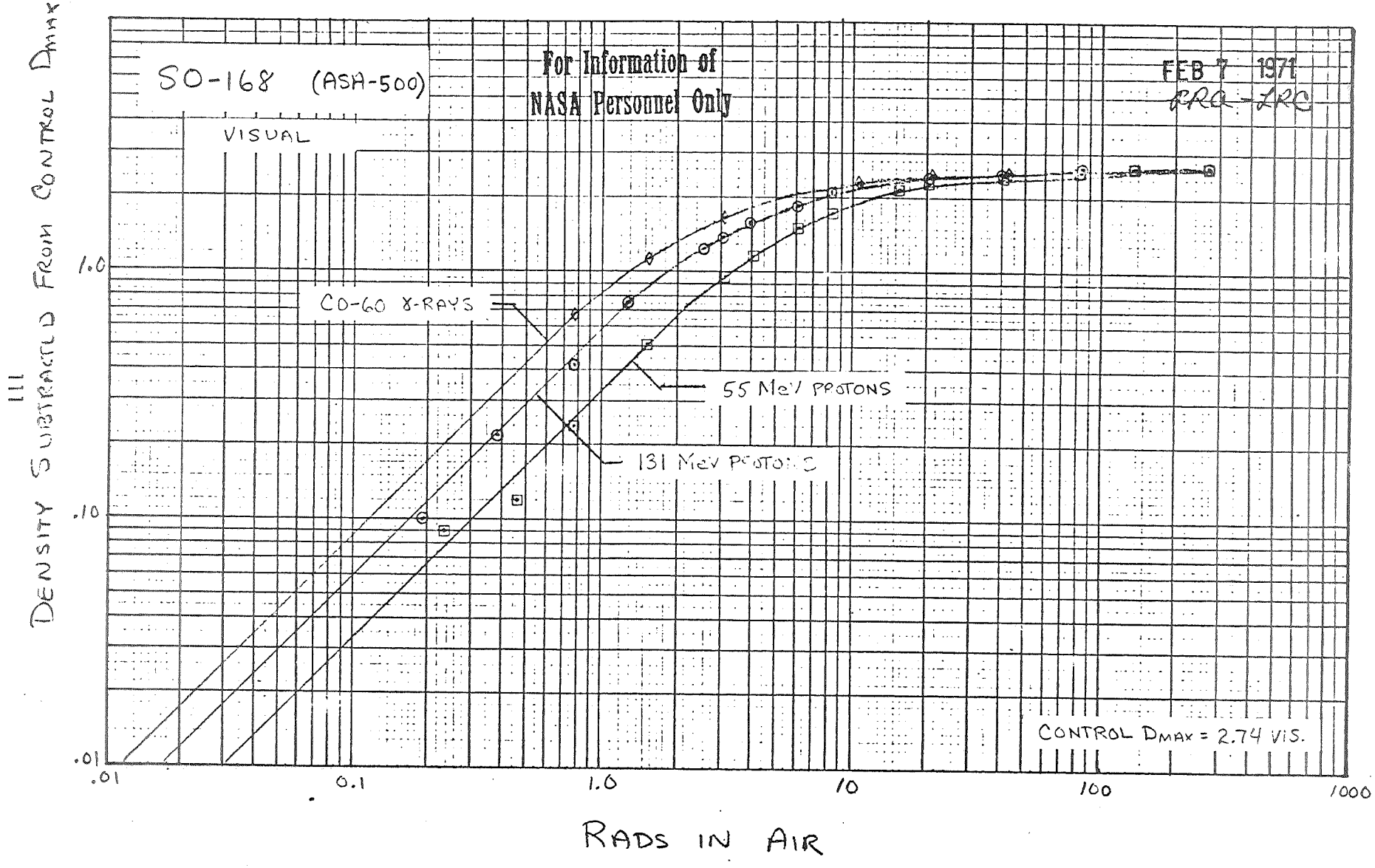
SO-168 (ASA-500)
For Information of
NASA Personnel Only
FEB 7 1971
GRC-LRC
VISUAL
CO-60 X-RAYS
55 MeV PROTONS
131 MeV PROTONS
CONTROL DMAX = 2.74 VIS.
DENSITY SUBTRACTED FROM CONTROL DMAX
1.0
.10
.01
.01
0.1
1.0
10
100
1000
RADS IN AIR

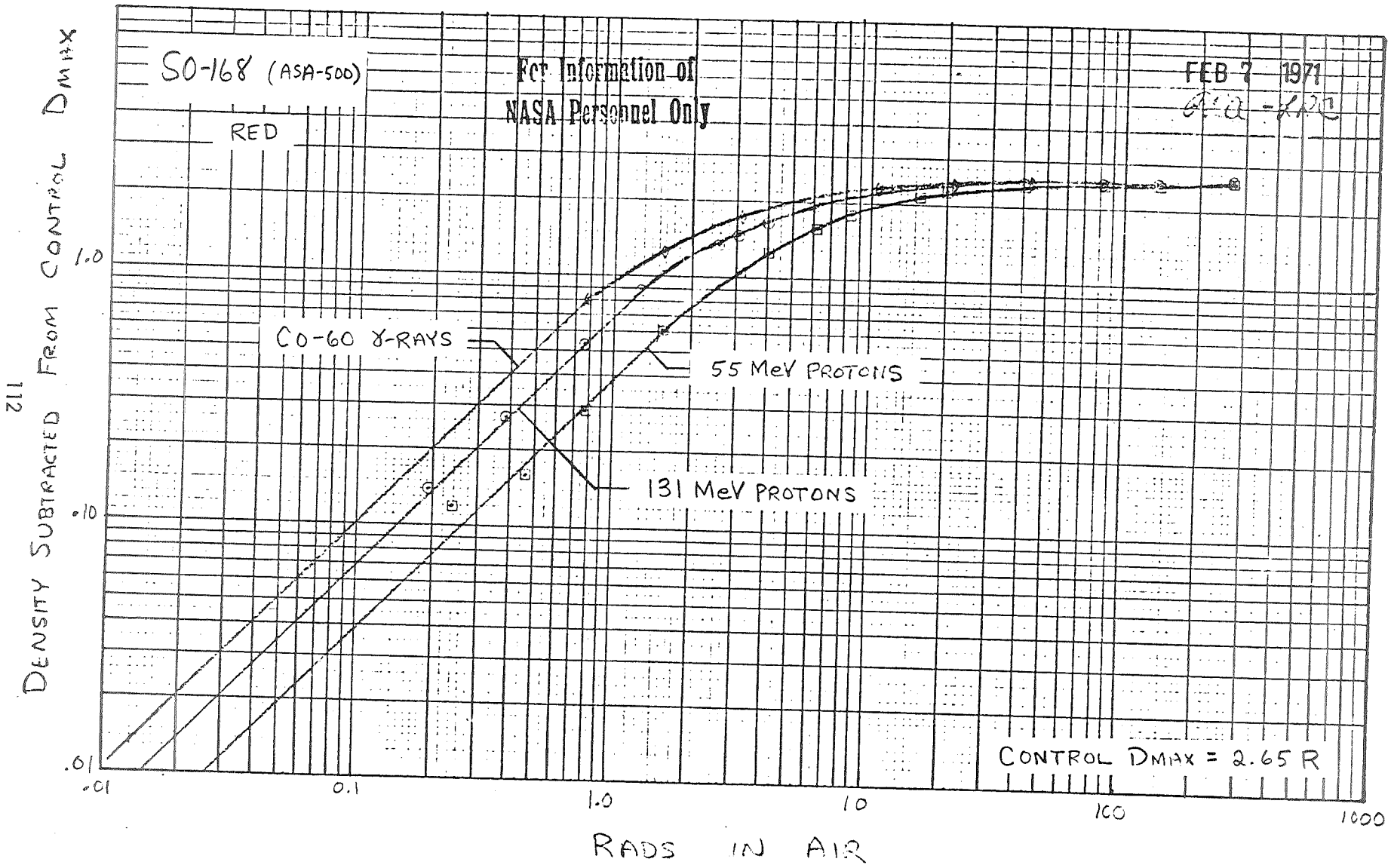
SO-168 (ASA-500)
RED
For Information of
NASA Personnel Only
FEB 7 1971
CO-60 γ-RAYS
55 MeV PROTONS
131 MeV PROTONS
CONTROL DMAX = 2.65 R
DENSITY SUBTRACTED FROM CONTROL DMAX
RADS IN AIR
.01
.10
1.0
.01
0.1
1.0
10
100
1000

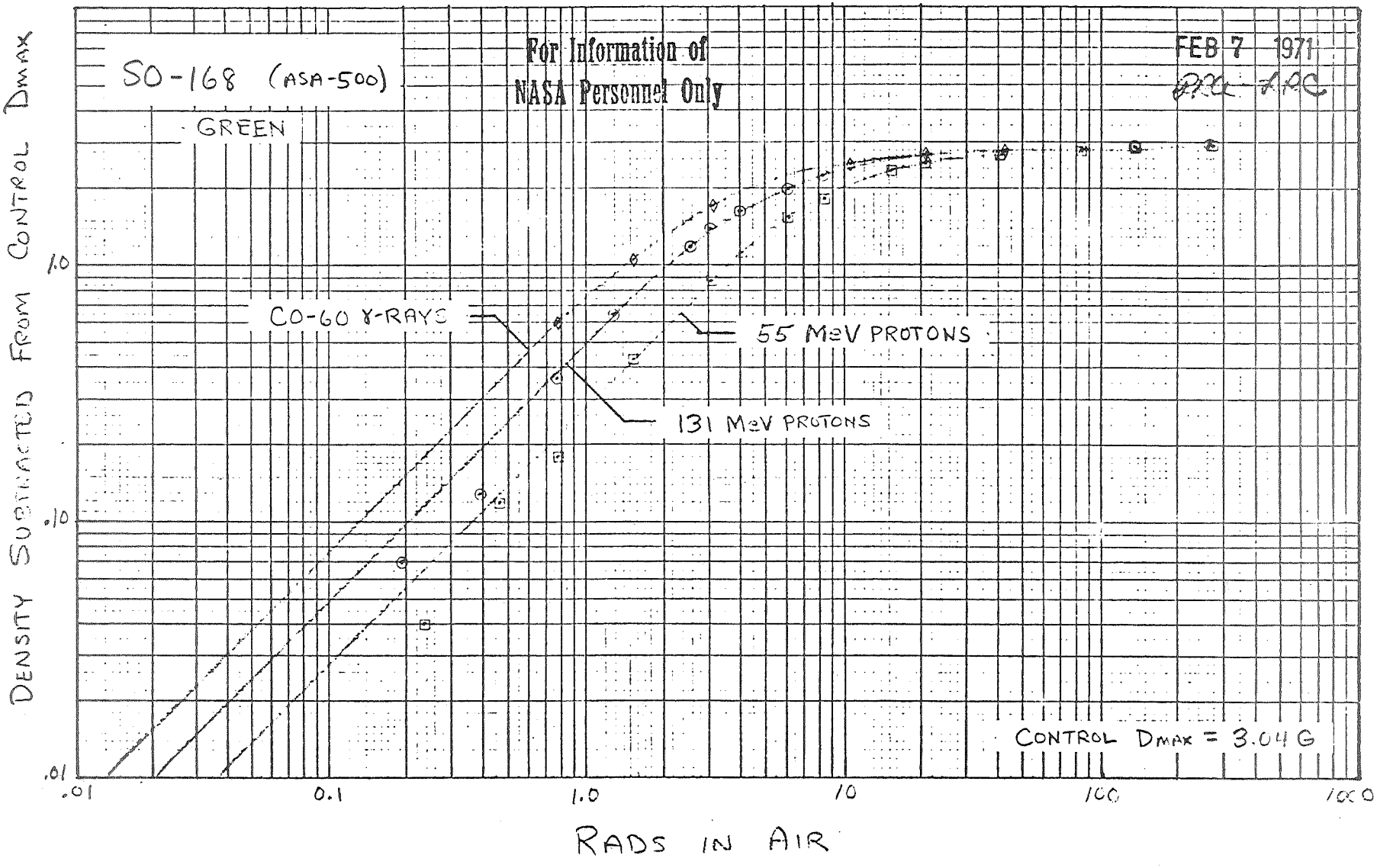
SO-168 (ASA-500)
GREEN
For Information of
NASA Personnel Only
FEB 7 1971
CO-60 γ-RAYS
55 MeV PROTONS
131 MeV PROTONS
CONTROL DMAX = 3.04 G
DENSITY SUBTRACTED FROM CONTROL DMAX
RADS IN AIR
.01
.10
1.0
.01
0.1
1.0
10
100
1000

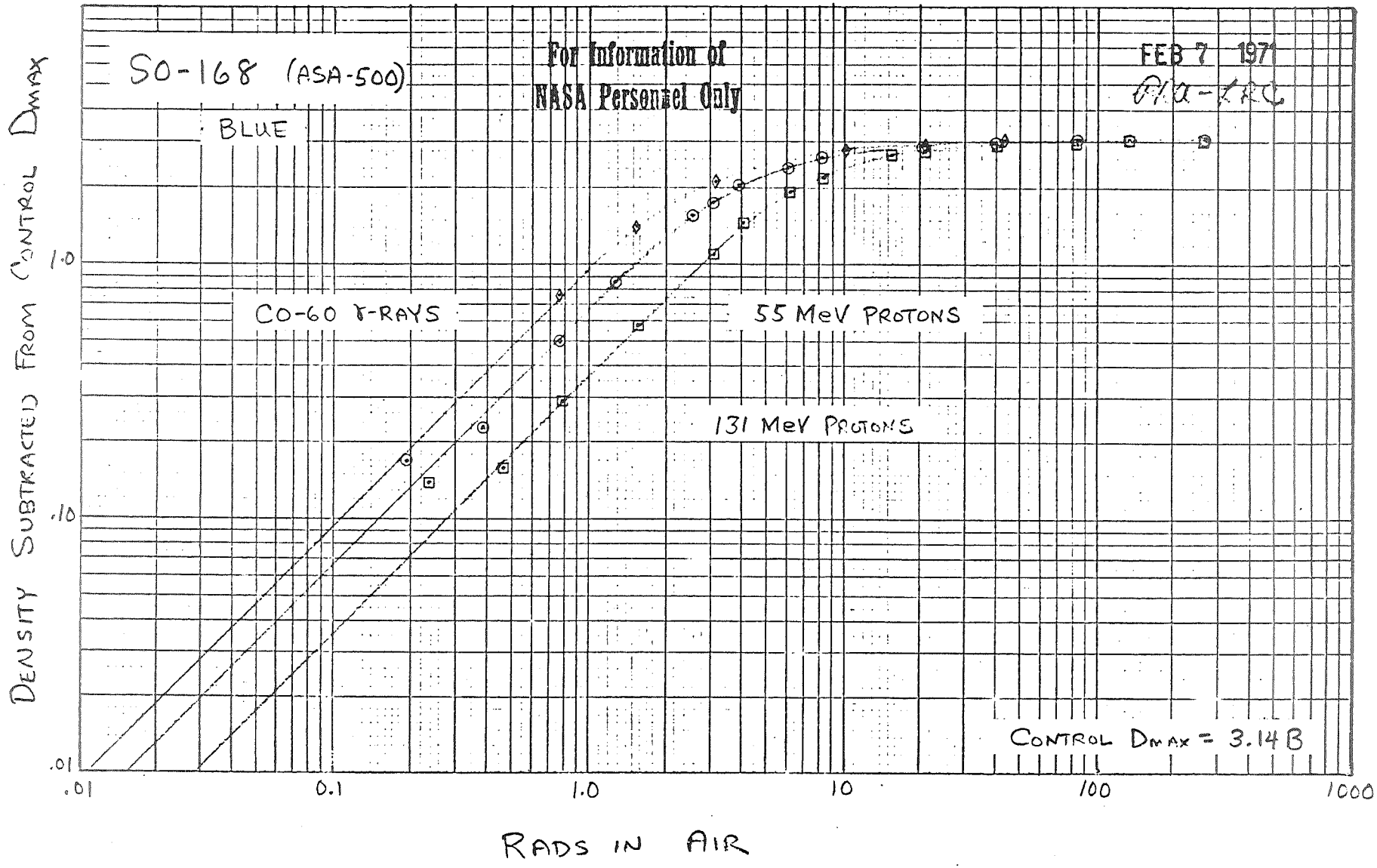
SO-168 (ASA-500)
BLUE
For Information of
NASA Personnel Only
FEB 7 1971
CO-60 γ-RAYS
55 MeV PROTONS
131 MeV PROTONS
CONTROL DMAX = 3.14 B
DENSITY SUBTRACTED FROM CONTROL DMAX
1.0
.10
.01
.01
0.1
1.0
10
100
1000
RADS IN AIR

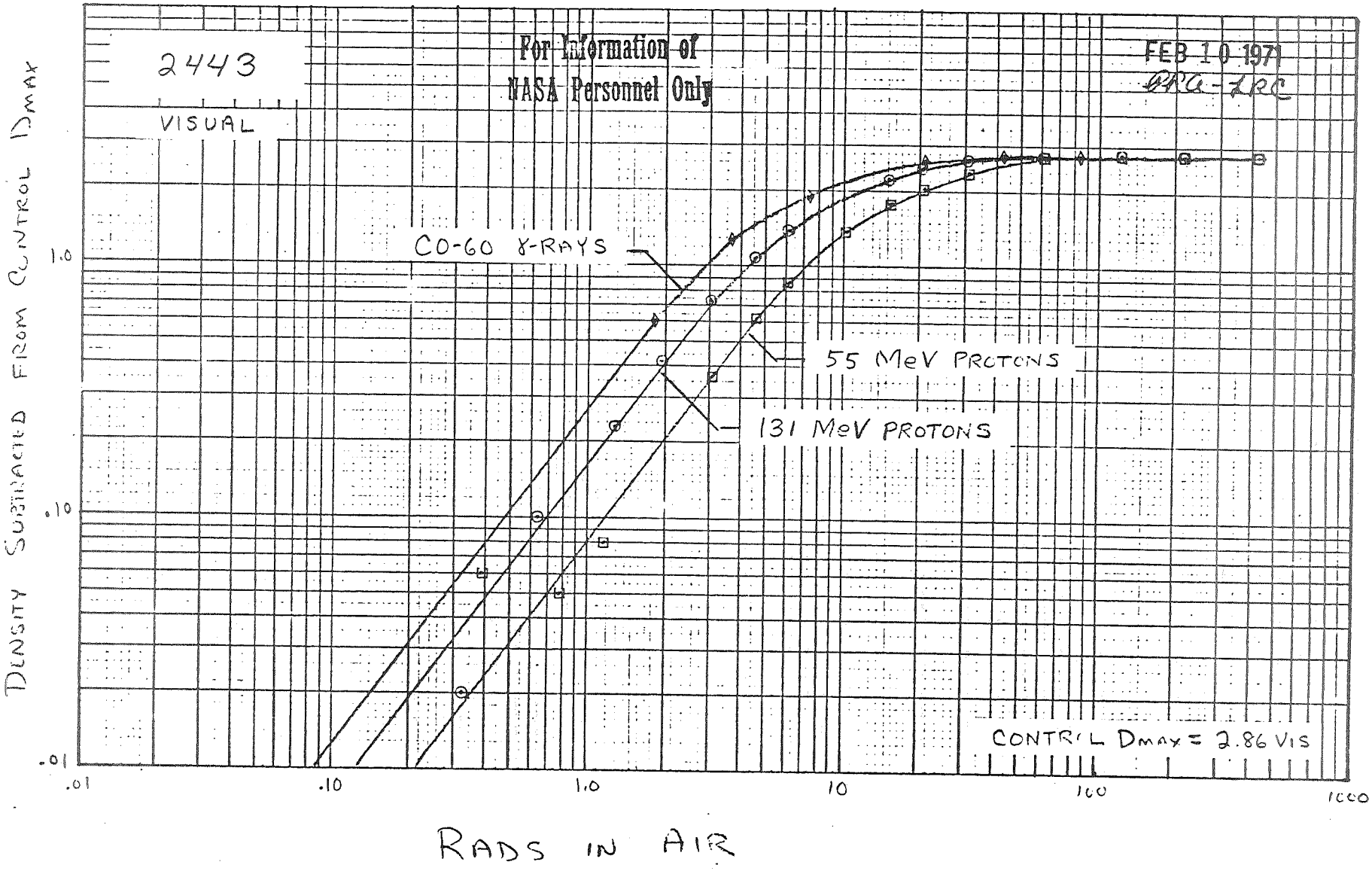
2443
VISUAL
For Information of
NASA Personnel Only
FEB 10 1971
ARC-LRC
CO-60 X-RAYS
55 MeV PROTONS
131 MeV PROTONS
CONTROL DMAX = 2.86 VIS
DENSITY SUBTRACTED FROM CONTROL DMAX
1.0
.10
.01
.01
.10
1.0
10
100
1000
RADS IN AIR

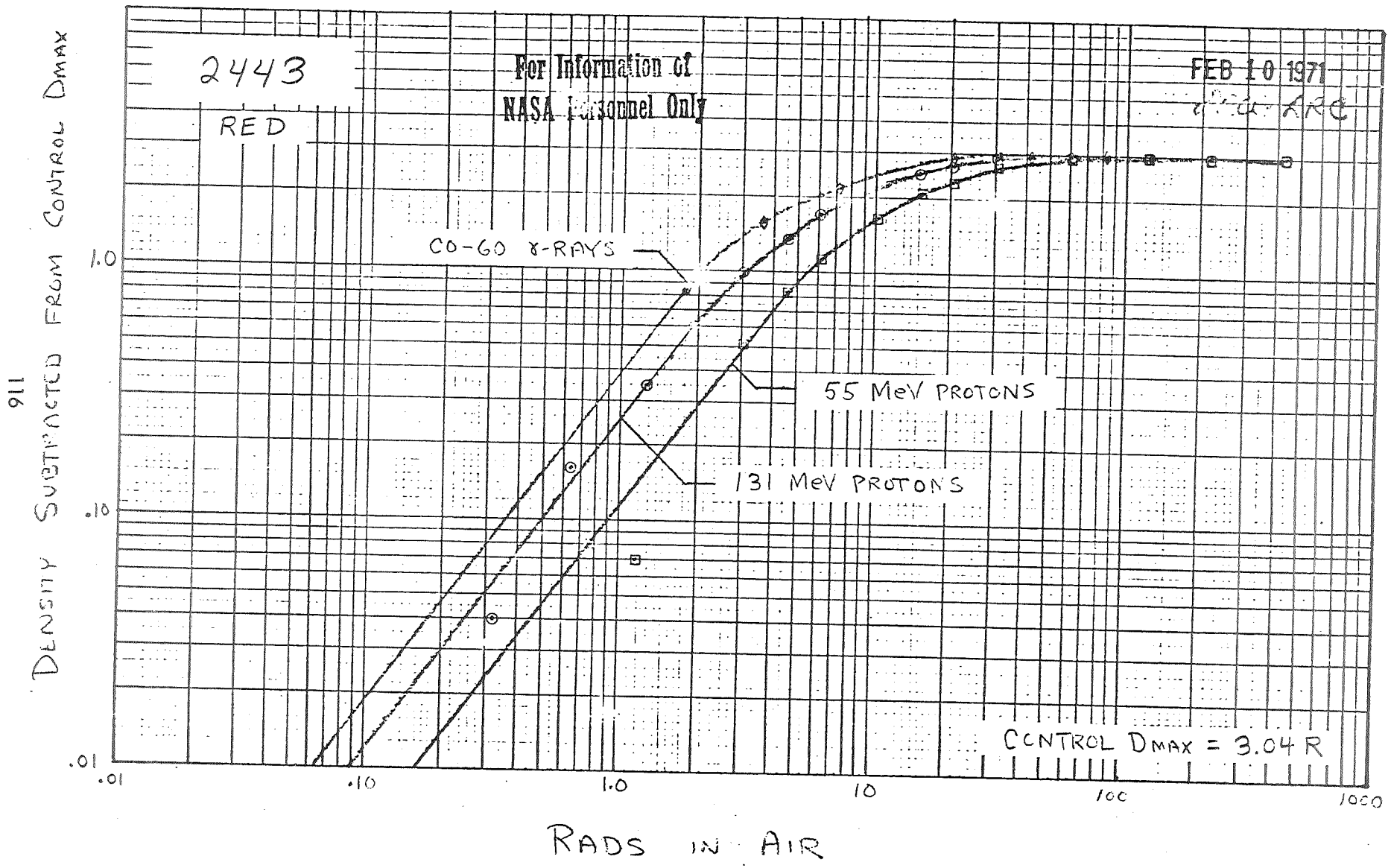
2443
RED
For Information of
NASA Personnel Only
FEB 10 1971
ARC
CO-60 γ-RAYS
55 MeV PROTONS
131 MeV PROTONS
CONTROL DMAX = 3.04 R
911
DENSITY SUBTRACTED FROM CONTROL DMAX
1.0
.10
.01
.01
.10
1.0
10
100
1000
RADS IN AIR

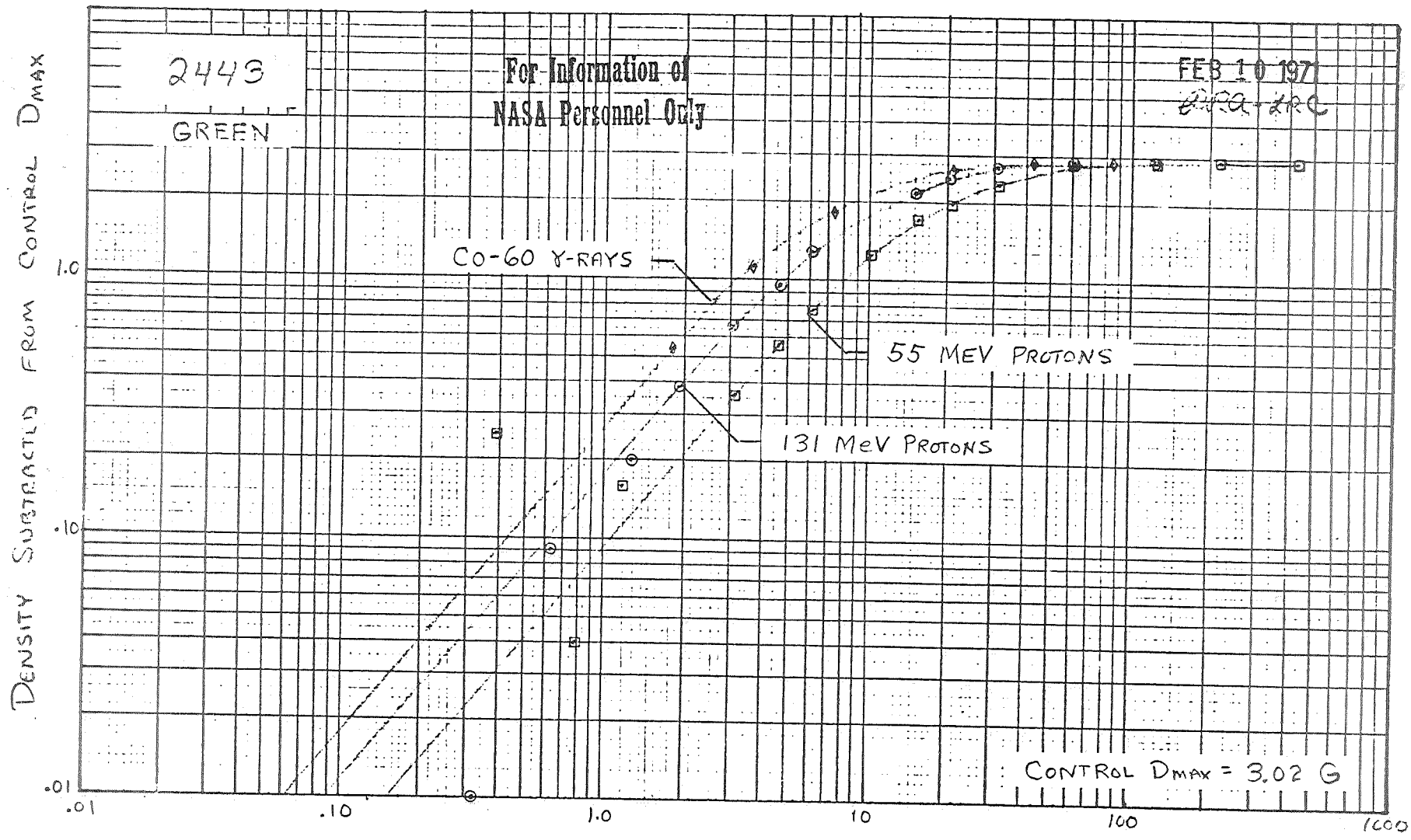
2443
GREEN
For Information of
NASA Personnel Only
FEB 10 1971
CO-60 γ-RAYS
55 MEV PROTONS
131 MeV PROTONS
CONTROL DMAX = 3.02 G
DENSITY SUBTRACTED FROM CONTROL DMAX
1.0
.10
.01
.01
.10
1.0
10
100
1000
RADS IN AIR

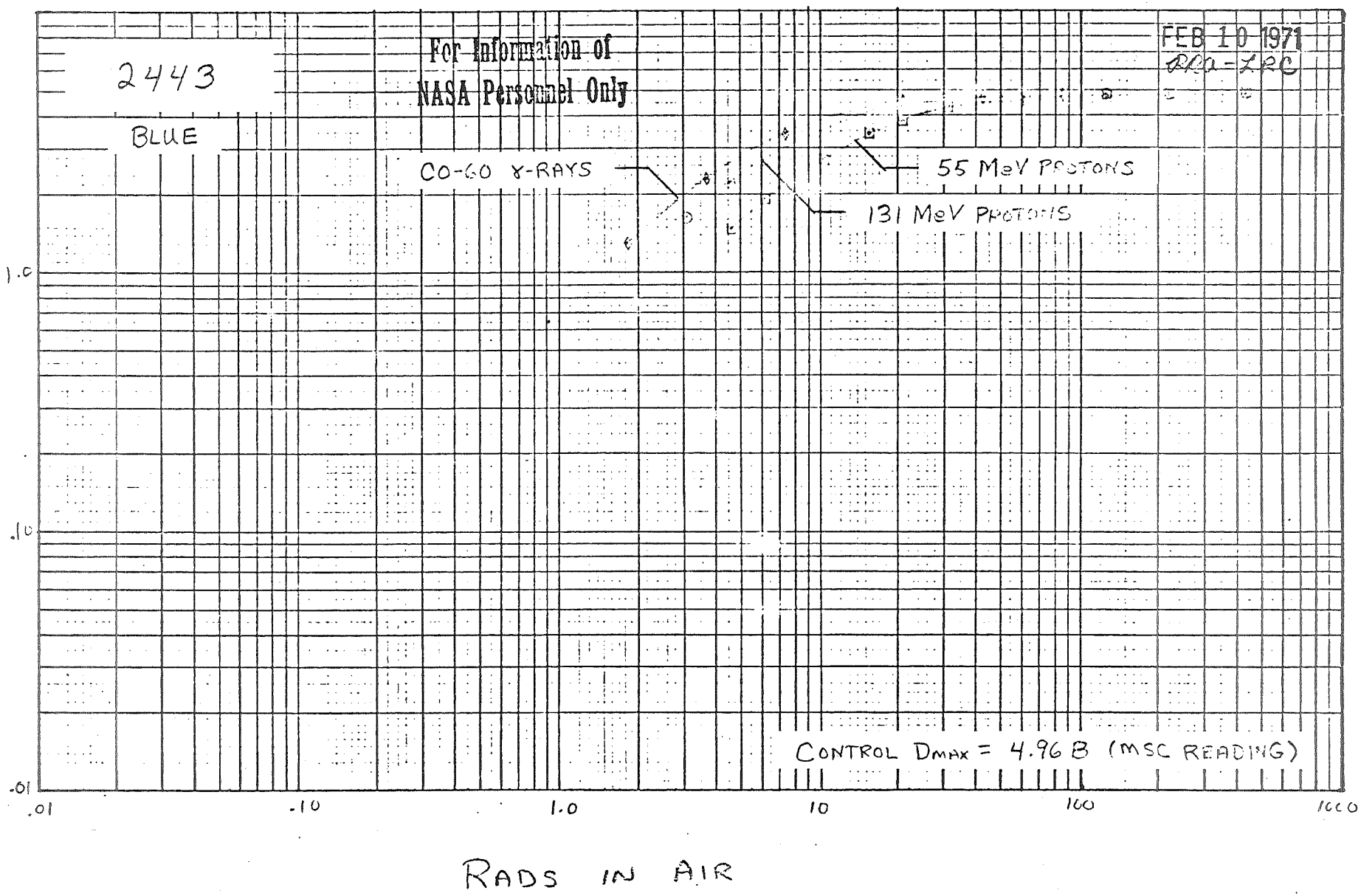
2443
BLUE
For Information of
NASA Personnel Only
FEB 10 1971
RCA-LRC
CO-60 γ-RAYS
55 MeV PROTONS
131 MeV PROTONS
CONTROL DMAX = 4.96 B (MSC READING)
DENSITY SUBTRACTED FROM CONTROL DMAX
1.0
.10
.01
.01
.10
1.0
10
100
1000
RADS IN AIR

REFERENCES

1. Adams, R. R. : The Photographic Effects of Ionizing Radiation on 13 Skylab Candidate Film Types - Preliminary Data, (Unpublished), Langley Research Center - NASA, February 23, 1971.

2. Braly, J. : Martin-Marietta Corporation, Denver, Colorado, Private Communication.

3. Burrell, M.O., and Wright, J.J.: MSFC-NASA, Private Communication.

4. Cormack, D.V. and Johns, H.E.: Electron Energies and Ion Densities in Water Irradiated with 200 KeV, 1 MeV, and 25 MeV Radiation, Vol. XXV, No. 295, Brit. Jour. Rad., July 1952.

5. Dudley, R. A. : "Dosimetry with Photographic Emulsions," in Radiation Dosimetry, Vol. II, edited by F. H. Attix and W. C. Roesch, Academic Press, 1966.

6. Greening, J.R. : The Photographic Action of X-rays, B64,977, Proc. Phys. Soc. (London), 1954.

7. Heckman, H.H., and Nakano, G.H. : East-West Asymetry in the Flux of Mirroring Geomagnetically Trapped Protons, No. 8, Vol. 68, Journal of Geophysical Research, April 15, 1963.

8. Hill, C. W.; Davis, D. N.; and Davis, J.H. : Space Radiation Hazards to Project Skylab Photographic Film, ER-10725, Lockheed-Georgia Company, Marietta, Georgia, June 1970.

9. Hill, C. W.; Davis, D.N.; and Parker, H.K., Jr.: Space Radiation Hazards to Photographic Film in the Apollo Telescope Mount and Orbiting Workshop, ER-10156, Lockheed-Georgia Company, Marietta, Georgia, May 1969.

10. Hill, C. W.; Ritchie, W. B.; and Simpson, K. M., Jr.: Data Compilation and Evaluation of Space Shielding Problems, Volume IV, LSVDC4 Program System, ER-7777, Lockheed-Georgia Company, Marietta, Georgia, 1967.

11. Holt, E. C.; Ruffin, R. L. Jr.; McClendon, J. A.; and Edgeton, R. L.: Film Radiation Damage Data Analysis - Draft, ASD-ASTN-13004, Teledyne Brown Engineering, Huntsville, Alabama, April 30, 1971.

12. Huff, K. E., and Cleare, H. M. : Eastman Kodak Company, Rochester, New York, Private Communication.

13. Lewis, J. C. and Watts, H. V. : Effects of Nuclear Radiation on the Sensitometric Properties of Reconnaissance Films, AFAL-TR-65-113, April 1965.

14. Nelson, William : ATM Experiment Office, MSFC-NASA, Private Communication.

15. Oldham, L. P.: Trip Report to Eastman Kodak Co., Rochester, N.Y., 16-17 September 1970, Martin Marietta Corporation, Unpublished Data, 1970.

16. Oran, W. : Radiation Degradation of Selected Films, NASA TMX-64524, MSFC-NASA, June 22, 1970.

17. Ress, R. B.; Oldham, L. P.; Dean, J. W.; and Burghardt, J. E. : Skylab Radiation Film Studies, ED-2002-1110 Martin Marietta Corporation, Denver, Colorado, June 1970.

18. Spear, J. D.; and Capone, T. A.: Radiation Protection Study for Photographic Space Film, Report, (N69-18734) Chrysler Corporation Space Division, New Orleans, La., January 1969.

19. Tochilin, E. and Golden, R. : Investigations on the Relative Beta - to Gamma -ray Response of Photographic Emulsions, 4, 244, Health Physics, 1961.

20. Tochilin, E.; Shumway, B.W.; and Kohler, G.D.: Response of Photographic Emulsions to Charged Particles and Neutrons, 4, 467, Radiation Research, (1956)

21. Vette, J. I., et al.: Models of the Trapped Radiation Environment, Vols I - VI, NASA SP-3024, 1966 - 1970.

22. Weinstein, M.: Radiation Tests, Memorandum, Data Corporation, December 16, 1970.

MSFC—RSA, Ala